University of Modena and Reggio Emilia
Department of Life Sciences
Ph.D. School in Agri-Food Sciences, Technologies and Biotechnologies
XXXII Cycle

Development of Active Chitosan-Based Films for Sustainable Food Packaging Applications

Ph.D. Candidate: **Hossein Haghighi**
Tutor: **Prof. Dr. Andrea Pulvirenti**
Co-Tutor: **Prof. Dr. Fabio Licciardello**
Coordinator: **Prof. Dr. Alessandro Ulrici**

2016-2019

To:

My wife, my parents and my sister

Contents

Abstract

The current trend in food packaging is oriented towards the substitution of non-biodegradable petroleum-based polymers by packaging materials that are eco-friendly and can prolong the food shelf life as well. In this context, this Ph.D. project aims to the development and characterization of chitosan-based films enriched with natural (essential oils) and synthetic (ethyl lauroyl arginate) antimicrobial compounds for sustainable food packaging applications. The overall project has been divided into five main parts. The brief description of each chapter is presented here:

Chapter I presents a review of the recent advances of chitosan-based blend films for food packaging applications. The reason for selecting chitosan as the main biopolymer in this study and literature review concerning blending chitosan with other natural and synthetic biopolymers has been described.

Chapter II aims to develop blend and bilayer bio-based active films by solvent casting technique, using chitosan and gelatin as biopolymers, glycerol as a plasticizer and ethyl lauroyl arginate (LAE) as an antimicrobial compound. The results showed that blend films had higher tensile strength and elastic modulus and lower water vapor permeability than bilayer films ($p<0.05$). Bilayer films demonstrated as effective barriers against UV light and showed lower transparency values ($p<0.05$). FT-IR spectra indicated that interactions existed between chitosan and gelatin due to electrostatic interactions and hydrogen bond formation. However, addition of LAE did not interfere in the network structure. Active films containing LAE (0.1%, v/v) inhibited the growth of four food bacterial pathogens including *Listeria monocytogenes, Escherichia coli, Salmonella typhimurium,* and *Campylobacter jejuni*.

Chapter III focuses to develop films based on chitosan-gelatin blend enriched with cinnamon, citronella, pink clove, nutmeg, and thyme essential oils (1%, v/v) and evaluating their physical, optical, mechanical, water barrier and microstructural

properties for active food packaging applications. The results confirmed intermolecular interactions between functional groups of the essential oils with the hydroxyl and amino groups of the chitosan-gelatin film network. The incorporation of different essential oils notably improved the UV barrier properties. The developed films, with special regards for those including thyme essential oil, were effective against four common food bacterial pathogens.

Chapter IV aims to develop active films based on chitosan and polyvinyl alcohol enriched with LAE at different concentrations (1-10%, w/w). The results showed that high LAE levels negatively affected mechanical and water barrier properties. Addition of LAE improved UV barrier properties. The developed active films were effective against four common food bacterial pathogens.

Chapter V summarizes the highlights and concludes significant findings of this study.

Sviluppo e caratterizzazione di film biodegradabili a base di chitosano attivo per il food packaging

Abstract

L'attuale tendenza nel confezionamento degli alimenti è orientata alla sostituzione di polimeri non biodegradabili a base di petrolio con materiali di imballaggio ecologici e che possono prolungare anche la shelf-life degli alimenti. In questo contesto, il progetto Ph.D. ha preso in considerazione lo sviluppo e la caratterizzazione di film misti a base di chitosano arricchiti con composti antimicrobici naturali (oli essenziali) e di sintesi (etil lauroil arginato) per applicazioni di confezionamento alimentare. L'intero progetto è stato diviso in cinque parti principali.

Il capitolo I presenta una breve introduzione sui recenti progressi dei film costituiti da miscele a base di chitosano. Il motivo per cui è stato scelto il chitosano come biopolimero principale in questo studio e nella revisione della letteratura riguardante la miscelazione del chitosano con altri biopolimeri è stata descritta.

Capitolo II, i film attivi a base biologica e doppio strato sono stati sviluppati mediante tecnica solvent casting, usando chitosano e gelatina come biopolimeri, glicerolo come plastificante e etil lauroil arginato (LAE) come composto antimicrobico. I risultati hanno mostrato che i film di miscelazione presentavano una resistenza alla trazione e un modulo elastici più elevati e una permeabilità al vapore acqueo inferiore rispetto ai film a doppio strato ($p<0,05$). I film bilayer hanno dimostrato una efficace barriera contro la luce UV e valori di trasparenza inferiori ($p<0,05$). Gli spettri FT-IR hanno indicato che esistevano interazioni tra chitosano e gelatina a causa di interazioni elettrostatiche e formazione di legami idrogeno. Tuttavia, l'aggiunta di LAE non ha interferito nella struttura della rete. I film attivi contenenti LAE (0,1% v/v) hanno inibito la crescita di quattro patogeni alimentari tra cui L*isteria monocytogenes, Escherichia coli, Salmonella typhimurium* e *Campylobacter jejuni*.

Nel capitolo III, sono stati sviluppati film a base di miscela chitosano-gelatina arricchita con cannella, citronella, chiodi di garofano rosa, noce moscata e oli essenziali di timo (1%, v/v) e le loro proprietà fisiche, ottiche, meccaniche, di barriera all'acqua e microstrutturali sono state valutate per applicazioni di confezionamento alimentare attivo. I risultati hanno confermato le interazioni intermolecolari tra i gruppi funzionali degli oli essenziali con i gruppi idrossile e amminico della rete di film di chitosano-gelatina. L'incorporazione di diversi oli essenziali ha migliorato notevolmente le proprietà di barriera UV. I film sviluppati, con particolare riguardo a quelli integrati con l'olio essenziale di timo, erano efficaci contro i quattro comuni patogeni alimentari testati.

Il capitolo IV si è concentrato sullo sviluppo di film attivi basati sulla miscelazione di biopolimeri naturali (chitosano) e sintetici (polivinilico alcool). Sono stati sviluppati film in miscela di alcool chitosano-polivinilico e LAE, incorporato in questi film a diverse concentrazioni (1-10%, p/p). I risultati hanno mostrato che alti livelli di LAE hanno influenzato negativamente sulle proprietà di barriera meccanica e permeabilità all'acqua. Anche in questo caso film attivi sviluppati erano efficaci contro quattro agenti patogeni alimentari testati.

Il capitolo V rappresenta la conclusione di questa tesi, e presenta una sintesi dei punti salienti dei risultati importanti, ottenuti in questo studio.

Abbreviations and symbols list

a*	Redness value
AFM	Atomic force microscopy
ANOVA	Analysis of variance
ASTM	American society for testing and materials
b*	Yellowness value
BHIA	Brain heart infusion agar
BHIB	Brain heart infusion broth
CS	Chitosan
CS-GL	Chitosan-Gelatin blend
CS/GL	Chitosan/Gelatin bilayer
CS-GL/LAE	Chitosan-Gelatin-Ethyl lauroyl arginate blend
CS/GL/LAE	Chitosan/Gelatin-Ethyl lauroyl arginate bilayer
CS/LAE	Chitosan-Ethyl lauroyl arginate blend
CS-PVA	Chitosan-Polyvinyl alcohol blend
ΔE^*	Total color difference
DDA	Disk diffusion assay
DNA	Deoxyribonucleic acid
E%	Elongation at break
EM	Elastic modulus
EO	Essential oil
FDA	Food and drug administration
EFSA	European food safety authority
FFS	Film-forming solution
ATR/FT-IR	Attenuated total reflectance/Fourier transform infrared
GC-MS	Gas chromatography-Mass spectrometer
GL	Gelatin
L*	Lightness value
GRAS	Generally recognized as safe
LAE	Ethyl lauroyl arginate
Log CFU	Logarithm of colony forming units
LRV	Log reduction value

MC	Moisture content
PLA	Polylactic acid
PVA	Polyvinyl alcohol
PVP	Polyvinylpyrrolidone
RH	Relative humidity
R_a	Roughness value
R_q	Root mean square
RNA	Ribonucleic acid
SD	Standard deviation
SEM	Scanning electron microscopy
TS	Tensile stress
UV	Ultraviolet
UV/Vis	Ultraviolet/Visual light
WC	Water content
WS	Water solubility
WVP	Water vapor permeability
WVTR	Water vapor transmission rate

Chapter 1

Recent advances of chitosan-based films for sustainable food packaging applications – a review

Highlights

- Low mechanical properties and high-water sensitivity represent actual drawbacks.
- Chitosan provides films with additional antioxidants and/or antimicrobial features.
- Blending with other biopolymers is a simple and cost-effective route to improvement.
- Blending success depends on specific miscibility and polymer-polymer interactions.
- Chitosan-based films may replace fossil-based packaging for some applications.

Abstract

Background: The recent sharp increase of sensitivity towards environmental issues and the plastic issue, in particular, has boosted interest towards sustainable alternative packaging materials which would, nevertheless, offer suitable performances to the food. This new trend in the food sector will finally promote the industrial exploitation of the knowledge acquired in the last decades on chitosan-based materials.

Scope and Approach: Chitosan is commercially derived from the deacetylation of chitin. It is the second most abundant polysaccharide in nature behind cellulose and is extensively used due to the unique biological and functional properties. However, inherent drawbacks of chitosan including low mechanical properties and high sensitivity to humidity are causing a major restriction for its industrial applications, in particular for food packaging applications. Blending chitosan with natural and synthetic biopolymers is a simple and efficient method to prevail over these limitations and to

reduce the cost as well. This paper reviews the latest advances in the development of chitosan-based films for their potential application in the food packaging industry.

Key Findings and Conclusions: Blending chitosan with natural and synthetic biopolymers leads to the improvement of microstructural, physical, mechanical and barrier properties depending on the specific miscibility and polymer-polymer components interactions. In addition, chitosan provides antioxidant and/or antimicrobial activities to the films. Blending chitosan with other biopolymers appears to have a bright future for the design of innovative food packaging with bio-functional properties to partially replace existing synthetic plastic packaging materials for some applications.

1. Introduction

Annually, more than 350 million tons of plastics are produced in the world (Ritchie & Roser, 2018). Packaging is one of the largest application fields for plastics. It is expected that plastics will account for 20% of total oil consumption by 2050. Food packaging is represented as a coordinated system for processing, transporting, distributing, retailing, protecting and preserving food to satisfy the consumer demand with optimal cost. The main purpose of food packaging is to possess food in a cost-effective route that satisfies industry demands and consumer desires, retain food safety and protect food from external contamination (Shin & Selke, 2014).

Food packaging can be classified into different levels: the primary packaging is referred to as the package that directly contacts the food; the secondary packaging comprises two or more primary packages and supports the product from physical damage during transportation and storage. The distribution packaging is proposed to protect the product during distribution and to provide adequate handling, while a load unit is a group of distribution packagings that are collected into a single unit for automated approach of large amounts of products (Shin & Selke, 2014).

Plastic durability has raised concerns about post-consumer waste and end-of-life disposal over the years. Accumulation of huge amounts of plastic waste in the environment, and also rapid depletion of fossil reserves and increases in the cost of petroleum, force the food packaging industries toward the development and application of eco-friendly materials such as bioplastics (Arikan & Ozsoy, 2015). Bioplastics can be referred to plastics formed from renewable resources (biobased), plastics that are biodegradable and/or compostable or materials that feature both properties. Hence, not all biobased materials are also biodegradable and not all biodegradable materials are produced from renewable resources (Rujnić-Sokele & Pilipović, 2017). A schematic classification of biodegradable polymers according to their source is presented in Fig. 1.

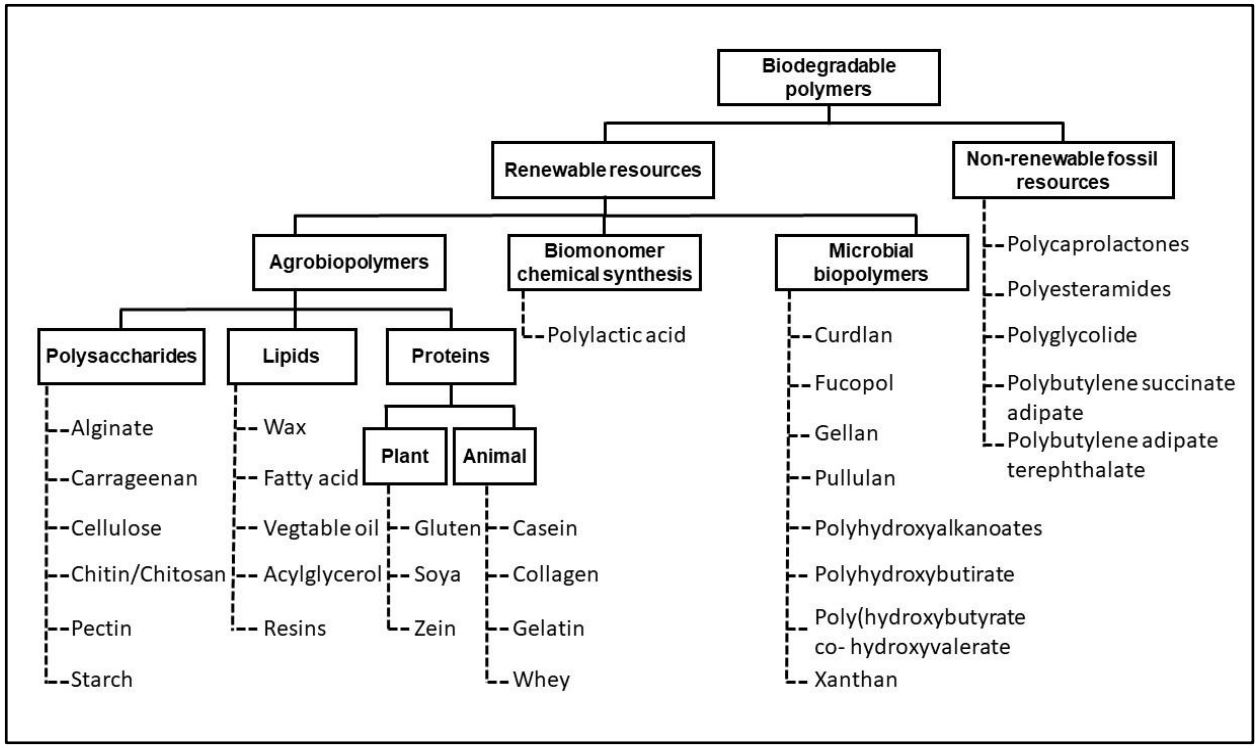

Fig. 1. Schematic classification of biodegradable polymers.

The term “biobased” refers to the derivation of material from biomass. The term “biodegradable” indicates materials that can disintegrate or break down naturally into CO_2, CH_4, H_2O, inorganic compounds, or biomass in which the prevalent process is the enzymatic function of microorganisms (Peelman et al., 2013), that can be

measured by standardized tests (ASTM Standard D-5488-94d). Some of these polymers can also be compostable, which means disintegration occurs in a compost site at a rate consistent with known compostable materials and without releasing toxic substances (Siracusa, Rocculi, Romani, & Rosa, 2008).

As stated by the European Bioplastic Organization, bioplastics constitute approximately 1% of the total global plastics production annually (Rujnić-Sokele & Pilipović, 2017). Packaging, as one of the largest application fields for bioplastics, shares almost 65% of the total bioplastics market. This number is predicted to rise continuously in the upcoming years mainly due to the increasing consumer requirements for sustainable products and growing awareness of environmental impacts (van den Oever, Molenveld, van der Zee, & Bos, 2017).

Bioplastics, whether biobased, biodegradable or both, have unique advantages over conventional plastics including reducing reliance on limited fossil resources, reducing carbon costs and greenhouse gas emissions, increasing resource efficiency and extra waste management or disposal options such as organic recovery (Arikan & Ozsoy, 2015).

Recently, biodegradable polymers derived from renewable resources have been proposed as the future generation of packaging materials. The basic material employed to form biobased films are polysaccharides, proteins, lipids, and their derivatives. Proteins and polysaccharides have acceptable mechanical and gas barrier properties but high sensibility to humidity. On the contrary, lipid films show acceptable water vapor barrier properties, high oxygen permeability but poor mechanical properties (Vodnar, Pop, Dulf, & Socaciu, 2015). Among polysaccharides, chitosan has received considerable attention from academics and industry for food packaging applications owing to its particular physicochemical features, biodegradability, non-toxicity, biocompatibility, good film-forming properties, chemical stability, high

reactivity, also having intrinsic antioxidant and antimicrobial activities against fungi, molds, yeasts, and bacteria (Leceta, Guerrero, & De La Caba, 2013).

The objective of the present review paper is to provide a comprehensive overview of recent advances in the development of chitosan-based films for food packaging applications, highlighting the strategies adopted for the improvement of performances on the basis of the rich literature reviewed.

2. Features and potential of chitosan

Chitosan is a unique natural biopolymer, commercially originated from the deacetylation (to varying degrees) of chitin (Ahmed & Ikram, 2017). It is the second most abundant natural polysaccharide behind cellulose (Fig. 2). Chitin can be obtained from terrestrial arthropods (e.g., spiders, scorpions, beetles, cockroaches, and brachiopods), marine crustaceans (e.g., crab, lobster, prawn, and krill), mollusca (e.g., squid) and microorganisms (e.g. fungi cell walls) (Zargar, Asghari, & Dashti, 2015). The waste of marine food production (particularly exoskeleton of crabs, lobsters, and shrimps) is currently the main industrial source of biomass for chitin production, with approximately 1560 million tons available universally (Gutiérrez, 2017).

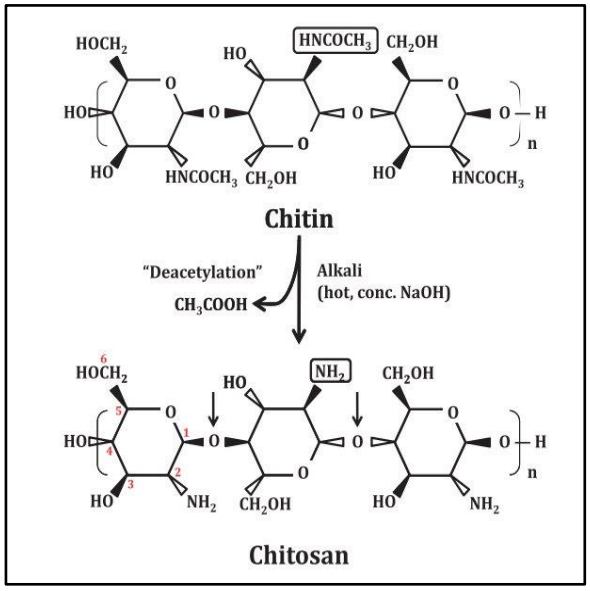

Fig. 2. Chemical structure of chitin and chitosan (adapted from Raafat & Sahl (2009)).

The first report on chitin traces back to 1811 by French Professor of natural history Henri Braconnot. He found out the alkaline-insoluble fraction from mushrooms and named it “fungine”. In 1823, Antoine Odier separated this alkaline-insoluble fraction from the cuticle of insects and named it “chitine”, originated from the Greek word “*khiton*” meaning “tunic” or “envelope”. Twenty years later, Jean Louis Lassaigne proved the presence of nitrogen in chitin. In 1859, Prof. C. Rouget discovered deacylated form of chitin. He treated chitin with concentrated potassium hydroxide solution and heat to become soluble in dilute organic acids and named it “modified chitin” (Rouget, 1859). In 1878, Ledderhose identified that chitin was made of glucosamine and acetic acid. In 1894, Hoppe-Seyler treated the shells of crabs, scorpions, and spiders with potassium hydroxide solution at 180 °C and dissolved the product in dilute acid solution and named it “chitosan”. In 1894, Gilson proved the presence of glucosamine in chitin. In 1930, Rammelberg found more chitin sources apart from insects and fungi. He hydrolyzed chitin in several ways and extracted chitosan from marine arthropods *(*e.g.*,* crab, shrimp, and lobster). In the 1940s, both chitin and chitosan attracted considerable attention as evidenced by about 50 patents. In 1950, the structure of chitosan was discovered using an X-ray device (Darmon & Rudall, 1950). 140 years after Braconnot initial observations*,* the first book about chitosan was published by Albert Glenn Richards in 1951 (Richards, 1951).

Nowadays, chitin and chitosan are simply described as copolymers of *N*-acetyl-D-glucosamine and D-glucosamine units linked with β-(1–4)-glycosidic bonds. They attract considerable attention and are employed worldwide for a broad range of applications. In the food industry, they are applied as antimicrobial (bactericidal and fungicidal) agents, edible films (e.g. controlled respiration rate), additives (e.g., natural flavor extender, emulsifying agents, thickeners, stabilizing agents and color

stabilizers), integrators (e.g., dietary fiber,), and in the purification of water (e.g. removal of dyes) (Ahmed & Ikram, 2017; Zargar et al., 2015).

Chitosan exhibits antioxidant and antimicrobial activity against a broad range of pathogenic and spoilage microorganisms, including fungi (yeasts and molds), Gram-positive and Gram-negative bacteria (van den Broek, Knoop, Kappen, & Boeriu, 2015). The antimicrobial activity of chitosan has drawn attention as a potential natural food preservative (Del Nobile, Di Benedetto, Suriano, Conte, Corbo, & Sinigaglia, 2009; No, Meyers, Prinyawiwatkul, & Xu, 2007). Several hypotheses have been suggested to elucidate the mechanism of antimicrobial activity of chitosan: the most reasonable hypothesis is electro statistic interaction between protonated amino groups (NH_3^+) of glucosamine in the chitosan backbone and microbial negative cell membrane constituents such as phosphoryl groups of the phospholipid components, proteins, amino acids, and various lipopolysaccharides (Elsabee & Abdou, 2013). This interaction affects the membrane integrity and permeability, interfering with energy metabolism and nutrient transport and provoking the permeation of proteinaceous and other intracellular components, causing disruptions that lead to cell death of microorganisms (Elsabee & Abdou, 2013). Another possible mechanism is the interaction of chitosan with cellular DNA of microorganisms, preventing DNA transcription, RNA translation and protein synthesis (Raafat & Sahl, 2009). Moreover, chitosan acts as a chelating agent that selectively binds essential trace metals, spores, prevents the production of toxins and microbial growth (Vodnar et al., 2015). Growth inhibition through blockage of essential nutrient flow has been proposed as another mechanism of action by several researchers (No et al., 2007; Raafat & Sahl, 2009).

3. Strategies for the improvement of properties of chitosan-based films

Inherent drawbacks of chitosan such as high sensitivity to water, low mechanical properties, and high production cost have limited its applications in food packaging

(Elsabee & Abdou, 2013; Li, 2008). Therefore, different strategies have been proposed to tackle these issues and to improve the properties of chitosan-based materials, including chemical cross-linking (Jahan, Mathad, & Farheen, 2016), enzyme treatment (Águila-Almanza, Salgado-Delgado, Vargas-Galarza, García-Hernández, & Hernández-Cocoletzi, 2019), graft copolymerization (Argüelles-Monal, Lizardi-Mendoza, Fernández-Quiroz, Recillas-Mota, & Montiel-Herrera, 2018), complexation (Wang, Wang, & Heuzey, 2016), surface coating (Khwaldia, Basta, Aloui, & El-Saied, 2014), fillers incorporation (Abdelrazek, Elashmawi, & Labeeb, 2010), high-energy irradiation (Shahbazi, Rajabzadeh, & Ahmadi, 2017) and blending with other biopolymers (Wang, Zhang, et al., 2018). Among them, blending chitosan with other polymers, among the plethora of biopolymers available, is a simple and effective way to enhance the barrier and mechanical properties (Campos, Gerschenson, & Flores, 2011). Blending chitosan with other polymers to form a composite film could combine the advantages of the base polymers into a film with higher performances compared with those of each constituent. In order to get an idea of the complexity of the theme and of the work that has been done in the last years, an interrogation of the Web of Science database (performed on 8th November 2019) searching “chitosan, film, blend, food packaging” within title, abstract and keywords has produced 164 records in the timeframe 2015 – 2020. A series of natural and synthetic polymers have been reported to blend with chitosan, such as pectin (Baron, Pérez, Salcedo, Córdoba, & Sobral, 2017), cellulose and its derivatives (Valizadeh, Naseri, Babaei, Hosseini, & Imani, 2019), starch (Ren, Yan, Zhou, Tong, & Su, 2017), gelatin (Bonilla, Poloni, Lourenço, & Sobral, 2018; Guo et al., 2019), soy protein isolate (Li et al., 2017), polyvinyl alcohol (Jahan et al., 2016; Yoon, Kim, Kim, & Je, 2017), polylactic acid (Liu, Wang, Zhang, Lan, & Qin, 2017), etc. In the present study, we have extensively reviewed the scientific literature of the last five years addressing chitosan blend films for food packaging

applications. Nevertheless, for the sake of synthesis, among the very large number of papers available dealing with a wide range of characteristics and functionalities, only the most significant studies and achievements will be analyzed and discussed, in the light of their potential food packaging applications.

4. Chitosan blends

A polymer blend is a compatible or phase-separated mixture of at least two polymers or copolymers, that is produced to enhance the physical properties of each individual component (Cazón & Vázquez, 2019; Khan, Mansha, & Mazumder, 2018). The objective of polymer blending is to develop composite materials in a simple and cost-effective route which would combine the features of components, possibly enhancing their useful attributes and minimizing their drawbacks (Unger, Sedlmair, Siesler, & Hirschmugl, 2014).

The success of polymer blending as a strategy for packaging material improvement relies on the wide range of resulting physical, thermal, mechanical, barrier and optical properties. Therefore, studying these properties is of key importance for the suitable formulation of blends addressed to specific applications (Li, 2008).

The growing interest towards chitosan for packaging applications has resulted in the publication of many studies focusing on the production and investigation of properties of films obtained from chitosan blended with other natural and synthetic biopolymers (Jahan et al., 2016). In this study, we have classified chitosan blends into two main groups, respectively *chitosan-natural biopolymer blends* and *chitosan-synthetic biopolymer blends*. A synopsis of the literature published in the last five years is presented in each subsection considering: type of biopolymer and its concentration, active compounds and other additives incorporated in the blend and the main properties of the blend films addressed for food packaging applications.

4.1. Chitosan-natural biopolymer blends

The functional properties of chitosan-based films can be improved by blending with other natural biopolymers such as polysaccharides, proteins and their derivatives (Cazón & Vázquez, 2019; Elsabee & Abdou, 2013). Compatibility between chitosan and these polymers depends on the ability to associate through electrostatic interaction owing to chitosan cationic character at appropriate pH conditions and the availability of high-polarity groups, such as NH/NH_2, OH, C=O, C-O-C, in its backbone to form intermolecular hydrogen bonds or dipole association with the corresponding functional groups of other biopolymers (Bonilla et al., 2018). It has been reported that polysaccharides such as pectin, starch, alginate, carrageenan, cellulose, and its derivatives can be blended with chitosan. A synopsis of recent advances in chitosan-polysaccharide blend films for packaging applications is presented in Tab. 1.

Table 1. Synopsis of research published between 2015 and 2019 addressing chitosan-polysaccharide blend films for food packaging applications.

Biopolymer	Additives	Key findings	Reference
• Potato starch (4% w/v) • Chitosan (1.5% w/v)	• Citric acid (5, 10, 15, and 20% w/w based on a dry biopolymer basis)	• Citric acid addition into the biopolymers blends improved the tensile strength and elasticity values. • Active films containing citric acid showed a homogenous and compact structure. • Moisture content and water solubility reduced while water vapor permeability, mechanical and antimicrobial properties were improved by addition of citric acid to the biopolymers blend. • Both control and films containing citric acid showed antibacterial activity against *E. coli* and *S. aureus.*	(Wu et al., 2019)
• Hemicellulose (2% w/v) • Chitosan (2% w/v)	• Cellulose nanofiber (5, 10, 15, and 20% w/w based on biopolymers • Glycerol, xylitol, sorbitol (10, 20, 30 and 40% v/w on a dry biopolymer basis	• Adding 5% cellulose nanofiber to the biopolymers blend increased the tensile strength. Films containing glycerol showed better mechanical properties than films containing xylitol and sorbitol. • Films containing glycerol, xylitol, sorbitol showed higher water solubility, barrier properties to water vapor and oxygen, and lower contact angle, and opacity values.	(Xu, Xia, Zheng, Yuan, & Sun, 2019)
• Carboxy methyl chitosan (1% w/v) • Chitosan (2% w/v)	• Nisin (1000 and 6000 IU/mL of film forming solution).	• Blending carboxymethyl chitosan with chitosan increased elasticity while thermal stability reduced. • Incorporation of nisin into the biopolymers blend showed antibacterial activity against *L. monocytogenes.*	(Zimet et al., 2019)
• Starch (1.5% w/v) • Chitosan	• Clove essential oil (3, 6, 9, and 12% w/w)	• Addition of nano titanium dioxide into the biopolymers blend caused an increase in tensile strength and antioxidant activity while	(W. Li et al., 2019)

(1.5% w/v)	• Nano titanium dioxide (1, 3, 5, and 7% w/w)	water vapor permeability, and elasticity decreased. • Addition of clove essential oil into the biopolymers blend reduced tensile strength, water content and water vapor permeability while antioxidant and antibacterial activity against *E. coli,* and *S. aureus* improved.	
• Carboxymethyl cellulose (2% w/v) • Chitosan (1% w/v)	• Cinnamon essential oil (1.5% v/v) • Oleic acid (1% w/v) • Glutaraldehyde (0.01% w/v)	• Addition of glutaraldehyde into the biopolymers blend caused an improvement in mechanical property, water solubility, and water vapor permeability. • Addition of cinnamon essential oil into the biopolymers blend showed antioxidant and antimicrobial activities against *L. monocytogenes* and *P. aeruginosa.* • Addition of cinnamon essential oil and glutaraldehyde at the same time into the biopolymers blend increased the antioxidant and antibacterial activities. • Addition of oleic acid into the biopolymers blend reduced the water solubility, tensile strength, antioxidant and antimicrobial activities while elasticity and water vapor permeability increased.	(Valizadeh, Naseri, Babaei, Hosseini, & Imani, 2019)
• Gum Arabic (1.5% w/v) • Chitosan (1.5%w/v)	• Cinnamon essential oil (8% w/w of total solid)	• Increasing gum arabic proportion in biopolymers blend reduced the thickness, water content, tensile strength, elasticity, and water vapor permeability values. • Addition of cinnamon essential oil into the biopolymers blend showed antioxidant activity.	(Xu, Gao, et al., 2019)
• Corn starch (3% w/v) • Cassava starch (3% w/v) • Chitosan (0.5% w/v)	• Glutaraldehyde (10% w/v based on a dry biopolymer basis)	• Composite films showed antibacterial activity against aerobic mesophilic bacteria.	(Luchese et al., 2018)
• Hardleaf oatchestnut starch (0.5, 2, and 8% w/v) • Chitosan (2% w/v)	• Litsea cubeba oil (4, 8, 12, and 16% w/w, based on biopolymers total weight)	• Blending chitosan and hardleaf oatchestnut (ratio 1:1) caused an increase in tensile strength and an improvement in water vapor permeability. • The incorporation of litsea cubeba oil into the biopolymers blend (ratio 1:1) decreased tensile strength, elasticity, water vapor permeability, water content, and water solubility while contact angle values increased. • Addition of litsea cubeba oil into the biopolymers blend showed antimicrobial activity against *E. coli* and *S. aureus*.	(Zheng et al., 2018)
• Cassava starch • Chitosan (0, 25, 50, 75, 100, and 150 mg chitosan/g starch ratios)	• Gallic acid	• Increasing chitosan proportion in biopolymers blends decreased the moisture content, water activity, water vapor permeability, total phenolic contents, and antioxidant activities. • Blending chitosan and cassava starch postponed the growth of spoilage microorganisms and prolonged the shelf life of cooked ham.	(Zhao, Teixeira, Gänzle, & Saldaña, 2018)
• Burdock root inulin (4% w/v) • Chitosan (2.5% w/v)	• Oregano-thyme essential oils blend (1:1; 1, 1.5, and 2% w/w)	• Water vapor permeability, water-solubility, water content, tensile strength and lightness value of inulin-chitosan films reduced with increasing oregano-thyme essential oils blend. • Addition of oregano-thyme essential oils blend into the biopolymers blend increased the elasticity, opacity, a^*, and b^* values. • Active films containing oregano-thyme essential oils blend showed antioxidant and antibacterial activity against *E. coli, L.*	(Cao, Yang, & Song, 2018)

		monocytogenes, S. aureus, and *S. typhimurium*.	
• Corn starch (5% w/v) • Chitosan (1, 2, 3 and 4% w/v)		• Blending chitosan and corn starch showed an increase in water solubility, total color differences, tensile strength and elasticity, and a reduction in crystallinity, elastic modulus, and water vapor permeability. • Increasing concentration of chitosan in biopolymers blend caused an increase in water vapor permeability and water content values.	(Ren et al., 2017)
• Rice starch (2% w/v) • Chitosan (2% w/v)	• Cranberry, blueberry, beetroot, pomegranate, oregano, pitaya and resveratrol extract (0.5, 2, and 5% w/w based on a dry biopolymer weight)	• Addition of plant extracts into the biopolymers blend improved UV-Vis light barrier properties. • Active films containing beetroot, cranberry, and blueberry extracts showed higher antibacterial activity against *E. coli,* aerobic mesophilic bacteria, and fungi (*P. notatum*, *A. niger*, and *A. fumigatus*).	(Lozano-Navarro et al., 2017)
• Pectin (2% w/v) • Chitosan (2% w/v)		• Increasing pectin proportion in biopolymers blends caused an increase in water solubility, water content and swelling index values. • Increasing chitosan proportion in biopolymers blends caused an increase in tensile strength and reduced elasticity values.	(Baron et al., 2017)
• Tapioca starch (3% w/w) • Chitosan (20, 40, 60, and 80% w/w of dry starch solid weight)		• Increasing chitosan proportion in biopolymers blend up to 60% w/w caused an increase of tensile strength and elastic modulus while elasticity values reduced.	(Shapi'i & Othman, 2016)
• Carboxymethyl cellulose (1% w/v) • Chitosan (2% w/v)	• Zinc oxide nanoparticles (2, 4, and 8 % w/w)	• Incorporation of zinc oxide nanoparticles into the biopolymers blend caused antimicrobial activity against *S. aureus*, *P. aeruginosa*, *E. coli, C. albicans* and prolonged the shelf life of white soft cheese.	(Youssef, El-Sayed, El-Sayed, Salama, & Dufresne, 2016)
• Carboxymethyl cellulose (2% w/v) • Qaternized Chitosan (5% w/v)		• Increasing carboxymethyl cellulose proportion in biopolymers blend caused an improvement in tensile strength, thermostability, and water vapor permeability values while oxygen permeability and opacity values increased. • Increasing carboxymethyl cellulose proportion in biopolymers blend caused a reduction in antibacterial activity against *E. coli* and *S. aureus.* • Higher proportion of quaternized chitosan in biopolymers blends postponed the deterioration of banana fruit.	(Hu, Wang, & Wang, 2016)

Protein-based films from animal source (gelatin, collagen, casein and whey protein) and plant source (soy protein isolate, corn zein, kidney bean protein isolate, quinoa protein, and wheat gluten) have been studied for the development of biodegradable films owing their high abundance, acceptable mechanical properties, excellent gas barrier properties to non-condensable gases (oxygen, carbon dioxide, and nitrogen)

and aromas (Arfat, Ahmed, Hiremath, Auras, & Joseph, 2017). However, these films display a high affinity to water because of the hydrophilic nature of protein molecules (Basta, Khwaldia, Aloui, & El-Saied, 2015; Ma et al., 2012). The chitosan-protein blend film could render better functional properties than single proteins and chitosan film, thus promoting their application in food packaging (Wang, Qian, & Ding, 2018). A synopsis of recent advances in chitosan-protein blend films for packaging applications is presented in Tab. 2

Table 2. Synopsis of research published between 2015 and 2019 addressing chitosan-protein blend films for food packaging applications.

Biopolymer	Additives	Key findings	Reference
• Gelatin (2% w/v) • Chitosan (2% w/v)	• Polyphenols from the fruits of Chinese hawthorn (2, 4, and 6% w/w on the total biopolymer weight)	• Addition of the polyphenol extract into the biopolymers blend increased thickness, tensile strength, elasticity, opacity, and total color difference values while water content, water vapor permeability reduced. • Antioxidant activity of biopolymers blends films significantly improved by increasing concentration of polyphenol extract.	(Kan et al., 2019)
• Gelatin (5% w/v) • Chitosan (3, 6, and 9 % w/w based on gelatin)	• Citric acid (10 and 20% w/w based on gelatin weight)	• Incorporation of citric acid into the biopolymer blend improved elasticity values. • Higher concentration of chitosan and citric acid in biopolymers blend led to better antibacterial activity against *E. coli*.	(Uranga et al., 2019)
• Gelatin (2% w/v) • Chitosan (2% w/v)	• Cinnamon, citronella, pink clove, nutmeg and thyme essential oils (1% w/w based on weight)	• Addition of essential oils into the biopolymers blend improved UV light barrier properties and increased thickness, water content, water vapor permeability, opacity, and total color difference values. • Incorporation of essential oils into biopolymers blend showed antibacterial activity against *C. jejuni*, *E. coli*, *L. monocytogenes,* and *S. typhimurium.*	(Haghighi, Biard, et al., 2019)
• Sheep bone collagen (1.5% w/v) • Skin gelatin (1.5% w/v) • Chitosan (1.5% w/v)		• Addition of chitosan into bone collagen improved transparency and tensile strength of bone collagen film. • Increasing proportion of chitosan upper than 50% in the biopolymers blend improved the elasticity value. • Blending chitosan and bone collagen led to the improvement in UV barrier properties, solubility in water and thermal stability while water barrier permeability increased	(Hou et al., 2019)
• Gelatin (1% w/v) • Chitosan (1% w/v)	• Cinnamon essential oil (0.4% w/w based on a dry biopolymer weight)	• Addition of cinnamon essential oil into the biopolymer blend improved elasticity, thermal stability, water vapor permeability, UV barrier properties, and contact angle values. • Active films containing cinnamon essential oils showed antibacterial activity against *E. coli* and *S. aureus*.	(Guo et al., 2019)
• Collagen (3.5% w/v) • Chitosan (1% w/v)	• Pomegranate peel extract (1, 3, and 5% v/v)	• Addition of 5% pomegranate peel extract into the biopolymers blend caused a reduction in water solubility values and enhanced antibacterial activity against *B. saprophyticus*, *B. subtilis*, *S. typhi,* and *E. coli*.	(Bhuimbar, Bhagwat, & Dandge, 2019)

• Zein (10% w/v) • Chitosan (6 wt%)	• TiO_2 nanoparticles (0.05, 0.1, 0.15, 0.2, and 0.25 % w/w)	• Addition of TiO_2 nanoparticles up to 0.2% into the biopolymers blend enhanced water absorption, water vapor permeability. • Biopolymers blend containing TiO_2 nanoparticles showed antibacterial activity against *S. aureus, E. coli,* and *S. enteritidis.*	(Qu et al., 2019)
• Gelatin (2% w/v) • Chitosan (2% w/v)	• Ethyl lauroyl arginate (0.1% v/v)	• Blending chitosan and gelatin caused an improvement in mechanical and water barrier properties. • Addition of ethyl lauroyl arginate into the biopolymer blend showed antibacterial activity against *C. jejuni*, *E. Coli*, *L. monocytogenes* and *S. typhimurium.*	(Haghighi, De Leo, et al., 2019)
• Gelatin (3% w/v) • Chitosan (1% w/v)	• Gallic acid (1% w/w total dry weight of film) • Tween 80 (50 and 100% w/w based on the weight of the gallic acid • β-cyclodextrin • Ethanol	• Addition of gallic acid into the biopolymers blend increased opacity and elasticity values. • Incorporation of β-Cyclodextrin and gallic acid into the biopolymers blend reduced water barrier properties.	(Rezaee, Askari, EmamDjomeh, & Salami, 2018)
• Gelatin (4% w/v) • Chitosan (1% w/v)	• Eugenol and ginger essential oils (0.5% w/w based on dry biopolymers weight)	• Addition of essential oils into the biopolymers blend improved elasticity and UV barrier properties. • Incorporation of essential oils into biopolymers blend showed significant antioxidant activity.	(Bonilla et al., 2018)
• Gelatin (3% w/v) • Chitosan (1% w/v)	• Procyanidin (0.25, 0.5, 0.75, and 1 mg/mL)	• Addition of procyanidin into the biopolymers blend improved elasticity, water vapor permeability, water solubility, and swelling index and UV barrier properties while tensile strength reduced. • Incorporation of procyanidin into the biopolymers blend showed antioxidant activity and antibacterial activity against *S. aureus* and *E. coli* strains.	(Ramziia, Ma, Yao, Wei, & Huang, 2018)
• Soy protein isolate (2% w/w) • Chitosan (2% w/w)		• Elasticity, thermal stability, and homogeneity of chitosan film increased by blending with soy protein isolate.	(Xing, Zhang, Li, Li, & Shi, 2018)
• Soy protein isolate • Chitosan (1% w/w)	• Cu nanoclusters (20 mmol/L)	• Incorporation of copper nanoclusters into the biopolymers blend improved tensile strength, elasticity, water vapor permeability, contact angle, and thermal stability values.	(K. Li et al., 2017)
• Eggshell membrane gelatin (3% w/v) • Chitosan (1.5% w/v)		• Blending chitosan and gelatin showed an improvement in elasticity, water solubility, and water barrier property values.	(Mohammadi et al., 2018)
• Gelatin (4%w/v) • Chitosan (1% w/w)	• Cinnamon, guarana, rosemary and boldo-do-chile ethanolic extract (1% v/v)	• Increasing chitosan proportion in biopolymers blends improved the mechanical properties and water vapor permeability. • Addition of ethanolic extracts into the biopolymers blend enhanced antioxidant and antibacterial activity against *S. aureus* and *E. coli.*	(Bonilla & Sobral, 2016)
• Gelatin (10% w/v) • Chitosan (2% w/v)	• Boric acid (2, 3, 4, and 5% w/w) • Polyethylene glycol	• Blending chitosan and gelatin showed UV barrier property. • Addition of boric into the biopolymer blend improved tensile strength and water solubility,	(Ahmed & Ikram, 2016)

	(5, 10, and 20% v/v)	moisture content and water vapor permeability values. • Addition of polyethylene glycol into the biopolymers blend caused an increase in elasticity, water content and water solubility.	
• Corn starch (2 and 5% w/v) • Gelatin (2 and 5% w/v) • Chitosan (2% w/v)	• Glycerol and sorbitol (1, 2, 5, and 10% w/w)	• Addition of sorbitol into the chitosan-starch or chitosan-gelatin blend films showed enhancement in water vapor permeability values than films containing glycerol. • Addition of glycerol and sorbitol into the biopolymers blend showed antioxidant activity.	(Badawy, Rabea, & El-Nouby, 2016)
• Quinoa protein (6.7% w/v) • Chitosan (1.5 and 2% w/v) • Chitosan-tripolyphosphate nano particles (0.3 w/v)	• Thymol nanoparticles (0.1% w/v)	• Addition of chitosan-tripolyphosphate nanoparticles into the biopolymers blend improved water vapor permeability. • Chitosan-tripolyphosphate-thymolnanoparticles incorporation into the biopolymers blends enhanced antibacterial activity against *L. innocua*, *S. aureus, S. typhimurium*, *E. aerogenes, P. aeruginosa,* and *E. coli.*	(Caro et al., 2016)
• Gelatin (3% w/v) • Chitosan (2% w/v)	• Red grape seed extract (1 and 2% w/w) • Ziziphora clinopodioides essential oil (1 and 2% w/w)	• Addition of red grape seed extract and ziziphora clinopodioides into the biopolymers blend showed antibacterial activity against *L. monocytogenes*, total mesophilic and psychrotrophic bacteria*, Pseudomonas spp., P. fluorescens, S. putrefaciens,* lactic acid bacteria, and *Enterobacteriaceae* family. • Packing minced rainbow trout fillets with chitosan-gelatin blend enriched with red grape seed extract and ziziphora clinopodioides extend the shelf life at refrigerated condition due to the delay of lipid oxidation and inhibition of bacterial growth.	(Kakaei & Shahbazi, 2016)
• Brewer's spent grain protein (3% w/v) • Chitosan (2% w/v)		• Blending brewer's spent grain protein with chitosan caused an improvement in Water vapor permeability and mechanical properties. Blend films showed antioxidant and antibacterial activity against *S. aureus*, *E. coli*, *L. monocytogenes,* and *S. typhimurium.*	(Lee, Lee, Yang, & Song, 2015)
• Mung bean (vicilin-rich) protein isolate (5 %w/v) • Chitosan (1 %w/v)	• Nisin	• Addition of chitosan into the biopolymer blend improved mechanical properties.	(Huang & Zhang, 2015)

4.2. Chitosan-synthetic biopolymers blends

Blending chitosan with synthetic biopolymers (polyvinyl alcohol - PVA, polyvinyl pyrrolidone - PVP, polylactic acid - PLA, etc.), has been extensively studied for the positive effects on the physical, mechanical and biological features of composite films. The success of synthetic polymers as biomaterials depends on their diverse range of mechanical properties, chemical resistance, and low production costs compared to natural polymers (Bourakadi et al., 2019). Chitosan is potentially miscible with some synthetic biopolymers mainly due to the formation of intermolecular hydrogen bonds

between hydroxyl groups of synthetic polymer and hydroxyl and amine groups of chitosan. Depending on the interactions between polymer components, blending chitosan with synthetic biopolymers can enhance the mechanical and moisture barrier properties of films in some cases. A synopsis of recent advances in chitosan-synthetic biopolymer blend films for packaging applications is presented in Tab. 3.

Table 3. Synopsis of research published between 2015 and 2019 addressing chitosan-synthetic biopolymer blend films for food packaging applications.

Biopolymer	Additives	Key findings	Reference
• PVA (5% w/v) • Chitosan (1% w/v)	• Ethyl lauroyl arginate (1, 2.5, 5, and 10% w/w)	• Addition of ethyl lauroyl arginate into the biopolymers blend had a negative impact on elasticity, tensile strength, and water barrier properties values while barrier properties to the UV light improved. • Chitosan-gelatin blend enriched with ethyl lauroyl arginate exhibited antibacterial activity against *C. jejuni*, *E. coli*, *L. monocytogenes,* and *S. typhimurium.*	(Haghighi et al., 2020)
• Poly(ε-capro-lactone) (6% w/v) • Chitosan (1% w/v)	• Oregano essential oil (1, 3, and 5% w/w)	• Addition of oregano essential oil into the biopolymers blend caused a reduction in tensile strength and elastic modulus while water vapor permeability and elasticity values increased. • Poly(ε-caprlactone)-chitosan blend mats containing 5% oregano essential oil showed antibacterial activity against *S. aureus*, *L. monocytogenes*, *S. enteritidis,* and *E. coli.*	(Hasanpour Ardekani-Zadeh & Hosseini, 2019)
• PVA (2% w/v) • Fish gelatin (2% w/v) • Chitosan (1.5% w/v)		• Increasing fish gelatin proportion in biopolymers blend caused an increase in water vapor permeability, water absorption, and opacity values while water solubility, tensile strength, and elasticity values reduced.	(Ghaderi, Hosseini, Keyvani, & Gómez-Guillén, 2019)
• PVA (4% w/v) • Chitosan (1.25% w/v)	• Thiabendazol-ium-montmorillonite (5% w/w)	• Addition of thiabendazolium into the biopolymers blend caused an increase in tensile strength and elastic modulus values. Chitosan-PVA blend films containing thiabendazolium showed antibacterial activity against *P, aeruginosa, S. aureus,* and *E. coli.*	(Bourakadi et al., 2019)
• PVA (2% w/v) • Chitosan (2% w/v)		• Increasing chitosan proportion in the biopolymer blend caused a reduction in tensile strength and elasticity values while UV barrier properties improved.	(Wu, Ying, Liu, Zhang, & Huang, 2018)
• Microcrystallin e cellulose (3, 4 and 5% w/w) • PVA (2 and 4% w/w) • Chitosan (0.5 and 1% w/w)		• Addition of chitosan-PVA blend into the cellulose-based films caused an improvement in mechanical properties. • Blending chitosan and cellulose improved barrier properties to the UV light. • Addition of PVA into the biopolymers blend caused an improvement in light transmittance values.	(Cazón, Vázquez, & Velazquez, 2018)
• PVA (3% w/v) • Chitosan (1.5% w/v)	• Cellulose nanocrystals from rice straw (1, 3, and 5 % w/w base on polyvinyl alcohol-chitosan blend)	• Addition of cellulose nanocrystals into PVA-chitosan blend improved tensile strength and thermal properties. • PVA-chitosan blend films enriched with cellulose nanocrystal from rice straw showed antifungal activity against *C. gloeosporioides* and antibacterial activity against *S. mutans*, *S.aureus*, *E.coli,* and *P.aeruginosa.*	(Perumal, Sellamuthu, Nambiar, & Sadiku, 2018)

• PVA (1% w/v) • Chitosan (2% w/v)	• SiO_2 (0.3, 0.6, and 0.9 %w/w)	• Addition of silicon dioxide into the biopolymers blend caused an enhancement in mechanical, water and oxygen barrier properties.	(Yu, Li, Chu, & Zhang, 2018)
• PVA (10 %w/v) • Chitosan (2, 2.5, 3, and 3.5% w/v)		• In comparison to neat PVA film, blending PVA and chitosan caused an improvement in elasticity and oxygen barrier properties while water barrier propertied decreased. Increasing proportion of chitosan in biopolymer blend showed better antibacterial activity against *S. aureus* and *E. coli.*	(Liu, Wang, & Lan, 2018)
• PVA (2% w/v) • Chitosan (2% w/v)	• Sulfosuccinic acid (5, 10, 15, 20, and 30 wt%) • Glycerol (0-60 wt%) • Xylitol (0-60 wt%) • Sorbitol (0-60 wt%)	• Addition of sulfosuccinic acid int the biopolymer blend caused an enhancement in tensile strength, elasticity, swelling degree, water-solubility, thermal stability, and optical properties.	(Yun, Lee, Kim, & Yoon, 2017)
• PVA (1% w/v) • Chitosan-gallic acid (0.1, 0.5, and 1 % w/v)		• Increasing chitosan-gallic acid concentration into the biopolymers blend and UV treatment caused an increase in tensile strength while elasticity reduced. • Films containing chitosan-galic acid (1% w/v) showed antibacterial activity against *E. coli*, *S. typhimurium*, *S. aureus,* and *B. cereus.*	(Yoon et al., 2017)
• PVA (5% w/v) • Sodium lactate loaded chitosan (2% w/v)	• Montmorillonite (0, 5, 10, 15, and 20 % w/w, based on the dry weight of CS/PVA)	• Increasing montmorillonite concentration up to 15% in biopolymers blend improved tensile strength and elastic modulus while elasticity values reduced. • Addition of montmorillonite into the biopolymer blend enhanced barrier properties to water vapor, oxygen and carbon dioxide. Blend films showed antibacterial activity against *E. coli*.	(Zhang et al., 2017)
• PVA (5% w/v) • Chitosan (0.15% w/w)	• Carvacrol (5% w/v) • Cellulose nanocrystals (3% w/w)	• Addition of carvacrol and cellulose nanocrystal into the biopolymer blend caused an improvement in mechanical properties while color and transparency value not affected. • Blend films showed antioxidant activity and antibacterial activity against *P. carotovorum* subsp. *odoriferum,* and *X. axonopodis*.	(Luzi et al., 2017)
• PVA (2% w/v) • Chitosan (2% w/v)		• Increasing proportion of PVA in the biopolymer blend caused an increase in tensile strength and elasticity. • Increasing proportion of chitosan in biopolymer blend improved antioxidant activity and antibacterial activity against *S. aureus*, *B. cereus M. luteus*, *S. enterica*, *E. coli,* and *S. typhimurium.*	(Hajji et al., 2016)
• PVA (10, 20 and 30 % w/w) • Montmorillonite (5 %w/v) • Chitosan (2% w/v)		• Addition of PVA into the biopolymers blend caused a plasticizing effect and increased the plasticity while tensile strength reduced. In addition, barrier properties to water and oxygen improved. • Incorporation of montmorillonite into the biopolymer blend enhanced the mechanical and antimicrobial activities while barrier properties to water and oxygen reduced.	(Giannakas et al., 2016)
• EVOH (4% w/v) • Chitosan	• Nano zinc oxide (1 and 2 %w/w)	• Addition of nano zinc oxide into the biopolymers blend caused an improvement in barrier properties against water vapor and oxygen. • Presence of chitosan and nano zinc oxide caused excellent antibacterial and antibacterial activities against *A. niger* and *E.coli*. Adding	(Sadeghi & Shahedi, 2016)

		nano zinc oxide improved barrier, mechanical and antimicrobial properties	
• PVA • Chitosan (1% w/v)	• Potassium nitrate (0.1, 0.2, 0.3, 0.4, and 0.5 % w/w)	• Addition of potassium nitrate into the biopolymers blend caused an improvement in tensile strength and elasticity values owing to its crosslinking effect. • The degradation behavior can be improved with addition of potassium nitrate.	(Jahan et al., 2016)
• PLA (1% w/v) • Chitosan (1% w/v)	• Methyldiphenyl diisocyanate (0.2, 1, 2, and 3 % w/w of the final PLA/chitosan solution)	• Increasing concentration of methyldiphenyl diisocyanate in biopolymers blends caused an improvement in tensile strength and contact angle values.	(Gartner, Li, & Almenar, 2015)

5. Conclusions

Application of conventional packaging materials such as synthetic plastics and their derivatives cause severe environmental issues that label food industry as a source of pollution and social concern. The adoption of chitosan as packaging material could contribute to mitigating the environmental concern, despite some drawbacks in terms of thermal stability, barrier and mechanical properties, and production costs. Blending chitosan with other natural and synthetic polymers is an effective way to improve these limitations and to reduce costs. Thus, this approach appears to have a bright future for innovative food packaging design since it will allow the partial replacement of the existing synthetic plastic packaging materials presently available in the market.

Chapter 2

Comparative analysis of blend and bilayer films based on chitosan and gelatin enriched with Ethyl Lauroyl Arginate (LAE) with antimicrobial activity for food packaging applications

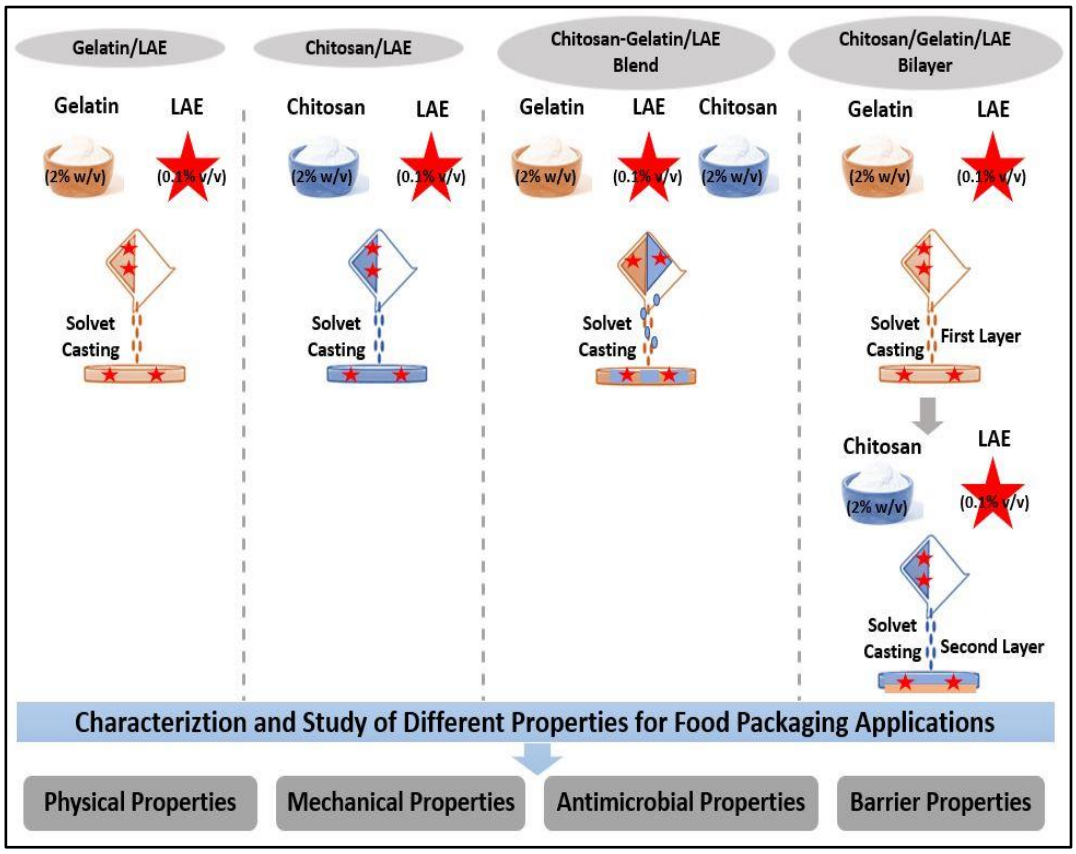

Highlights

- Blend and bilayer active films based on chitosan and gelatin were developed.
- Physical, mechanical, barrier and antimicrobial properties of films were characterized.
- Potential interaction between chitosan and gelatin was confirmed by FT-IR analysis.
- Films enriched with LAE showed a bactericidal effect against common food pathogens.

Abstract

Blend and bilayer bio-based active films were developed by solvent casting technique, using chitosan (CS) and gelatin (GL) as biopolymers, glycerol as a plasticizer and ethyl lauroyl arginate (LAE) as an antimicrobial compound. Blend films had higher tensile strength and elastic modulus and lower water vapor permeability than bilayer films ($p<0.05$). Bilayer films demonstrated as effective barriers against UV light and showed lower transparency values ($p<0.05$). FT-IR spectra indicated that interactions existed between CS and GL due to electrostatic interactions and hydrogen bond formation. However, the addition of LAE did not interfere in the network structure. Active films incorporated with LAE (0.1%, v/v) inhibited the growth of *Listeria monocytogenes, Escherichia coli, Salmonella typhimurium,* and *Campylobacter jejuni*. This study highlighted the development of blend and bilayer bio-based active films based on CS and GL enriched with LAE for food packaging applications with improved physical, mechanical, barrier and antimicrobial properties.

1. Introduction

The market for active packaging as a part of smart packaging technologies is expected to have a promising future due to the consumer's preference for safe and high-quality food (Musso, Salgado, & Mauri, 2017). In this context, active films based on renewable natural biopolymers such as polysaccharides, proteins, and lipids enriched with natural antimicrobial substances have received considerable attention in recent years in the food packaging industry. Bio-based active films have emerged as alternatives to traditional synthetic packaging due to their biocompatibility with human tissues, biodegradability and environmentally friendly properties (Poverenov, Rutenberg, Danino, Horev, & Rodov, 2014; Souza et al., 2017; Staroszczyk, Sztuka, Wolska, Wojtasz-Pająk, & Kołodziejska, 2014). They can improve food shelf life and quality by providing a barrier to protect the food from mechanical damage, reducing moisture

loss, oxidation rate, and respiration. Moreover, they have this potential to act as effective carriers of active compounds such as antimicrobials and antioxidants (Ponce, Roura, del Valle, & Moreira, 2008).

Among many natural biopolymers that can be used to form edible films, chitosan and gelatin have been proven to exhibit excellent film-forming properties, stability, flexibility, biocompatibility, biodegradability, non-toxicity and commercial availability (Cardoso et al., 2016; Qiao, Ma, Zhang, & Yao, 2017).

Chitosan is a linear polysaccharide, commercially obtainable as a seafood by-product from the deacetylation of chitin, which is the major constituent of the exoskeleton of crustaceans such as crab and shrimp. Chitosan is categorized as GRAS (generally recognized as safe) by U.S. Food and Drug Administration in 2005 (FDA, 2005a). According to the European Union regulation (No. 749/2012) in 2007, it has been approved for use as a food supplement for human consumption in Europe. This polycationic biopolymer is soluble in low-pH solutions due to the protonation of the amino group (Bonilla & Sobral, 2016). In conjunction with its cationic character, several studies have reported the wide inhibition spectrum of chitosan against yeasts, molds, Gram-positive and Gram-negative bacteria (Bellich, D'Agostino, Semeraro, Gamini, & Cesàro, 2016; Elsabee & Abdou, 2013; Leceta, Guerrero, & De La Caba, 2013). However, these beneficial characteristics are counterbalanced by limitations such as thermal stability, high water vapor permeability and ultraviolet (UV) degradation which restrict chitosan application in food packaging (Ahmed, Mulla, Arfat, & Thai T, 2017). Barrier and mechanical properties of chitosan films can be improved by blending or laminating with protein-based biopolymers to combine the advantages of these two biopolymers as well as to minimize their disadvantages (Galus & Kadzińska, 2015; Pereda, Ponce, Marcovich, Ruseckaite, & Martucci, 2011; Poverenov, Rutenberg, Danino, Horev, & Rodov, 2014; Ramos, Valdés, Beltrán, & Garrigós, 2016). Protein-

based films generally have impressive gas barrier properties compared to polysaccharide films and their mechanical properties are also better due to their unique structure and high intermolecular binding potential (Benbettaïeb, Kurek, Bornaz, & Debeaufort, 2014). Protein films have multiple sites for chemical interaction as a function of their diverse amino acid functional groups, which can allow for property improvement (Dangaran, Tomasula, & Qi, 2009)

Gelatin is a natural water-soluble protein, obtainable from the partial hydrolysis of collagen (Ramos, Valdés, Beltrán, & Garrigós, 2016). Gelatin consists of different amino acids and therefore has amphoteric properties. It can easily absorb UV light due to the presence of aromatic amino acids (Ahmed & Ikram, 2016). Since gelatin and chitosan are hydrophilic biopolymers with good affinity and compatibility, they are expected to form composite films (blend or bilayer) with improved properties. Negatively charged amino acids on gelatin macromolecular chains have the potential to interact electrostatically with positively charged chitosan to form blend or bilayer films (Poverenov, Rutenberg, Danino, Horev, & Rodov, 2014). In this context, the hydroxyl, amine and also carboxyl groups of gelatin are capable of forming hydrogen bonds with hydroxyl and amine groups of chitosan (Staroszczyk, Sztuka, Wolska, Wojtasz-Pająk, & Kołodziejska, 2014).

Active packaging or enrichment of packaging materials with certain additives is an innovative concept to improve food safety and quality (Gaikwad, Lee, Lee, & Lee, 2017). The capacity to release the active compound in a progressive way is an obvious advantage over conventional packaging systems in which the full amount of active agent is added in the food formulation (Pezo, Navascués, Salafranca, & Nerín, 2012). Ethyl lauroyl arginate (LAE) is considered as one of the most potent antimicrobial substances among novel food additives with strong and fast antimicrobial properties against foodborne pathogens in direct contact with them (Becerril, Manso, Nerin, &

Gómez-Lus, 2013). The incorporation of LAE into edible films can provide the films with activity against food pathogens and spoilage microorganisms including bacteria, yeasts, and molds to extend shelf life and quality of food. LAE acts as a cationic surfactant on the cytoplasmic membrane of microorganisms and inhibits the growth of microorganisms without causing cell lysis (Muriel-Galet, Carballo, Hernández-Muñoz, & Gavara, 2016). LAE has been evaluated for food safety as an antimicrobial compound by the U.S. Food and Drug Administration (FDA, 2005b) and as a food preservative by the European Food Safety Authority (EFSA, 2007). This compound has been classified as GRAS at concentrations up to 200 ppm, since it is hydrolyzed in the human body by chemical and metabolic pathways and quickly broken into its natural components such as lauric acid, L-arginine and ethanol (Asker, Weiss, & McClements, 2009). Incorporation of LAE as an antimicrobial compound into packaging films has been reported in several studies (Moreno, Gil, Atarés, & Chiralt, 2017; Muriel-Galet, Carballo, Hernández-Muñoz, & Gavara, 2016; Rubilar, Candia, Cobos, Díaz, & Pedreschi, 2016). However, limited information is available concerning the enrichment of chitosan and gelatin blend and bilayer films with LAE. Thus, the main objective of this study was to develop blend and bilayer active films based on chitosan and gelatin enriched with LAE to assess their physical, mechanical and barrier properties that are relevant for food packaging applications. Moreover, the antimicrobial activity of the films was tested against common pathogenic bacteria.

2. Material and methods

2.1. Materials and reagents

Chitosan (CS) with a molecular weight of 100-300 kDa was obtained from Acros Organics™ (China). Gelatin (GL) with bloom 128 - 192° was purchased from AppliChem GmbH (Darmstadt, Germany). Glycerol (≥ 99.5%) was purchased from Merck (Darmstadt, Germany). Acetic acid was obtained from Brenntag S.p.A (Milan,

Italy). Ethyl lauroyl arginate (LAE) was provided as Mirenat® - G (90% glycerol, 10% LAE) by Vedeqsa (Terrassa, Barcelona, Spain). Brain heart infusion agar (BHIA) was purchased from Biolife (Milan, Italy).

2.2. Preparation of film-forming solutions and films

Preparation of films was adapted from Pereda, Ponce, Marcovich, Ruseckaite, & Martucci (2011) with slight modifications. Eight different types of films were analyzed in this study. Four control films (without LAE) based on the chitosan (CS), gelatin (GL), chitosan-gelatin blend (CS-GL) and chitosan/gelatin bilayer (CS/GL) and four active films based on the same formulations enriched with LAE (CS/LAE, GL/LAE, CS-GL/LAE blend and CS/GL/LAE bilayer). All film-forming solutions (FFSs) with and without LAE were prepared separately. CS solution (2%, w/v) was prepared by dissolving CS in an acetic acid solution (1%, v/v) under continuous stirring at room temperature for 2 h. GL solution (2 %, w/v) was prepared by dissolving GL in distilled water under continuous stirring at 55 °C for 15 min. Glycerol (0.9 g/g GL or CS) was then added as a plasticizer into both FFS that was stirred for an additional 30 min. CS-GL blend solution was prepared by mixing the same volume of CS (2%, w/v) FFS and GL (2%, w/v) FFS, respectively. CS/GL bilayer consisted of two separates FFS of GL and CS prepared as previously described. The first layer was cast from FFS of GL and dried at 25 ± 2 °C overnight. Then, a second layer was cast from the FFS of CS which was kept at 25 ± 2 °C the night before. Moreover, LAE (0.1%, v/v) was added to each FFS which was stirred at 35 °C for an additional 30 min to obtain active films (Rubilar, Candia, Cobos, Díaz, & Pedreschi, 2016). All FFSs were degasified with a vacuum pump (70 kPa) for 15 min to remove bubbles in the solution. Films were obtained by casting 20 mL of the FFS into Petri dishes (14.4 cm in diameter) and dried at 25 ± 2 °C overnight in the chemical hood at an ambient relative humidity (RH) of 45%.

2.3. Scanning electron microscopy (SEM)

Scanning electron microscopy (SEM) from cross-section images of the films were obtained with the use of a scanning electron microscope (FEI, Quanta 200, Oregon, USA). Film samples were fixed on a stainless-steel support with a double side conductive adhesive. The analysis was conducted in a low vacuum (0.6 Torr) at an acceleration voltage of 20 kV.

2.4. Attenuated Total Reflectance (ATR)- Fourier Transform Infrared (FT-IR) Spectroscopy

The infrared spectra of different films were obtained using an ATR-FT-IR spectrometer (type Alpha, Bruker Optik GmbH, Ettlingen, Germany). Spectra were collected from two different locations from the top and bottom of the same samples in the 4000 - 400 cm^{-1} wavenumber by accumulating 64 scans with a spectral resolution of 4 cm^{-1}.

2.5. Thickness

Film thickness was measured with a digital micrometer (Model CDJAAB15, Borletti-LTF S.p.A., Antegnate, Bergamo, Italy) at five different random positions (one at the center and four on the edges). The means of these five separate measurements were recorded.

2.6. Mechanical properties

The tensile stress (TS), elongation at break (E%) and elastic modulus (EM) were determined using a dynamometer (Z1.0, Zwick/Roell, Italy) according to ASTM standard method D882 (ASTM, 2001a). The films with known thickness were cut into rectangular strips (9 x 1.5 cm^2). The initial grip separation and cross-head speed were set at 70 mm and 50 mm/min, respectively. The measurements were repeated 18 times. The software TestXpert® II (V3.31) (Zwick/Roell, Ulm, Germany) was used to record the TS curves. TS was calculated by dividing the maximum load to break the film by the cross-sectional area (thickness) of the film and expressed in MPa. E% was

calculated by dividing film elongation at rupture by the initial grip separation expressed in percentage (%). EM was calculated from the initial slope of the stress-strain curve and expressed in MPa.

2.7. UV barrier, light transmittance and transparency value

Films were cut into square stripes (2 x 2 cm^2). The barrier properties of films against UV and visible light were determined at the UV (200, 280 and 350 nm) and visible (400, 500, 600, 700 and 800 nm) wavelengths, using a Jasco V – 550 UV/Vis spectrophotometer (Jasco Corporation, Tokyo, Japan). The transparency of the films was calculated by Eq. (1):

$$\text{Transparency value} = \frac{-\log T_{600}}{x} \quad (1)$$

where T_{600} is the fractional transmittance at 600 nm and x is the film thickness (mm). The greater transparency value represents the lower transparency of the film.

2.8. Color

The color of films was measured with a CR-400 Minolta colorimeter (Minolta Camera, Co., Ltd., Osaka, Japan) at room temperature, with D65 illuminant and 10° observer angle. The instrument was calibrated with a white standard (L* = 99.36, a*= -0.12, b* = -0.07) before measurements. Results were expressed as L* (luminosity), a* (red/green) and b* (yellow/blue) parameters. The total color difference (ΔE^*) was calculated using the following Eq. (2):

$$\Delta E^* = \sqrt{[(\Delta L^*)^2 + (\Delta a^*)^2 + (\Delta b^*)^2]} \quad (2)$$

where ΔL^*, Δa^* and Δb^* are the differences between the corresponding color parameter of the samples and that of a standard white plate used as the film background. For each film, five readings were taken at different points and the average values were determined from the top and bottom sides.

2.9. Moisture content and water solubility

Moisture content (MC) of the films was determined by measuring the weight loss of film upon drying in an oven at 105 ± 2 °C for 24 h according to the following Eq. (3):

$$MC\ (\%): \frac{Mw-Md}{Mw} \times 100 \quad (3)$$

Where Mw is the initial weight (g) of the film and Md is the dry weight (g) of the film. Triplicate tests of MC were conducted for each type of film and an average was taken as the result.

The solubility of films (2 × 2 cm^2) in water was determined by drying to constant weight in an oven at 105 ± 2 °C (Wi) and then each film was immersed in 50 mL distilled water at 25 °C. After 24 h, the film samples were dripped and dried to constant weight at 105 ± 2 °C (Wf) to determine the weight of dry matter which was not solubilized in water. The measurement of water solubility (WS) was determined according to the following Eq. (4):

$$WS\ (\%): \frac{Wi-Wf}{Wi} \times 100 \quad (4)$$

where Wi is the initial weight (g) of the film and Wf is the final weight (g) of the film.

2.10. Water vapor transmission rate and water vapor permeability

Water vapor transmission rate (WVTR) and water vapor permeability (WVP) of the films was determined gravimetrically in triplicate according to the ASTM E96 method (ASTM, 2001b) with some modifications. Films were sealed on top of glass test cups with an internal diameter of 10 mm and a depth of 55 mm filled with 2 g anhydrous $CaCl_2$ (0% RH). The cups were placed in an environmental chamber at 45 °C and 75% RH. A fan located inside the chamber was used to move the internal air ensuring uniform conditions at all test locations. WVTR was determined using the weight gain of the cups and was recorded and plotted as a function of time. Cups were weighed daily for 7 days to guarantee the steady-state permeation. The slope of the mass gain

versus time was obtained by linear regression ($r^2 \geq 0.99$). WVTR (g/day m^2) and WVP (g mm/kPa day m^2) were calculated according to the following Eqs. (5) and (6):

$$WVTR = \frac{\Delta W}{\Delta t \times A} \quad (5)$$

$$WVP = \frac{WVTR \times L}{\Delta P} \quad (6)$$

where $\Delta W/\Delta t$ is the weight gain as a function of time (g/day), A is the area of the exposed film surface (m^2), L is the mean film thickness (mm) and ΔP is the vapor pressure difference across the film (kPa), calculated based on the chamber temperature and the relative humidity inside and outside the cup

2.11. In vitro antimicrobial activity

Antibacterial activity of films assessed against four typical food bacterial pathogens including *Listeria monocytogenes* (UNIMORE 19115), *Escherichia coli* (UNIMORE 40522), *Salmonella typhimurium* (UNIMORE 14028) and *Campylobacter jejuni* (UNIMORE 33250) using the disk diffusion assay according to Pereda, Ponce, Marcovich, Ruseckaite, & Martucci (2011). Films (sterilized with UV light) were cut into a disc shape (15 mm diameter) and placed on the surface of BHIA agar plates, which had been previously seeded with 0.1 mL of inocula containing 10^6 CFU/mL of tested bacteria. The plates were then incubated at 30 °C for 24 h (*C. jejuni* plates were incubated at 37 °C). The diameter of the inhibition zones (mm) was measured with a caliper. All tests were performed in triplicates.

2.12. Statistical analysis

The statistical analysis of the data was performed through analysis of variance (ANOVA) using SPSS statistical program (SPSS 20 for Windows, SPSS INC., IBM, New York). The differences between means were evaluated by Tuckey's multiple range test ($p<0.05$). All tests were repeated three times. The data were expressed as the mean ± SD (standard deviation).

3. Results and discussion

3.1. Microstructural properties

The microstructural properties of the edible films depend on the compatibility and miscibility between film components, which affects the final physical, mechanical, barrier and optical properties (Acosta, Jiménez, Cháfer, González-Martínez, & Chiralt, 2015). SEM images of the control (without LAE) and active films (with LAE) based on Chitosan (CS), Gelatin (GL), CS-GL blend and CS/GL bilayer are displayed in Fig. 1.

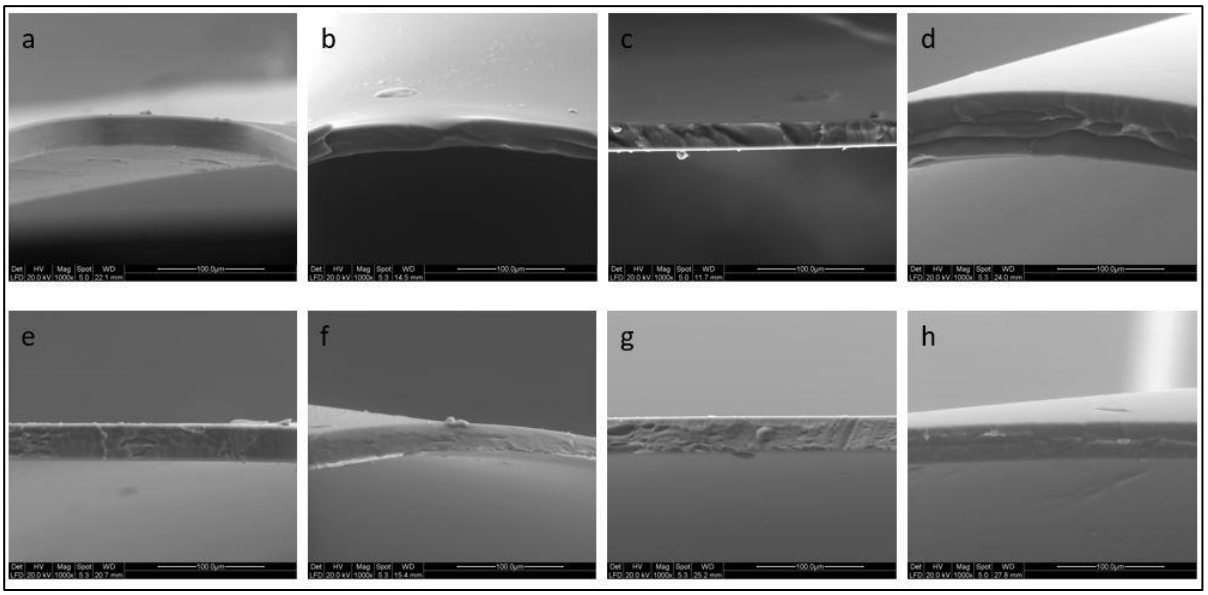

Figure 1. SEM images on cross-sections of films based on a: chitosan, b: gelatin, c: chitosan-gelatin blend, d: chitosan/gelatin bilayer, e: chitosan/LAE, f: gelatin/LAE, g: chitosan-gelatin/LAE blend, h: chitosan/gelatin/LAE bilayer.

The SEM images indicated that both CS and GL films were homogeneous (Fig. 1a and b). The SEM image of CS-GL blend showed dense, homogeneous and compact structures without discontinuous or porous structures (Fig 1c). Phase separation could not be detected in CS-GL blend indicating high compatibility and homogeneity between CS and GL due to associative interactions (Galus & Kadzińska, 2015). This represents excellent structural integrity for CS-GL blend. The SEM image of CS/GL bilayer film revealed sheets stacked in layers (Fig. 1d). Interactions could take place at the interface of the bilayer film, increasing the bonding strength between layers which prevent manual peeling of single film components (Pereda, Ponce, Marcovich,

Ruseckaite, & Martucci, 2011). Active films enriched with LAE revealed some holes, porous and free spaces (Fig. 1e, f, g, and h). The SEM image of GL/LAE film showed a smoother structure than other active films (Fig. 1f). This might be due to the good dispersion of LAE as a cationic surfactant inside the GL film-forming solution (Rubilar, Candia, Cobos, Díaz, & Pedreschi, 2016).

3.2. Attenuated Total Reflection (ATR) / Fourier-Transform Infrared (FT-IR) Spectroscopy

The FT-IR spectra of the control and active films based on CS, GL, CS-GL blend and CS/GL bilayer recorded in the wavenumber range of 4000 - 400 cm^{-1} are shown in Fig. 2. The characteristic band at 1631 cm^{-1} (amide-I) in the GL film spectrum is primarily due to the ν(C=O) stretching vibration (Fig. 2a). This amide-I band is the most sensitive spectral signal to characterize protein secondary structure (Jridi et al., 2013). Proteins with predominantly β-sheet structure exhibit amide-I bands between 1630 - 1640 cm^{-1} (Jackson & Mantsch, 1995). A strong peak at 1631 cm^{-1} may be taken as evidence of the presence of a significant amount of β-sheet secondary structures in GL film. The peak at 1545 cm^{-1} corresponds to a combination band of the ν(C-N) stretching and δ(N-H) bending vibrations (amide-II) and the low-intensity band at about 1237 cm^{-1} (amide III) has been assigned to another coupled vibration of the –CONH- functionality. The band situated around 1034 cm^{-1} can be assigned to a ν(C-O) stretching vibration and could be related to possible interactions arising between plasticizer (hydroxyl group of glycerol) and film structure. The absorption band at 3291 cm^{-1} corresponds mainly to the ν(N-H) stretching vibration of hydrogen-bonded N-H functionalities. The band doublet at about 2930/2870 cm^{-1} can be assigned to antisymmetric and symmetric, respectively, $\nu_{as}(CH_3/CH_2)$/$\nu_s(CH_3/CH_2)$ stretching vibrations of CH_3 and CH_2 functionalities. Similar spectra for GL film have been reported by Qiao, Ma, Zhang, & Yao, (2017) and Wu, Sun, Guo, Ge & Zhang, (2017).

CS (Fig. 2b) shows bands at 1655 and 1586 that can be assigned to the amide-I and amide-II bands of the residual acetamide structures, respectively. Peaks at 853, 926, 990, 1026 and 1152 cm^{-1} can be assigned to saccharide structures (Bonilla, & Sobral, 2016). The broad band between 3600 and 3000 cm^{-1} is composed of ν(OH), ν(NH) and $\nu_{as}(NH_2)/\nu_s(NH_2)$ vibrational contributions.

The band doublet at about 2921/2870 cm^{-1} corresponds to $\nu_{as}(CH_3/CH_2)$/ $\nu_s(CH_3/CH_2)$ vibrations. The band at 1377 cm^{-1} is assigned to acetamide groups, which indicates that CS is not totally deacetylated (Leceta, Guerrero, Ibarburu, Dueñas & De La Caba, 2013).

If two polymers are compatible, the IR spectrum of the blends should differ from the spectra of the individual components by band shifts and intensity changes depending on the degree of chemical interactions. Analysis of FT-IR spectrum of CS-GL blend film (Fig. 2c) revealed a slight shift of the ν(N-H) band to 3289 cm^{-1} which indicates the formation of additional intermolecular hydrogen bonds between CS and GL. Moreover, the amide-I band shifted from 1631 cm^{-1} to 1638 cm^{-1} in the blend. This change can be interpreted as a conformational change of the secondary structure of GL. The amide-II peak slightly shifts from 1545 to 1550 cm^{-1} in the blend and indicates the formation of further hydrogen bonds. Furthermore, the shift of the amide-II peak of CS from 1586 to 1550 cm^{-1} confirms the presence of the electrostatic interactions between the carboxyl groups of GL and amino groups of CS (Qiao, Ma, Zhang, & Yao, 2017). Thus, our spectroscopic data suggest that blending CS and GL resulted in the conformational and hydrogen bonding changes in the GL polypeptide structure. Similar results were reported by Mohammadi et al., (2017).

Due to the limited penetration depth (only a few micrometers) of infrared radiation into the sample in the ATR/FT-IR measurement geometry, the spectra measured from the

bottom- and the top-side of the CS/GL bilayer films (Fig. 2d and 2e) showed exactly the spectral characteristics of the individual components.

Active films enriched with LAE showed similar major bands as the control films indicating that their structural characteristics were not significantly influenced by the incorporation of LAE. The absence of changes in the intensities and positions of the major CS and GL bands suggest a low interfacial interaction between these biopolymers and the LAE. Similar results were reported by Gaikwad, Lee, Lee, & Lee, (2017) and Rubilar, Candia, Cobos, Díaz, & Pedreschi, (2016).

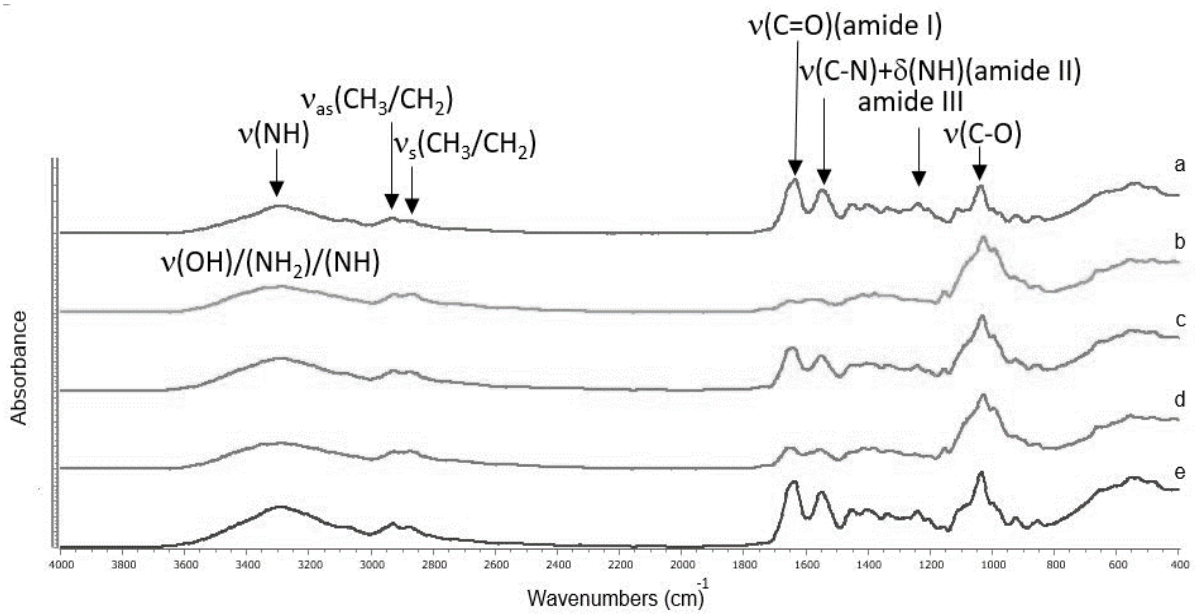

Figure 2. ATR-FT-IR spectra of active films based on a: gelatin/LAE, b: chitosan/LAE, c: chitosan-gelatin/LAE blend, d: chitosan/gelatin/LAE bilayer (top layer) and e: chitosan/gelatin/LAE bilayer (bottom layer).

3.3. Thickness

The thickness of control and active films based on CS, GL, CS-GL blend and CS/GL bilayer is shown in Tab. 1. In this study, control and active films based on the CS, GL, and CS-GL blend were obtained by casting the same volume of film-forming solution (FFS) onto Petri dishes while control and active films based on the CS/GL bilayer were obtained by two-step casting method. Thus, the thickness of control and active CS/GL bilayer films were higher than other films ($p<0.05$). The incorporation of LAE did not influence the thickness ($p>0.05$). This could be due to the low amount of LAE (0.1%,

v/v) incorporated into active films which was not sufficient to significantly increase the average thickness. Similar results were reported by Rivero, García, & Pinotti (2009) and Poverenov, Rutenberg, Danino, Horev, & Rodov (2014).

3.4. Mechanical properties

Mechanical properties including tensile strength (TS), elongation at break (E%) and elastic modulus (EM) of control and active films based on CS, GL, CS-GL blend and CS/GL bilayer are presented in Tab. 1. The mechanical properties of films represent their ability to keep the integrity and endure external stress during the processing, subsequent transportation, handling and storage of the packaged materials. Sufficient mechanical strength and extensibility are generally required for food packaging applications (Ahmed, Mulla, Arfat, & Thai T, 2017; Jridi et al., 2014). Our results showed that TS, E%, and EM were not affected by the addition of LAE into the films ($p>0.05$). This might be due to the low amount of active compound incorporated into the films.

The TS of control and active CS films (21 and 22.8 MPa, respectively) showed higher values than control and active GL film (8.9 and 09.3 MPa, respectively) ($p<0.05$). This is in agreement with other studies that demonstrated GL film is brittle and susceptible to cracking due to the strong cohesive energy density of the polymer (Jridi et al., 2014; Rivero, García, & Pinotti, 2009). The TS of control and active CS-GL blend films (both 31.9 MPa) showed higher values than bilayer and single component films ($p<0.05$), leading to stronger and tougher films. This could be attributed to the formation of intermolecular hydrogen bonds between ammonium of the CS backbone and hydroxyl of the GL in the blend formulations (Leceta, Guerrero, Ibarburu, et al., 2013). Considering that TS is in correlation with the microstructure of the polymer matrix and intermolecular forces within the film components, the higher TS of the films might be due to the condensed structure of the CS-GL blend film (Mohammadi et al., 2017).

Control and active bilayer films showed TS values (22.7 and 24.3 MPa, respectively) similar to CS film. In contrast to this result, Pereda, Ponce, Marcovich, Ruseckaite, & Martucci (2011) reported that TS of CS-GL blend and CS/GL bilayer films was decreased compared to the single component films.

E% is the maximum change in length of a film until it breaks compared to the initial length. E% helps to determine the flexibility and stretchability of a film (Jantrawut, Chaiwarit, Jantanasakulwong, Brachais, & Chambin, 2017). No significant difference was observed in the E% of control and active films based on CS, GL, CS-GL blend and CS/GL bilayer ($p>0.05$). Souza et al. (2017) also found that the incorporation of different essential oils and hydroalcoholic extracts into CS film did not induce significant differences in E% values.

EM is the fundamental measure of film intrinsic stiffness. EM stands for the resistance of the film to elastic deformation and this can be perceived as reflecting the stiffness and strength of the film. A low EM value corresponds to a flexible film while higher values stand for more stiffness (Jantrawut et al., 2017). Control and active GL films showed the lowest EM values (344.5 and 361.3 MPa, respectively) while control and active CS films showed higher EM values (548.7 and 565.2 MPa, respectively) ($p<0.05$). Control and active CS-GL blend films showed EM value similar to CS film (592.2 and 534.6 MPa, respectively). CS/GL bilayer films showed intermediate values (436.1 and 462.6 MPa, respectively). Hosseini, Rezaei, Zandi, & Ghavi (2013) found that GL and CS were totally compatible to form films. The addition of positively charged CS improved the mechanical properties of films made from GL. The addition of CS caused a significant increase in the TS and EM, leading to stronger films as compared to GL film, but significantly decreased the E%. Our results suggested that blend films provided greater mechanical properties compared to the bilayer and single component films. However, the comparison of the data in the literature for mechanical properties

of CS and GL film provide contrary conclusions and depend on multiple factors such as the molecular mass of the polymer, deacetylation degree of CS, pH of the FFS, drying conditions, solubilization method, water content, film preparation, and film thickness.

Table 1. Thickness, tensile strength (TS), elongation at break (E%) and elastic modulus (EM) of the films based on chitosan (CS), gelatin (GL), chitosan-gelatin blend (CS-GL) and chitosan/gelatin bilayer (CS/GL) and those enriched with LAE.

Film sample	Thickness (μm)	TS (MPa)	E (%)	EM (MPa)
CS	31 ± 0.3^{ab}	21.0 ± 0.9^{b}	27.6 ± 0.8^{a}	548.7 ± 30.5^{c}
GL	28 ± 0.9^{a}	8.9 ± 0.1^{a}	27.2 ± 1.7^{a}	344.5 ± 10.7^{a}
CS-GL	29 ± 1.9^{a}	31.9 ± 1.6^{c}	29.8 ± 0.3^{a}	592.2 ± 5.7^{c}
CS/GL	54 ± 2.7^{c}	22.1 ± 2.8^{b}	31.1 ± 1.6^{a}	436.1 ± 14.3^{b}
CS/LAE	35 ± 1.6^{b}	22.8 ± 0.6^{b}	28.9 ± 0.5^{a}	565.2 ± 23.7^{c}
GL/LAE	29 ± 2.0^{ab}	9.3 ± 0.1^{a}	29.4 ± 1.8^{a}	361.3 ± 8.9^{a}
CS-GL/LAE	32 ± 1.3^{ab}	31.9 ± 1.7^{c}	28.7 ± 0.5^{a}	534.6 ± 6.4^{c}
CS/GL/LAE	58 ± 3.1^{c}	24.3 ± 3.2^{b}	31.6 ± 0.6^{a}	462.6 ± 10.2^{b}

Values are given as mean ± SD (n = 3).
Different lowercase letters in the same column indicate significant differences ($p<0.05$).

3.5. UV barrier, light transmittance and transparency value

Protecting food from the effect of light and UV radiation is an important property to evaluate due to their influence on product performance and consumer acceptance. The UV barrier, visible light transmittance and transparency values in the wavelength range 200 - 800 nm of control and active films based on CS, GL, CS-GL blend, and CS/GL bilayer are shown in Tab. 2. Control and active bilayer films showed the lowest UV light transmission (0.18% and 0.16%, respectively). UV barrier property of films (200 - 350 nm) is an important characteristic to avoid lipid oxidation induced by UV light in the food (Wu, Sun, Guo, Ge, & Zhang, 2017). However, the mechanisms of blocking UV light can affect visual transparency which is an interesting sensory factor for consumers and one of the major goals within the packaging industry (Cárdenas, Díaz, Meléndrez, & Cruzat, 2008). In general, CS films are not good UV barriers. In contrast, GL films exhibited excellent UV barrier properties due to the UV absorption

of peptide bonds in the polypeptide chains and their high amount of aromatic amino acids (Liu et al., 2015). Control and active blend films showed UV barrier values similar to single component films while control and active bilayer films showed lower values. This might be due to the higher thickness of the bilayer films compared to the blend and single component films.

In contrast to the UV range, the light transmission of the films in the visible range (400 - 800 nm) showed higher values leading to transparent films. Control and active bilayer films showed less light transmission compared to blend and single component films. The presence of LAE in the film matrix inhibited the light transmission for both UV and visible ranges. The highest transparency value was observed for CS/LAE film in the visible light range. If compatibility between film constituents was not good, then due to reflection or dispersion of light at the phase interface, the transparency would be low (Ahmed & Ikram, 2016; Pereda, Ponce, Marcovich, Ruseckaite, & Martucci, 2011).

Table 2. Light transmittance (T%) and transparency value (600 nm) of the films based on chitosan (CS), gelatin (GL), chitosan-gelatin blend (CS-GL) and chitosan/gelatin bilayer (CS/GL) and those enriched with LAE.

Film sample	Light Transmission (%) at different wavelengths (nm)								Opacity value
	200	280	350	400	500	600	700	800	
CS	0.27	53.6	72.1	85.8	89.0	89.1	88.6	88.5	1.6 ± 0.2^{c}
GL	0.23	60.1	88.1	91.4	91.5	90.9	90.1	90.0	1.3 ± 0.1^{ab}
CS-GL	0.24	61.2	82.7	90.5	91.8	91.3	90.5	90.3	1.3 ± 0.1^{ab}
CS/GL	0.18	42.1	74.1	87.3	90.4	90.3	89.7	89.5	0.8 ± 0.1^{a}
CS/LAE	0.20	37.9	52.4	62.8	70.5	74.8	77.5	88.5	3.6 ± 0.4^{d}
GL/LAE	0.23	60.7	89.4	92.0	91.8	91.1	90.3	90.2	1.3 ± 0.2^{ab}
CS-GL/LAE	0.23	61.2	82.8	89.3	90.2	89.9	89.2	89.1	1.4 ± 0.2^{ab}
CS/GL/LAE	0.20	36.7	67.3	79.2	83.9	85.9	86.3	86.3	1.3 ± 0.3^{ab}

Values are given as mean ± SD (n = 3).
Different lowercase letters in the same column indicate significant differences ($p<0.05$).

Active films had higher transparency values than the control film. The transparency value of the films depends on the type of biopolymer, differences in thickness and the distribution of LAE in the film network. The higher transparency value indicated that the film was less transparent. Control and active CS films showed the highest

transparency values ($p<0.05$). Interestingly, the CS/GL bilayer film showed the lowest transparency value ($p<0.05$) despite a higher thickness. These results suggested that the bilayer film with the strong absorbance in the UV range and lower transparency value revealed better UV and light barrier properties than blend and single component films.

3.6. Color

Optical properties are essential in food packaging applications since they can directly affect food appearance and consumers' purchasing decisions (Leceta, Guerrero, Ibarburu, et al., 2013). Color values of control and active films based on CS, GL, CS-GL blend and CS/GL bilayer are shown in Tab. 3. The lightness (L*), redness (a*), yellowness (b*) offer objective evaluation of the appearance of films while the total color difference (ΔE*) measures the color change of treatment from a reference color. CS/LAE film showed the lowest L* value (97.7) making this film darker compared to other films. This result confirmed the higher transparency value of CS/LAE film. Despite some significant differences observed in the L* of control and active films, this value varied between 97.7 to 98.7 which means that all films were almost clear.

The parameter a* corresponding to the redness of films ranged between -0.3 to -0.6, which means that films were not truly red. A more visible effect was observed in the parameter b*. The b* value varied between 0.8 and 2.9. The b* value was higher in CS/LAE, control and active bilayer films ($p<0.05$) presented more yellow color which might be due to the higher thickness of the bilayer films and the presence of b-1-4 linked 2-amino-2-deoxy-D-glucopyranose repeat units at CS (Pereda, Ponce, Marcovich, Ruseckaite, & Martucci, 2011).

CS/LAE, CS/GL, and CS/GL/LAE bilayer films showed ΔE* values higher than 3 mainly related to the higher b* value of the yellow color intensity of these films. It is well known

that when the ΔE* value is higher than 3, the color difference can be detected by the human eyes (Kim, Daeschel, & Zhao, 2008).

Table 3. Color parameters (L*, a* and b*) and total color difference (ΔE*) of the films based on chitosan (CS), gelatin (GL), chitosan-gelatin blend (CS-GL) and chitosan/gelatin bilayer (CS/GL) and those enriched with LAE.

Film sample	Color parameters			
	L*	a*	b*	ΔE*
CS	98.4 ± 0.04^{bc}	-0.4 ± 0.2^{ab}	1.8 ± 0.4^{b}	2.1 ± 0.4^{b}
GL	98.7 ± 0.1^{c}	-0.3 ± 0.1^{b}	0.8 ± 0.04^{a}	1.1 ± 0.1^{a}
CS-GL	98.5 ± 0.1^{bc}	-0.4 ± 0.2^{ab}	1.8 ± 0.5^{b}	2.0 ± 0.5^{b}
CS/GL	98.1 ± 0.2^{ab}	-0.6 ± 0.1^{a}	2.7 ± 0.4^{c}	3.1 ± 0.4^{c}
CS/LAE	97.7 ± 0.2^{a}	-0.6 ± 0.1^{a}	3.0 ± 0.4^{c}	3.5 ± 0.2^{c}
GL/LAE	98.5 ± 0.2^{bc}	-0.4 ± 0.1^{ab}	1.3 ± 0.2^{ab}	1.7 ± 0.3^{ab}
CS-GL/LAE	98.5 ± 0.2^{bc}	-0.5 ± 0.1^{a}	1.9 ± 0.2^{b}	2.2 ± 0.2^{b}
CS/GL/LAE	97.8 ± 0.5^{a}	-0.6 ± 0.1^{a}	2.9 ± 0.3^{c}	3.4 ± 0.4^{c}

Values are given as mean ± SD (n = 3).
Different lowercase letters in the same column indicate significant differences ($p<0.05$).

3.7. Moisture Content and water solubility

The moisture content (MC) of the films is a parameter related to the total empty volume occupied by water molecules in the network microstructure of the film (Pereda, Ponce, Marcovich, Ruseckaite, & Martucci, 2011). This parameter is very important for food packaging applications since it could be greatly related to physical properties and microbial growth. The MC of control and active films based on CS, GL, CS-GL blend and CS/GL bilayer are shown in Tab. 4. The incorporation of LAE did not affect the MC ($p>0.05$). Control and active CS films had higher MC values than the control and active GL films ($p<0.05$) due to the availability of free hydroxyl and amine groups of CS to interact with water (Ahmed & Ikram, 2016). Control and active blend and bilayer films showed intermediate MC values. The hydrophilic nature of CS biopolymer may represent a drawback, as tends to swell, dissolve, or disintegrate upon contact with the surface of foodstuff with high MC. However, this drawback could be improved in blend and bilayer films (Gómez-Guillén, Giménez, López-Caballero, & Montero, 2011).

Water solubility (WS) of control and active films based on CS, GL, CS-GL blend and CS/GL bilayer is shown in Tab. 4. The WS was not influenced by the addition of LAE

to the films ($p>0.05$). Control and active GL films were completely soluble in water while control and active CS films showed slight solubility in water. Control and active blend and bilayer films showed WS values lower than GL films but slightly higher than CS films ($p<0.05$). Considering the interaction between CS and GL that occurred in the film matrix, this might lower the availability of hydroxyl and amino groups that can interact with water, thus decreasing the water solubility of the blend and bilayer films. Pereda, Ponce, Marcovich, Ruseckaite, & Martucci (2011) reported that a polyelectrolyte positively charged (CS) and a polyampholyte negatively charged (GL) can make associative interactions due to hydrogen bond formation and electrostatic forces resulting in a reduction of water solubility of soluble polyelectrolyte complex.

Table 4. Moisture content (MC), water solubility (WS), water vapor transmission rate (WVTR) and water vapor permeability (WVP) of the films based on chitosan (CS), gelatin (GL), chitosan-gelatin blend (CS-GL) and chitosan/gelatin bilayer (CS/GL) and those enriched with LAE.

Film sample	MC (%)	WS (%)	WVTR (g day^{-1} m^{-2})	WVP 75:0% RH (g mm/kP day m^2)
CS	21.1 ± 1.2^{d}	19 ± 0.7^{a}	3885 ± 22.9^{b}	2.2 ± 0.02^{b}
GL	11.0 ± 3.0^{ab}	100 ± 0^{c}	4274 ± 35.5^{c}	2.1 ± 0.02^{b}
CS-GL	14.8 ± 1.6^{bc}	26 ± 0.6^{b}	3314 ± 20.0^{a}	1.7 ± 0.01^{a}
CS/GL	14.3 ± 2.8^{bc}	27 ± 0.5^{b}	3824 ± 65.7^{b}	3.7 ± 0.06^{c}
CS/LAE	17.6 ± 3.0^{cd}	17 ± 0.6^{a}	3795 ± 34.0^{b}	2.4 ± 0.02^{b}
GL/LAE	7.5 ± 1.2^{a}	100 ± 0^{c}	4262 ± 53.6^{c}	2.2 ± 0.03^{b}
CS-GL/LAE	16.3 ± 3.7^{bc}	26 ± 0.6^{b}	3202 ± 53.7^{a}	1.8 ± 0.03^{a}
CS/GL/LAE	15.2 ± 2.6^{bc}	26 ± 0.7^{b}	3690 ± 32.9^{b}	4.0 ± 0.14^{c}

Values are given as mean ± SD (n = 3).
Different lowercase letters in the same column indicate significant differences ($p<0.05$).

3.8. Water vapor transmission rate and water vapor permeability

The water vapor permeability (WVP) is a key parameter to ensure the organoleptic qualities of food which are highly associated with the shelf life. An effective control of moisture transfer is a desirable property for the food packaging industry. The WVP should be as low as possible to avoid or to reduce moisture transfer between the food and the surrounding atmosphere (Cao, Yang, & Fu, 2009). The water vapor transmission rate (WVTR) and WVP of control and active films based on CS, GL, CS-

GL blend and CS/GL bilayer are shown in Tab. 4. WVTR and WVP were not influenced by the addition of LAE to the films ($p>0.05$).

Our result showed that the WVTR of control and active blend films was lower than that of control and active bilayer and single component films ($p<0.05$).

Control and active bilayer films showed the highest WVP values among the tested films ($p<0.05$). This could be explained by the higher thickness of bilayer films compared to other films. McHugh, Avena-Bustillos, & Krochta (1993) reported that a positive relationship existed between thickness and WVP of hydrophilic films since the increase in film thickness could increase the relative humidity and equilibrium water vapor partial pressure at the inner film surface and provide an increased drive to mass transfer across it. Control and active blend films demonstrated the lowest WVP ($p<0.05$) where the hydrogen and covalent interactions between CS and GL network reduced the availability of the hydrophilic groups, and subsequently lead to a decrease in the water affinity. This result is in accordance with the SEM analysis revealing that blend films have dense, homogenous and compact structures without discontinuous or porous structures.

3.9. Antimicrobial activity

Antimicrobial activity of films was evaluated by the disk diffusion assay. The details of antimicrobial activity of control and active CS, GL, CS-GL blend and CS/GL bilayer films against *E. coli*, *S. typhimurium*, *L. monocytogenes,* and *C. jejuni* are shown in Tab. 5. The control films without LAE did not show an inhibitory effect against any of the tested microorganisms. Similar results were shown by Pranoto, Rakshit, & Salokhe (2005). The absence of inhibitory character could be explained by the limitation of CS diffusion in agar medium or incapability of GL to inhibit bacterial growth as it has been reported by other authors (Leceta, Guerrero, Ibarburu, et al., 2013). Incorporating LAE into films even at low concentrations revealed an antimicrobial effect. All active films

effectively inhibited the growth of tested microorganisms. The high antimicrobial activity of LAE has been attributed to its action as a cationic surfactant by increasing the permeability of the cytoplasm and outer membrane of Gram-negatives and the cell membrane and cytoplasm of Gram-positives, through denaturation of a membrane protein, where it alters their metabolic processes such as inhibition of cellular ATP generation. These changes produce disturbances in membrane potential, resulting in cell growth inhibition and loss of viability (Bonnaud, Weiss, & McClements, 2010; Moreno, Cárdenas, Atarés, & Chiralt, 2017). In addition, LAE has been reported to affect DNA structures by causing them to aggregate through ionic bridging (Ma, Davidson, Critzer, & Zhong, 2016). In summary, the results provided by the disk diffusion assay proved that the incorporation of LAE into the films even at low concentrations had the potential to inhibit target microorganisms.

Table 5. Inhibition zone diameters of the film disks (15 mm diameter) based on chitosan (CS), gelatin (GL), chitosan-gelatin blend (CS-GL) and chitosan/gelatin bilayer (CS/GL) and those enriched with LAE.

Film sample	***Listeria. monocytogenes***	***Escherichia. coli***	***Salmonella. typhimurium***	***Campylobacter. jejuni***
CS	N. D.	N. D.	N. D.	N. D.
GL	N. D.	N. D.	N. D.	N. D.
CS-GL	N. D.	N. D.	N. D.	N. D.
CS/GL	N. D.	N. D.	N. D.	N. D.
CS/LAE	16.4 ± 0.5^{aA}	17.7 ± 2.1^{aA}	16.0 ± 0.1^{aA}	23.3 ± 2.3^{aB}
GL/LAE	16.7 ± 0.6^{aA}	16.3 ± 0.6^{aA}	16.0 ± 1.0^{aA}	23.3 ± 1.5^{aB}
CS-GL/LAE	16.7 ± 0.5^{aA}	18.0 ± 1.7^{aA}	17.0 ± 0.1^{aA}	23.7 ± 0.6^{aB}
CS/GL/LAE	16.7 ± 0.6^{aA}	17.7 ± 2.1^{aA}	16.0 ± 1.0^{aA}	24.3 ± 0.6^{aB}

Values are given as mean ± SD (n = 3). N.D: not detected.
Different lowercase letters in the same column indicate significant differences ($p<0.05$).
Different capital letters in the same row indicate significant differences ($p<0.05$).

4. Conclusions

In this study blend and bilayer films based on CS and GL were developed and some physical, mechanical and barrier properties of these films were compared to the single component films. Moreover, LAE at a low concentration was incorporated into the films to evaluate their antimicrobial activities. Blend films demonstrated higher TS and EM

values as well as lower WVP compared to the bilayer films. Bilayer films demonstrated as effective barrier against UV light. The incorporation of LAE did not influence the thickness, the mechanical properties and the water vapor permeability of the films. However, it affected the light transmittance of the films and improved their barrier properties against UV radiation. ATR/FT-IR analysis showed good compatibility between CS and GL due to the electrostatic interactions and hydrogen bond formation. Active films enriched with LAE showed antimicrobial activity against four major food bacterial pathogens including *E. coli*, *L. monocytogenes, S. typhimurium*, and *C. jejuni*. Overall, these findings demonstrated that blend and bilayer films based on CS and GL enriched with LAE presented as good potential materials in the development of biodegradable and renewable packaging with an additional bioactive function to ensure food safety and to extend the shelf-life of foods. However, further studies are required to investigate their optimal application on an industrial scale.

Chapter 3

Comprehensive characterization of active chitosan-gelatin blend films enriched with different essential oils

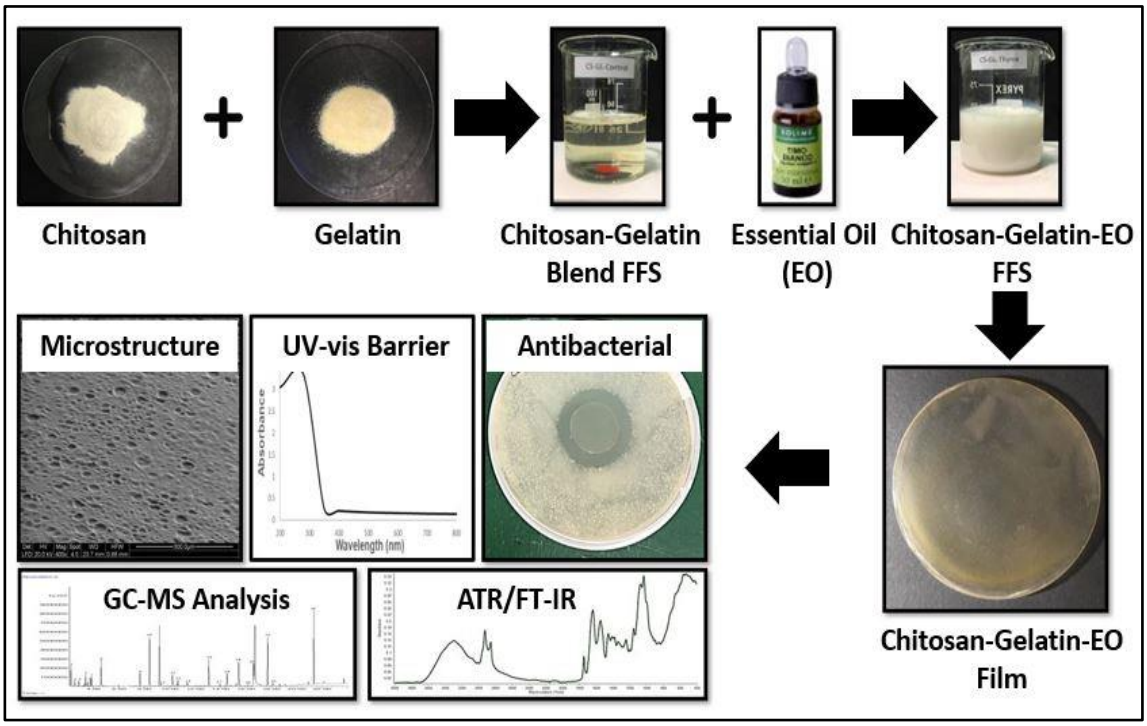

Highlights

- Production of films based on chitosan-gelatin enriched with essential oils.
- Determination of the physical, mechanical and barrier properties.
- Demonstration of the interaction between chitosan-gelatin and essential oils.
- Improving UV barrier of chitosan-gelatin film by addition of essential oils.
- Effectiveness of active films against common food bacterial pathogens.

Abstract

Natural extracts and plant essential oils (EOs) have long been recognized as valid alternatives to synthetic food additives owing to their proven wide-spectrum antimicrobial capacity. The main aim of this study was to characterize the physical, mechanical, water barrier, microstructural and antimicrobial properties of chitosan-gelatin blend films enriched with cinnamon, citronella, pink clove, nutmeg, and thyme EOs. The film microstructure determined by scanning electron microscopy showed that all active films had heterogeneous surfaces: in particular, films including cinnamon, nutmeg, and thyme EOs showed remarkable pores on the surface. The possible interaction of chitosan-gelatin blend film with incorporated EOs was investigated using Fourier-transform infrared (FT-IR) spectroscopy. Presence of new bands and changes in the FT-IR spectra confirmed intermolecular interactions between the chitosan-gelatin matrix and the EOs. The antimicrobial activity of films was determined using disk diffusion assay. Active films inhibited the growth of four major food bacterial pathogens including *Campylobacter jejuni, Escherichia coli, Listeria monocytogenes,* and *Salmonella typhimurium* and, among the tested EOs, thyme was the most effective ($p<0.05$). The active films can be considered as effective barriers against UV light. The incorporation of EOs to the chitosan-gelatin film increased thickness, moisture content, water vapor permeability, b* and ΔE* values ($p<0.05$) while it decreased L* value, light transparency, and opacity ($p<0.05$). Overall, the characterization of functional properties revealed that chitosan-gelatin films incorporated with EOs could be used as environmentally friendly active food packaging with antimicrobial properties and potential to extend the shelf-life of food products.

1. Introduction

Environmental concerns as well as consumer demand for natural, minimally processed, preservative-free and high-quality food, have raised the attention of food

packaging industries on the development of bio-based films enriched with natural compounds. Bio-based films have been considered as attractive alternatives to plastic packaging due to their excellent biodegradability, moreover, they can be blended with active compounds such as antimicrobial agents to protect food against microbial deterioration and to extend the shelf life of food products (De Leo et al., 2018; Shen & Kamdem, 2015).

Among biopolymers, chitosan (CS) and gelatin (GL) have shown outstanding film-forming property, non-toxicity, biocompatibility, biodegradability, stability and commercial availability. The CS is a linear polysaccharide, commercially obtainable from deacetylation of chitin. This polycationic biopolymer is soluble in solutions with pH below 6.5 due to the protonation of the amino group (Bonilla, Poloni, Lourenço, & Sobral, 2018). The positively charged amino group of CS interacts with negatively charged microbial cell membranes leading to the leakage of proteinaceous and other intracellular constituents of the microorganisms (Bonilla & Sobral, 2016). Owing to the intrinsic antimicrobial property, chitosan has attracted considerable commercial interest from food packaging companies as a natural alternative to synthetic plastics.

GL is a natural water-soluble protein, obtainable from the partial hydrolysis of collagen. It has a unique amino acid sequence with high contents of proline, glycine, and hydroxyproline, which help in the formation of a flexible film with excellent barrier properties to gases, volatile compounds, oils and UV light (Wu, Sun, Guo, Ge, & Zhang, 2017; Figueroa-Lopez, Andrade-Mahecha, & Torres-Vargas, 2018). Previous studies showed that CS and GL have good barrier to gases such as CO_2 and O_2. However, their use is currently limited due to weak mechanical and water barrier properties. Since CS and GL are hydrophilic biopolymers with good affinity and compatibility, blending CS and GL (CS-GL) to form a composite film may improve mechanical and water barrier response compared to single component films. This is

due to the ability to associate through electrostatic interaction between the negatively charged carboxyl group of GL and the positively charged amino group of CS at appropriate pH conditions, and strong hydrogen bond formation (Bonilla et al., 2018; Haghighi, De Leo, et al., 2019). Therefore, blending could combine the advantages of these two biopolymers as well as minimize their disadvantages (Hosseini, Rezaei, Zandi, & Ghavi, 2013; Wang, Qian, & Ding, 2018).

Natural extracts and plant EOs are secondary metabolites of plants that are complex mixtures of low molecular weight compounds. EOs have long been recognized as valid alternatives to synthetic food additive owing to their proven wide-spectrum antimicrobial capacity. Antimicrobial activity of EOs is due to the presence of mono- and sesquiterpenes, mono- and sesquiterpene hydrocarbons and phenolic compounds. These components interact with polysaccharides, fatty acids, and phospholipids of bacterial membranes and cause cell death due to the loss of ions and cellular contents (Burt, 2004).

Combination of CS and GL bio-based films with EOs to create bio-based active films is one of the promising strategies that is employed by the food industries to reduce the use of chemical additives (Jamróz, Juszczak, & Kucharek, 2018). The incorporation of EOs into the films instead of applying them directly on foods is an alternative to extend the shelf life of the food and to achieve the desired goal with lower oil concentrations, thus limiting strong aroma and possible changes in the organoleptic properties of the food (Salgado, López-Caballero, Gómez-Guillén, Mauri, & Montero, 2013). In many cases, the active compounds are released slowly onto the food surface from the active films, which act as an active compound reservoir for an extended period. Furthermore, owing to their hydrophobic nature, EOs could improve the water barrier properties of hydrophilic biopolymers such as CS and GL. In this study, cinnamon (*Cinnamomum zeylanicum*), citronella (*Cymbopogon nardus*), pink clove (*Eugenia caryphyllata*),

nutmeg (*Myristica fragrans*) and thyme (*Thymus vulgaris*) were selected for incorporation into CS-GL blend films due to their sensory acceptability and compatibility with food and for their proved antimicrobial properties (Figueroa-Lopez et al., 2018; Ojagh, Rezaei, Razavi, & Hosseini, 2010; Peng & Li, 2014; Shen & Kamdem, 2015; Wu, Sun, Guo, Ge, & Zhang, 2017). Due to the natural origin of EOs, the majority of them have been considered as GRAS by the US Food and Drug Administration (FDA, 2013). Upon addition of EOs into the films, it is also important to evaluate their effects on microstructure, optical properties, mechanical strength, water vapor permeability, moisture content and solubility of the resulting film. However, literature concerning the effects of these EOs on the functional properties of CS-GL blend film is not available. Therefore, the purpose of the present work was to characterize CS-GL films enriched with different EOs including cinnamon, citronella, pink clove, nutmeg, and thyme to evaluate some physical, optical, mechanical, water barrier and microstructural properties for potential applications as active food packaging. Moreover, their antimicrobial activity against four common food bacterial pathogens including *Campylobacter jejuni*, *Escherichia coli*, *Listeria monocytogenes,* and *Salmonella typhimurium,* was investigated.

2. Material and methods

2.1 Materials and reagents

Chitosan (CS) with a molecular weight of 100-300 kDa was obtained from Acros Organics™ (China). Gelatin (GL) with bloom 128 - 192° was purchased from AppliChem GmbH (Darmstadt, Germany). Glycerol (≥ 99.5%) was purchased from Merck (Darmstadt, Germany). Acetic acid (≥ 99.5%) was obtained from Brenntag S.p.A (Milan, Italy). Five types of commercial EOs including cinnamon, citronella, pink clove, nutmeg, and thyme were purchased from Solime S.r.l (Cavriago, Reggio Emilia, Italy).

Tween 80 was purchased from Sigma-Aldrich (Italy). Brain heart infusion agar (BHIA) was purchased from Biolife (Milan, Italy).

2.2. Preparation of film-forming solutions and films

Preparation of films was adapted from Bonilla & Sobral (2016) with slight modifications. In this study, five different types of films based on a CS-GL blend enriched with EOs (cinnamon, citronella, pink clove, nutmeg, and thyme) were analyzed. A film without EO was used as a control. All film-forming solutions (FFSs) with and without EOs were prepared separately. CS FFS (2%, w/v) was prepared by dissolving CS in an acetic acid solution (1%, v/v) under continuous stirring at 55 °C for 30 min. GL FFS (2 %, w/v) was prepared by dissolving GL in distilled water, first being allowed to swell at 7 °C for 15 min and then stirred at 55 °C for 30 min. Glycerol (25% w/w of CS or GL) was then added as a plasticizer into both FFS, followed by additional stirring for 30 min. CS-GL blend solution was prepared by mixing CS and GL FFS at 1:1 ratio. Moreover, different types of EOs (1%, v/v) together with Tween 80 (0.2%, v/v of EO) were added to FFS, followed by stirring at 55 °C for additional 30 min. All FFSs were degasified with a vacuum pump (70 kPa) for 15 min to remove bubbles from the FFS. Films were obtained by casting 20 mL of the FFS into Petri dishes (14.4 cm in diameter) and drying at 25±2 °C overnight in the chemical hood at ambient relative humidity (RH) of 45%.

2.3. Gas Chromatography-Mass Spectrometer (GC-MS) analysis of essential oils volatile profiles

The volatile profiling of the EOs used for incorporation in CS-GL films was carried out by GC–MS analyses using an Agilent (Palo Alto, CA, USA) 6890N GC equipped with a 30 m length, 0.25 mm i.d., 0.25 μm film thickness, fused silica capillary column (Stabilwax®-DA, Restek) coupled with an Agilent 5973 Network mass selective detector. EOs were suitably diluted with acetone and 1 μL was injected into the GC injector port set at 250 °C at 10:1 split ratio. The oven temperature program was as

follows: initial temperature 60 °C, then ramp to 200 °C at 8 °C/min and hold for 1 min, finally ramp to 240 °C at 20 °C/min and hold for 3.5 min. Helium was used as the carrier gas at a flow rate of 1.0 mL/min. Mass spectrometer parameters were as follows: ion source, 230 °C; electron energy, 70 eV; multiplier voltage, 1447 V; GC/MS transfer line, 250 °C; and a scan range of 33–650 mass units. Identification of compounds was carried out by comparison with spectra libraries.

2.4. Scanning electron microscopy (SEM)

Scanning electron microscopy (SEM) of the surface and cross-section of the films were obtained with the use of a scanning electron microscope (FEI, Quanta 200, Oregon, USA). Film samples were fixed on a stainless-steel support with a double side conductive adhesive. The analysis was conducted in a low vacuum (0.6 Torr) at an acceleration voltage of 20 kV.

2.5. Attenuated Total Reflection (ATR) / Fourier-Transform Infrared (FT-IR) Spectroscopy

The infrared spectra of different films were obtained using an ATR/FT-IR spectrometer (type Alpha, Bruker Optik GmbH, Ettlingen, Germany). Spectra were collected from two different locations from the top and bottom of the same samples in the 4000-400 cm^{-1} wavenumber range by accumulating 64 scans with spectral resolution of 4 cm^{-1}.

2.6. Thickness

Film thickness was measured with a digital micrometer (SAMA Tools measuring Instruments & NTD equipment, Viareggio, Italia) at five different random positions (one at the center and four at the edges). The means of these five separate measurements were recorded.

2.7. Mechanical properties

The tensile strength (TS), elongation at break (E%) and elastic modulus (EM) were determined using a dynamometer (Z1.0, ZwickRoell, Italy) according to ASTM

standard method D882 (ASTM, 2001a). The films with known thickness were cut into rectangular strips (9 x 1.5 cm^2). Initial grip separation and cross-head speed were set at 70 mm and 10 mm/s, respectively. Measurements were repeated 10 times. The software TestXpert® II (V3.31) (ZwickRoell, Ulm, Germany) was used to record the TS curves. TS was calculated by dividing the maximum load to break the film by the cross-sectional area (thickness) of the film and expressed in MPa. E% was calculated by dividing film elongation at rupture by the initial grip separation expressed in percentage (%). EM was calculated from the initial slope of the stress-strain curve and expressed in MPa. TS and E% were evaluated for ten samples from each type of film.

2.8. UV barrier, light transmittance, and opacity value

The barrier properties of films against UV and visible light were determined at the UV (200, 280 and 350 nm) and visible (400, 500, 600, 700 and 800 nm) wavelengths onto square film samples (2 × 2 cm^2) using a Jasco V – 550 UV/Vis spectrophotometer (Jasco Corporation, Tokyo, Japan) as described by Bellelli, Licciardello, Pulvirenti & Fava (2018). The opacity of the films was calculated by Eq. (1):

$$\text{Opacity value} = \frac{-\log T_{600}}{x} \quad (1)$$

where T_{600} is the fractional transmittance at 600 nm and x is the film thickness (mm). The greater opacity value represents the lower transparency of the film. For each film, four readings were taken at different points and average values were determined.

2.9. Color

The color of films was measured with a CR-400 Minolta colorimeter (Minolta Camera, Co., Ltd., Osaka, Japan) at room temperature, with D65 illuminant and 10° observer angle. The instrument was calibrated with a white standard (L* = 99.36, a* = -0.12, b* = -0.07) before measurements. Results were expressed as L* (luminosity), a* (red/green) and b* (yellow/blue) parameters. The total color difference (ΔE^*) was calculated using the following Eq. (2):

$$\Delta E^{*}= \sqrt{[(\Delta L^{*})^2+(\Delta a^{*})^2+(\Delta b^{*})^2]} \quad (2)$$

where ΔL^{*}, Δa^{*} and Δb^{*} are the differences between the corresponding color parameter of the samples and that of a standard white plate used as the film background. For each film, five readings were taken at different points and the average values were determined from the top and bottom sides.

2.10. Moisture content and water solubility

Moisture content (MC) of the films was determined by measuring weight loss upon drying to constant weight in an oven at 105 ± 2 °C according to the following Eq. (3):

$$\text{MC (\%)}: \frac{\text{Mw-Md}}{\text{Mw}} \times 100 \quad (3)$$

Where, Mw and Md are the initial weight and dry weight of the film, respectively.

The solubility of films (2 × 2 cm^2) in water was determined by drying to constant weight in an oven at 105 ± 2 °C (Wi) and then each film was immersed in 50 mL distilled water at 25 °C. After 24 h, the film samples were dripped and dried to constant weight at 105± 2 °C (Wf) to determine the weight of dry matter which was not solubilized in water. The measurement of water solubility (WS) was determined according to the following Eq. (4):

$$\text{WS (\%)}: \frac{\text{Wi-Wf}}{\text{Wi}} \times 100 \quad (4)$$

where, Wi and Wf are initial and final weight of the film, respectively.

2.11. Water vapor transmission rate and water vapor permeability

Water vapor transmission rate (WVTR) of the films was determined gravimetrically in triplicate according to the ASTM E96 method (ASTM, 2001b) with some modifications. Films were sealed on top of glass test cups with an internal diameter of 10 mm and a depth of 55 mm filled with 2 g anhydrous $CaCl_2$ (0% RH). The cups were placed in desiccators containing $BaCl_2$ (75% RH), which were maintained in incubators at 45 °C. WVTR was determined using the weight gain of the cups and was recorded and plotted

as a function of time. Cups were weighted daily for 7 days to guarantee the steady-state permeation. The slope of the mass gain versus time was obtained by linear regression ($r^2 \geq 0.99$). WVTR (g /day m^2) and WVP (g mm/kPa day m^2) were calculated according to the following Eqs. (5) and (6):

$$WVTR = \frac{\Delta W}{\Delta t \times A} \quad (5)$$

$$WVP = \frac{WVTR \times L}{\Delta P} \quad (6)$$

where $\Delta W/\Delta t$ is the weight gain as a function of time (g/day), A is the area of the exposed film surface (m^2), L is the mean film thickness (mm) and ΔP is the difference of vapor pressure across the film (kPa).

2.12. In vitro antimicrobial activity

Antibacterial activity test on films was assessed against four typical food bacterial pathogens including *Listeria monocytogenes* (UNIMORE 19115), *Escherichia coli* (UNIMORE 40522), *Salmonella typhimurium* (UNIMORE 14028) and *Campylobacter jejuni* (UNIMORE 33250) using the disk diffusion assay according to (Haghighi, Biard, et al., 2019). Films (sterilized with UV light) were cut into a disc shape of 22 mm diameter and placed on the surface of BHIA agar plates, which had been previously streaked with 0.1 mL of inocula containing 10^6 CFU/mL of tested bacteria. The plates were then incubated at 30 °C for 24 h (*C. jejuni* plates were incubated at 37 °C). The diameter of the inhibition zones was measured with a caliper and recorded in millimeters (mm). All tests were performed in triplicates.

2.13. Statistical analysis

The statistical analysis of the data was performed through analysis of variance (ANOVA) using SPSS statistical program (SPSS 20 for Windows, SPSS INC., IBM, New York). The differences between means were evaluated by Tukey's multiple range test ($p<0.05$). The data were expressed as the mean ± SD (standard deviation).

3. Results and discussion

3.1. Composition of the essential oils

The volatile profiles of the tested EOs are shown in Tab. 1, which reports the major compounds with their relative abundance (%). Typical chromatograms for each EO are available in the supplementary material (Appendix A). As it can be inferred, eugenol alone accounted for more than 51% of the total peak area of cinnamon EO, while 14 other components contributed from 1 to 6.7% to the total peak area, with β-caryophyllene and benzyl benzoate prevailing, followed by acetyleugenol and linalool, among the most represented. Some differences between our results and other studies were observed, as reported by Wang, Zhang, et al., (2018), cinnamaldehyde was the most representative components of cinnamon EO. The other main constituents were eugenol (19.188%), linalool (4.563%), and beta-caryophyllene (4.551%). In fact, the chemical compositions of the EOs may be varied depending on geographical and climate conditions, herbal species, age, ecotypes, geographical origins and method of drying and isolation of the EOs (Khezrian & Shahbazi, 2018).

The volatile profile of citronella was characterized by citronellal, geraniol, and β-citronellol, accounting for about 56%, δ-cadinene, citronellyl acetate, elemol and limonene which, together, made another 22.5%, while other 7 compounds added at least 1% each to the total peak area. Similar finding is reported by Chen et al. (2014) who noted that citronella EO was rich in citronellal (26.23%), geraniol (19.75%) and citronellol (12.96%).

Pink clove EO was the simplest among the studied substances, since it was mainly composed of eugenol (96.5% of total peak area), with minor contributions of carvacrol, β-caryophyllene, and vanillin.

Nutmeg EO was composed of about 22.7% sabinene, 14.9 and 10.3% α- and β-pinene, respectively, and many other terpenic compounds, 7 representing 3-7% and 7 more

ranging from 1 to 3% of total peak area. Our results on chemical profiling of the nutmeg EO was in accordance with Morsy (2016).

Thyme EO was characterized by p-cymene, thymol, and carvacrol, which, together, represented almost 80% of the total chromatographic area. Linalool, α-pinene, and borneol contributed for another 13%, while β-myrcene, limonene, β-caryophyllene, camphene, and 1,8-cineol accounted for about 1% each. Jouki, Yazdia, Mortazavia, Koocheki, & Khazaei (2014) also reported that thymol (46.42%), p-cymene (22.31%) and carvacrol (12.42%) were the most representative components of thyme EO.

Table 1. Relative volatile composition (main components) of the tested EOs.

NO.	RT* (min)	Compounds name	Cinnamon	Citronella	Pink clove	Nutmeg	Thyme
1	2.23	**α-pinene**	1.8	-	-	**14.9**	4.2
2	2.45	α-fenchene	-	-	-	-	0.2
3	2.52	camphene	0.6	-	-	0.3	1.2
4	2.85	**β-pinene**	0.5	-	-	**10.3**	0.4
5	2.97	**sabinene**	-	-	-	**22.7**	-
6	3.21	δ-3-carene	-	-	-	1.3	-
7	3.30	β-myrcene	-	-	-	2.4	1.3
8	3.37	α-phellandrene	1.1	-	-	1.1	-
9	3.52	α-terpinene	0.2	-	-	3.6	-
10	3.74	limonene	0.6	4.4	-	4.5	1.3
11	3.85	β-phellandrene	1.0	-	-	3.4	-
12	3.85	1,8-cineol	-	-	-	-	0.8
13	4.26	γ-terpinene	-	-	-	5.6	-
14	4.59	**p-cymene**	2.6	-	-	3.0	**34.9**
15	4.72	α-terpinolene	-	-	-	2.1	-
16	7.12	α-cubebene	1.5	-	-	0.2	-
17	7.25	trans thujan-4-ol	-	-	-	0.7	-
18	7.55	**citronellal**	-	**23.9**	-	-	-
19	7.65	α-copaene	-	-	-	0.9	-
20	8.13	camphor	-	-	-	-	0.5
21	8.39	linalool	4.6	1.1	-	0.3	6.6
22	8.51	β-terpineol	-	-	-	0.6	-
23	8.71	1-terpineol	-	-	-	0.3	-
24	8.87	isopulegol	-	3.1	-	-	-
25	8.93	α-fenchyl acetate	-	-	-	0.3	-
26	9.06	β-elemene	-	3.3	-	-	-
27	9.17	β-caryophyllene	6.7	0.1	0.8	1.0	1.2
28	9.31	4-terpineol	0.4	-	-	7.2	-
29	10.07	citronellyl acetate	-	5.4	-	-	-
30	10.16	isoborneol	-	-	-	-	0.4
31	10.21	α-humulene	1.3	0.3	-	-	-
32	10.43	α-amorphene	-	0.4	-	-	-
33	10.59	camphene	-	-	-	0.3	-
34	10.64	α-terpineol	0.6	-	-	0.7	-
35	10.65	borneol	-	-	-	-	2.3
36	10.77	β-cubebene	-	2.5	-	-	-
27	10.96	α-muurolene	-	1.1	-	-	-
38	11.21	citral	-	0.5	-	-	-

39	11.37	δ-cadinene	0.3	8.0	-	0.7	-
40	11.54	**β-citronellol**	-	**13.0**	-	-	-
41	11.99	nerol	-	0.2	-	-	-
42	12.66	**geraniol**	-	**19.2**	-	-	-
43	13.07	safrole	2.9	-	-	1.8	-
44	13.96	allylbenzene	0.2	-	-	-	-
45	14.51	caryophyllene oxide	1.3	-	0.3	-	0.4
46	14.83	methyleugenol	-	-	-	0.7	-
47	15.21	α-amorphene	-	0.8	-	-	-
48	15.43	cinnamaldehyde	2.7	-	-	-	-
49	15.59	elemol	-	4.6	-	-	-
50	16.18	spathulenol	0.2	-	-	-	-
51	16.61	cinnamyl acetate	3.4	-	-	-	-
52	16.69	**eugenol**	**51.2**	2.5	**96.5**	0.3	-
53	16.78	**thymol**	-	-	-	-	**30.2**
54	16.83	muurolol	-	0.6	-	-	-
55	17.12	**carvacrol**	-	-	1.1	-	**14.0**
56	17.28	α-eudesmol	-	0.4	-	-	-
57	17.35	elemicin	-	-	-	2.9	-
58	17.37	α-cadinol	-	1.4	-	-	-
59	17.71	acethyleugenol	4.7	-	-	-	-
60	17.80	**myristicin**	-	-	-	**4.8**	-
61	18.12	cinnamyl alcohol	0.4	-	-	-	-
62	18.68	chavicol	-	-	0.5	-	-
63	20.93	vanillin	-	-	0.8	-	-
64	21.36	benzyl benzoate	6.7	-	-	-	-

* Retention time
The dominant compounds are indicated in bold.

3.2. Microstructure

The surface and cross-section images of CS-GL film (control) and CS-GL film enriched with different EOs (active films) are presented in Fig. 1 and Fig. 2, respectively. The microstructure or internal morphological structures of the film depend on the interactions between film components which directly affect the final physical, optical, mechanical and barrier properties. The surface of control films was smooth and homogenous and did not show pores or cracks (Fig. 1a) indicating the formation of an ordered matrix. Active films showed heterogeneous surface that resulted from oil droplets after drying. Both CS and GL have a hydrophilic nature. The incorporation of EO in the FFS is usually carried out by emulsification of the aqueous solution containing the polymer; when the film is dried, droplets of lipid remain embedded into the polymer matrix (Siracusa et al., 2018), as observed in the surface of films incorporated with citronella, pink clove and thyme EOs (Fig. 1b, d, and f). Furthermore,

cinnamon and nutmeg films showed remarkable pores on the surface (Fig. 1b and e). The presence of pores might be attributed to the high volatility of these EOs during the drying process (Yao et al., 2017).

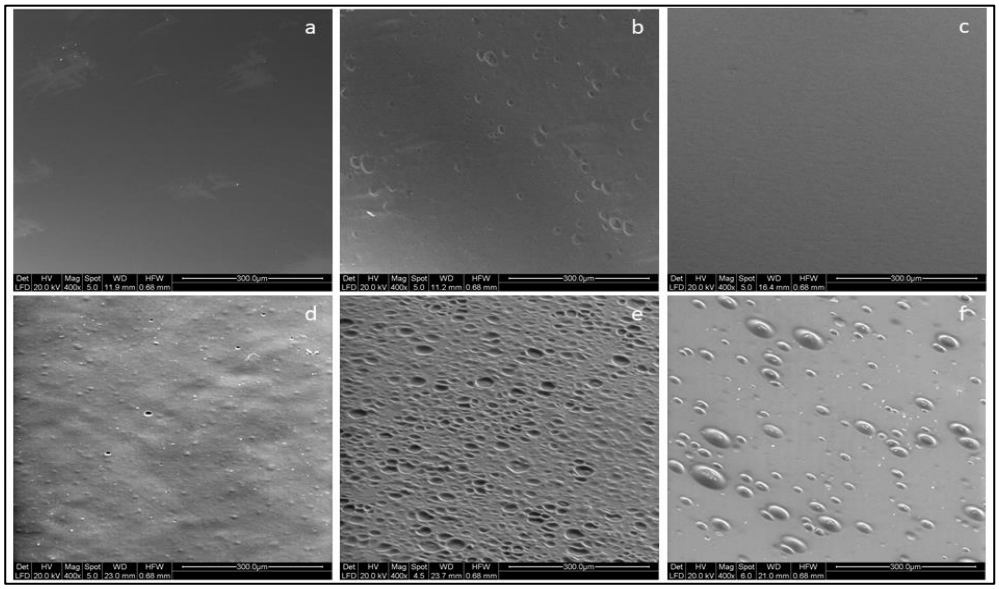

Fig. 1. Scanning electron microscopy (SEM) images of the surface of films. a: Chitosan-Gelatin blend (CS-GL) as a control; b: CS-GL-Cinnamon; c: CS-GL-Citronella; d: CS-GL-Pink Clove; e: CS-GL-Nutmeg; f: CS-GL-Thyme.

A compact and continuous structure without phase separation can be observed in the cross-section of the control film (Fig. 2a) indicating high compatibility among CS and GL to form a blend.

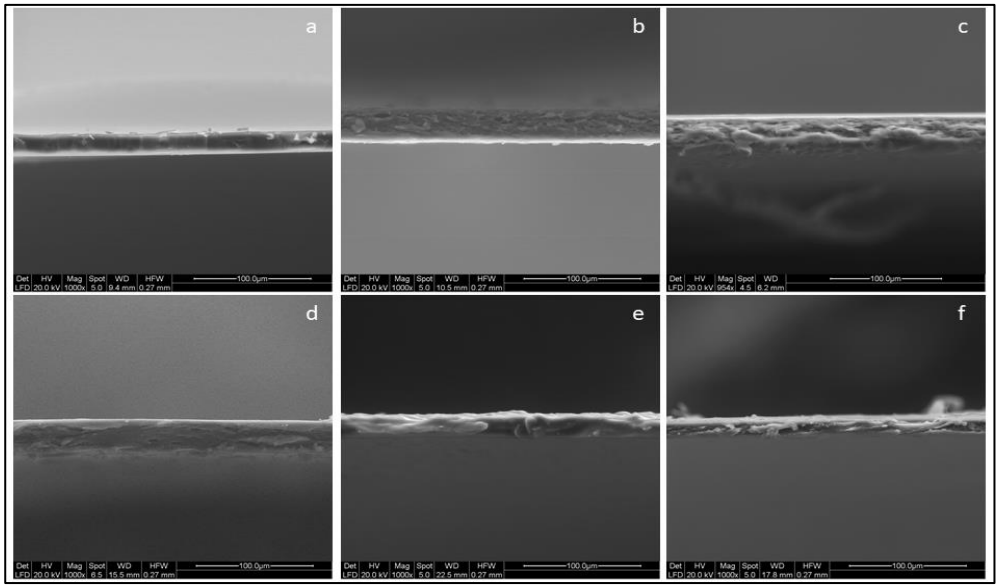

Fig. 2. Scanning electron microscopy (SEM) images on the cross-section of films. a: Chitosan-Gelatin blend (CS-GL) as a control; b: CS-GL-Cinnamon; c: CS-GL-Citronella; d: CS-GL-Pink Clove; e: CS-GL-Nutmeg; f: CS-GL-Thyme.

The cross-section of active films showed discontinuities and heterogeneous structure indicating the occurrence of oil droplets. Moreover, irregular structures with the presence of air bubbles in active films were observed (Fig. 2b, c, d, e, and f). Bonilla et al. (2018) also reported that CS-GL blend film containing eugenol and ginger EOs had incompact texture with sponge-like structure due to the uneven dispersion of EOs with hydrophobic nature from the aqueous phase during the film drying process.

3.3. Attenuated Total Reflection (ATR) / Fourier-Transform Infrared (FT-IR) Spectroscopy

ATR/FT-IR spectroscopy was performed to characterize the structural and spectroscopic changes due to the incorporation of the EOs into the CS-GL film matrix by measuring the absorbance in the wavenumber range of 4000 - 400 cm^{-1} at a resolution of 4 cm^{-1}. The FT-IR spectra of control and active films are shown in Fig. 3. The control film spectrum showed the characteristic band at 1636 cm^{-1} (amide-I) due to the ν(C=O) stretching vibration. A strong peak at 1636 cm^{-1} may be taken as evidence of the presence of a significant amount of β-sheet secondary structures of GL in CS-GL film (Haghighi, De Leo, et al., 2019). The peak at 1545 cm^{-1} (amide-II) corresponds to a combination band of the ν(C–N) stretching and δ(N-H) bending vibrations and the weak band at about 1245 cm^{-1} (amide III) has been assigned to another coupled vibration of the −CONH- functionality (Bonilla & Sobral, 2016). The broad absorption band between about 3600 and 3200 cm^{-1} corresponds to ν(O-H) and ν(N-H) stretching vibrations of hydrogen-bonded O-H and N-H functionalities. The band doublet at 2927/2874 cm^{-1} can be assigned to antisymmetric and symmetric $\nu_{as}(CH_3/CH_2)/\nu_s(CH_3/CH_2)$ stretching vibrations of CH_3 and CH_2 functionalities. The peaks at 849, 898, 995, 1030, 1150 cm^{-1} can be assigned to saccharide structures of the CS biopolymer in the CS-GL blend film network (Shen & Kamdem, 2015).

The ATR/FT-IR spectra of the active films showed partly characteristic additional bands of the incorporated EOs. It has to be mentioned, however, that due to the low amounts of admixed EOs, only the most intense absorptions of specific functionalities are observable in the spectra. In Fig. 3 the spectra have been arranged (from top to bottom) in the order of increasing ν(C=O) bands in the wavenumber range 1720 - 1740 cm^{-1} that can be assigned to ester, aldehyde or ketone functionalities of the EO admixtures. Thus, pink clove and thyme do not show these bands. However, while the spectrum of thyme is - with the exception of weak additional bands in the 2800 - 3000 cm^{-1} range due to aliphatic functionalities - very similar to the control spectrum, the spectrum of pink clove shows a very characteristic additional peak at 1515 cm^{-1} that belongs to the aromatic ring vibration of the main constituent (eugenol) of pink clove. The CS-GL-Citronella film showed a small new peak at 1733 cm^{-1} and slight changes in the ν(CH) absorption range originating from ester and aldehyde functionalities and aliphatic structures, respectively, of the citronella admixture. The ATR/FT-IR spectra of CS-GL-Cinnamon film showed new peaks in the aliphatic ν(CH) absorption range, at 1743 cm^{-1}, and a significant shoulder at 1515 cm^{-1}, due to aliphatic functionalities, ester and the aromatic structure of linalool, and eugenol components, respectively. The largest changes in the ν(CH) and ν(C=O) absorption ranges are reflected in the CS-GL-Nutmeg film. These changes can be traced back to a major component of nutmeg, trimyristin, a saturated fat which is the triglyceride of myristic acid.

Several of the admixed EOs contain alcoholic OH functionalities but their signatures are too weak and buried in the high-wavenumber wing of the intense, broad ν(NH) band of the CS-GL film. Nevertheless, it can be assumed that the admixed C=O and OH functionalities of the EOs contribute to intermolecular interactions with the hydroxyl and amino groups of the CS-GL film network.

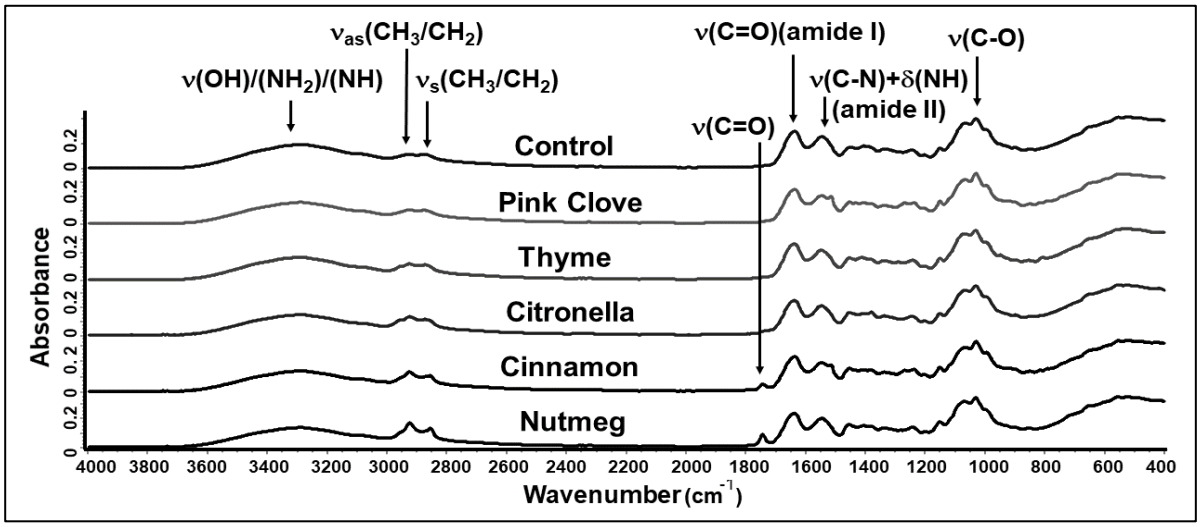

Fig. 3. ATR-FT-IR spectra of films based on a: Chitosan-Gelatin blend (CS-GL) as a control and those enriched with EOs (1%, v/v).

3.4. Thickness

The thickness values for control and active films are reported in Tab. 2. Thickness ranged from 21.66 µm to 33.41 µm: the control film had the lowest value ($p<0.05$), while incorporation of EOs into the CS-GL film increased the thickness ($p<0.05$). Bearing in mind that all films were prepared by casting the same amount of FFS on Petri dishes with the same surface, the difference in thickness might be explained by the different composition of FFS. Indeed, the addition of low molecular weight EOs into the FFS resulted in disrupting and restructuring of intermolecular interactions between CS and GL, increasing free volumes and the mobility of macromolecules, as it was confirmed by SEM images. Moreover, different chemical compounds present in EOs (Tab. 1) may enhance the spatial distance within the film matrix which led to thicker films (Khezrian & Shahbazi, 2018). A similar effect of EO on film thickness was reported by Ojagh et al. (2010). In contrast, Siracusa et al. (2018) found that addition of citral EO to pectin and sodium alginate films significantly reduced thickness. This might be due to an increase in homogeneity and to the creation of a well-organized and dense network upon addition of citral EO, but also to the extended drying time required.

Table 2. Thickness, tensile strength (TS), elongation at break (E%) and elastic modulus (EM) of the films based on chitosan-gelatin blend (CS-GL) as a control and those enriched with EOs (1%, v/v).

Film sample	Thickness (μm)	TS (MPa)	E (%)	EM (MPa)
CS-GL-Control	21.9 ± 1.2^{a}	41.5 ± 4.1^{bc}	2.6 ± 0.1^{a}	2231 ± 226^{bc}
CS-GL-Cinnamon	$32.8 \pm 1.\ 9^{c}$	29.5 ± 2.8^{a}	2.9 ± 0.1^{a}	1340 ± 056^{a}
CS-GL-Citronella	30.4 ± 1.6^{c}	36.4 ± 3.1^{ab}	2.2 ± 0.2^{a}	2017 ± 200^{b}
CS-GL-Pink clove	32.3 ± 2.2^{c}	32.4 ± 3.0^{a}	2.5 ± 0.3^{a}	2201 ± 074^{b}
CS-GL-Nutmeg	27.4 ± 2.3^{b}	47.7 ± 1.5^{c}	2.5 ± 0.2^{a}	2374 ± 205^{bc}
CS-GL-Thyme	26.7 ± 1.3^{b}	45.2 ± 3.8^{c}	2.6 ± 0.2^{a}	2661 ± 239^{c}

Values are given as mean ± SD (n = 3).
Different letters in the same column indicate significant differences ($p<0.05$).

3.5. Mechanical properties

The tensile strength (TS), percent elongation at break (E%) and elastic modulus (EM) are the most common mechanical parameters for food packaging applications (Acevedo-Fani, Salvia-Trujillo, Rojas-Graü, & Martín-Belloso, 2015). A bio-based film must be resistant to the normal stress that occurs in the application, shipping and handling to maintain the integrity and properties of foods. The mechanical properties of control and active films are presented in Tab. 2. The TS is the measurement of film strength: the films incorporated with cinnamon and pink clove EOs showed lower TS than the control film ($p<0.05$), whereas, films incorporated with citronella, nutmeg and thyme were as resistant as the control film. Several studies reported that the addition of EO reduced TS by decreasing cohesion forces within the polymers in the film matrix (Acevedo-Fani, Salvia-Trujillo, Rojas-Graü, & Martín-Belloso, 2015). It seems likely that strong polymer-polymer interactions between CS and GL molecules are partially replaced by the weaker polymer-oil interactions in the film matrix. Also, EO as a hydrophobic compound causes heterogeneous film network and discontinuous microstructure by rearrangement of biopolymers, leading to a decline in the mechanical resistance as it has been confirmed by SEM images (Atarés & Chiralt, 2016; Kim, Beak, & Song, 2018). In contrast, a different result was reported by Ojagh et al. (2010),

who found that the addition of EO to CS films significantly increased the TS value. Authors concluded that the strong interaction between CS and EO determined a cross-linking effect leading to an increase in TS. The TS of packaging film must be more than 3.5 MPa, according to conventional standards (Hosseini, Rezaei, Zandi, & Farahmandghavi, 2015). In this study, the TS value of control and active CS-GL films ranged from 29.5 to 47.7 MPa which is a high value for its application as packaging material.

E% is related to film flexibility and stretchability. The E% values ranged from 2.2% to 2.9% indicating that all films were quite brittle. No significant difference was observed in the E% of control and active films ($p>0.05$). Souza et al. (2017) also found that the incorporation of different EOs and hydroalcoholic extracts into CS film did not induce significant differences in E% values.

The EM stands for the resistance of the film to elastic deformation and this parameter indicates the rigidity or stiffness of the film. A low EM value corresponds to a flexible film while a larger EM value indicates a more rigid material. The cinnamon-added films showed the lowest EM value (1340 MPa) meaning that the CS-GL film lost its stiffness and became more flexible with the addition of cinnamon EO ($p<0.05$). However, films containing citronella, pink clove, nutmeg, and thyme EOs showed EM values similar to the control film. Overall, it seems that cinnamon EO acts as a plasticizer since it determines a lower TS and a higher E% (softer and more extensible film). Nutmeg and thyme seem to act as crosslinkers, slightly increasing TS. However, the effects on mechanical properties, are hardly noticeable and may depend on the low relative amounts of EO in the FFSs.

3.6. UV barrier, light transmittance, and opacity value

UV barrier, light transmittance and opacity value of control and active films are presented in Tab. 3. Active films behave as effective UV barriers, since transmittance

value was below 10% at 280 nm for these films. The UV barrier property of bio-based films is an important parameter for food packaging applications since it can retard lipid oxidation and preserve the organoleptic properties of the packaged food, thereby prolonging its shelf-life (Ramos, Valdés, Beltrán, & Garrigós, 2016).

Active films showed lower transmittance in the visible range (400 - 800 nm) than the control film indicating that the incorporation of EOs into the film matrix reduced the transparency of the film. The light barrier property is an important factor for food preservation to avoid photo-oxidation of organic compounds and degradation of vitamins and other pigments (Figueroa-Lopez et al., 2018). The control and CS-GL-Thyme films can be considered as transparent (opacity value: 2.6 and 5.2 respectively) while films containing cinnamon, citronella, pink clove, and nutmeg EOs were less transparent. Overall, the transparency of the films decreased with the addition of EOs due to the light scattering of oil droplets (with a different refractive index) in the CS-GL film network which interferes with the transmission of light. Similar result was reported by Bonilla, Poloni, Lourenco & Sobral (2018) and Kim et al. (2018).

Table 3. UV and visible light transmittance (T%) and opacity value (600 nm) of the films based on chitosan-gelatin blend (CS-GL) as a control and those enriched with EOs (1%, v/v).

Film sample	Light Transmission (%) at different wavelength (nm)								Opacity value
	200	280	350	400	500	600	700	800	
CS-GL-Control	0.16	38.2	67.1	78.8	85.6	87.6	88.5	88.8	02.6 ± 0.1^{a}
CS-GL-Cinnamon	0.02	0.01	11.4	21.5	25.9	28.4	30.4	31.6	16.7 ± 1.2^{d}
CS-GL-Citronella	0.03	3.05	16.7	22.1	27.8	31.4	34.9	37.6	15.3 ± 2.0^{bc}
CS-GL-Pink clove	0.02	0.01	07.9	26.8	35.2	41.2	44.5	46.6	12.0 ± 0.9^{b}
CS-GL-Nutmeg	0.05	7.53	28.8	37.1	45.0	49.5	53.6	56.3	11.1 ± 0.9^{b}
CS-GL-Thyme	0.09	0.05	57.7	64.4	69.7	72.8	75.1	76.5	05.2 ± 0.5^{a}

Values are given as mean ± SD (n = 3).
Different letters in the same column indicate significant differences ($p<0.05$).

3.7. Color

The color values (L*, a* and b*) and total color difference (ΔE*) of control and active films are shown in Tab. 4. The L* value, indicating lightness, decreased upon addition

of EOs. This value varied between 98.3 and 95.3, which means that all the films were almost clear. A similar result was reported by (Bonilla & Sobral, 2016).

The a* value, expressing the green-red color component, was negative for all films except for those added with cinnamon and pink clove, which showed a slightly positive a* value (+1.9 and +1.3, respectively) due to the presence of red-colored substances in the cinnamon and pink clove EOs. The b* value measures the blue-yellow color component. This value significantly increased upon addition of EOs ($p<0.05$), indicating the gain of a slight yellow color. The CS-GL films incorporated with cinnamon and pink clove showed the highest b* value (8.0 and 6.9, respectively) which, in agreement with the a* value, demonstrate the presence of colored compounds into the extracts. The total color difference (ΔE^*) measures the overall color change of a test sample compared with a reference color. The ΔE^* value varied from 2.5 in the control film to 8.7 in CS-GL-Cinnamon film. The addition of EOs to the CS-GL film generally increased the ΔE^* value ($p<0.05$). The CS-GL films incorporated with cinnamon and pink clove showed the highest ΔE^* values ($p<0.05$) mainly due to the lower brightness (L*) and to the increase observed in the colorimetric coordinate a* and b*. Some relation can be found also between the higher ΔE^* and the lowest light transmission values observed in the wavelength range 350 - 500 nm, which suggest that the compounds present in cinnamon and pink clove EOs absorb in this range, which corresponds to the yellow-red color measured by the a* and b* coordinates. Nevertheless, the color of the developed films can change the overall appearance of the food inside the packaging and affecting customer acceptance (Atarés & Chiralt, 2016).

Table 4. Color parameters (L*, a* and b*) and total color difference (ΔE*) of the films based on chitosan-gelatin blend (CS-GL) as a control and those enriched with EOs (1%, v/v).

Film sample	Color parameters			
	L*	a*	b*	ΔE*
CS-GL-Control	98.3 ± 0.3^{c}	-0.5 ± 0.1^{a}	2.2 ± 0.1^{a}	2.5 ± 0.2^{a}
CS-GL-Cinnamon	96.4 ± 1.3^{ab}	$+1.3 \pm 0.3^{b}$	8.0 ± 0.8^{c}	8.7 ± 0.4^{c}
CS-GL-Citronella	97.6 ± 0.2^{bc}	-0.9 ± 0.1^{a}	4.5 ± 0.2^{b}	4.9 ± 0.3^{b}
CS-GL-Pink clove	95.3 ± 0.4^{a}	$+1.9 \pm 0.9^{b}$	6.9 ± 0.3^{c}	8.3 ± 0.6^{c}
CS-GL-Nutmeg	97.5 ± 0.2^{bc}	-0.8 ± 0.1^{a}	4.7 ± 0.5^{b}	5.2 ± 0.6^{b}
CS-GL-Thyme	97.8 ± 0.1^{bc}	-0.6 ± 0.1^{a}	4.3 ± 0.2^{b}	4.6 ± 0.2^{b}

Values are given as mean ± SD (n = 3).
Different letters in the same column indicate significant differences ($p<0.05$).

3.8. Moisture content, water solubility, and water vapor permeability

The moisture content (MC), water solubility (WS) and water vapor permeability (WVP) of control and active films are presented in Tab. 5. The control film showed the lowest MC value (15.80%), while the addition of EOs increased the MC value ($p<0.05$). The MC is a parameter related to the total free volume occupied by water molecules in the network of the films. The loose microstructure of active films caused the film matrix to have a relatively high free volume and consequently increased the MC as confirmed by SEM images. Similarly, Abdollahi, Rezaei, & Farzi (2012) reported that the addition of rosemary EO to the CS film increased the MC. Authors concluded that the increase in the MC value might be related to the breakup of the film network, which caused an increasing amount of water molecules between polymer chains. In contrast, Nisar et al. (2018) reported that addition of clove EO to pectin film reduced the MC value due to the hydrophobic properties of the EOs and interaction of oil components with hydroxyl groups of pectin film. This could limit the interaction of hydroxyl groups with water molecules, leading to a reduction of MC.

The WS reflects the water resistance and the biodegradability of films (Zhang, Ma, Critzer, Davidson, & Zhong, 2015). Moreover, the WS can determine the release of antimicrobial substances from the films when placed in contact with the food surface (Abdollahi et al., 2012). Water resistance or insolubility is usually essential for potential

application of bio-based films for food packaging applications especially in humid environments (Nisar et al., 2018). The WS of control film was determined as 23.61 %. Addition of nutmeg EOs to the CS-GL film reduced the WS ($p<0.05$) due to the high hydrophobic nature of nutmeg, while, films incorporated with cinnamon, citronella, pink clove, and thyme EOs showed an increase in WS ($p<0.05$). This might be due to the difference in hygroscopic properties of these EOs by which they attract water molecules and the ability to establish polymer-oil interactions which weaken the CS-GL interactions (Gómez-Estaca, López de Lacey, López-Caballero, Gómez-Guillén, & Montero, 2010; Nisar et al., 2018).

The shelf life of some food products is directly related to the transfer of water between the product and the external environment in which they are introduced. Generally, packaging material should reduce this transfer of water to preserve foods from moisture (de Moraes Crizel et al., 2018; Hosseini, Rezaei, Zandi, & Farahmandghavi, 2016; Kim et al., 2018). Therefore, effective control of moisture transfer is a desirable property for the food packaging industry. The CS-GL films containing cinnamon, citronella, pink clove and thyme had higher WVP values compared to the control film ($p<0.05$). The irregular structures with the presence of air bubbles and oil droplets in these films might lead to a weakening of intermolecular interactions between polymer molecules, resulting in an open structure and increased water vapor transfer across the films and consequently an increase of the WVP value. A similar result was reported by Atarés, Bonilla, & Chiralt (2010) that addition of ginger EO to soy protein isolate increased the WVP. These authors concluded that addition of ginger EO might cause disruption in film network and affect the microstructure properties which is a determining factor in WVP value. In this study, despite the statistical differences, the WVP varied between 0.8 and 1.2 (g mm/kPa day m^2). In practical terms, this means that all films were highly permeable to water vapor.

Table 5. Moisture content (MC), water solubility (WS), water vapor transmission rate (WVTR) and water vapor permeability (WVP) of the films based on chitosan-gelatin blend (CS-GL) as a control and those enriched with EOs (1%, v/v).

Film sample	MC (%)	WS (%)	WVP 75:0% RH (g mm/kP day m^2)
CS-GL-Control	15.80 ± 0.33^{a}	23.61 ± 0.58^{b}	0.8172 ± 0.0027^{a}
CS-GL-Cinnamon	18.71 ± 0.80^{b}	30.24 ± 0.75^{d}	1.1344 ± 0.1298^{bc}
CS-GL-Citronella	19.15 ± 0.44^{b}	26.53 ± 0.53^{c}	1.1396 ± 0.2069^{bc}
CS-GL-Pink clove	23.78 ± 1.81^{c}	29.51 ± 1.40^{d}	1.2460 ± 0.4576^{c}
CS-GL-Nutmeg	17.71 ± 1.39^{ab}	20.36 ± 1.09^{a}	0.8853 ± 0.1237^{ab}
CS-GL-Thyme	18.78 ± 0.97^{b}	31.67 ± 1.71^{d}	1.2851 ± 0.3761^{c}

Values are given as mean ± SD (n = 3).
Different letters in the same column indicate significant differences ($p<0.05$).

3.9. In vitro antimicrobial activity

Antimicrobial activity of films was evaluated by the disk diffusion assay. The details of antimicrobial activity of control and active films against *C. jejuni, E. coli*, *L. monocytogenes,* and *S. typhimurium* are shown in Tab. 6. The control film did not show an inhibitory effect against any of the tested microorganisms. The absence of inhibitory character could be explained by the limitation of CS diffusion in agar medium or incapability of GL to inhibit bacterial growth as it has been reported by other authors (Leceta, Guerrero, Ibarburu, et al., 2013) so that only microorganisms in direct contact with the active sites of CS in the CS-GL film network are inhibited (Haghighi, De Leo, et al., 2019; Yuan, Chen, & Li, 2016).

Incorporating EOs into the films revealed an antimicrobial effect. In general, due to the hydrophobic nature of EOs, they can interact with polysaccharides, fatty acids and phospholipids of bacteria cell membranes and make them more permeable, so that leakage of ions and cell contents leads to bacterial cell death (Burt, 2004; Salvia-Trujillo, Rojas-Graü, Soliva-Fortuny & Martín-Belloso, 2015).

In this study, all active films inhibited the growth of the tested microorganisms. Thyme EO was the most effective ($p<0.05$). Thyme EO showed inhibition activity which was, for all pathogens excluding *L. monocytogenes*, at least double compared to the other

EOs. This might be due to the higher WS of CS-GL-Thyme films compared to the other films (Tab. 5). Moreover, thymol and carvacrol are two main phenolic compounds (monoterpenoids) representing 44.2% of the total chromatographic area in thyme EO (Tab. 1). The high antimicrobial activity of phenolic compounds such as thymol and carvacrol has been attributed to structural and functional damages to the bacterial cytoplasmic membrane and to the inhibition of intracellular metabolic pathways (Cao, Yang, & Song, 2018). It should be noted that thyme EO exerted the highest inhibition against *C. jejuni*, *E. coli* and *S. typhimurium*, while its antimicrobial effectiveness against *L. monocytogenes* was lower and comparable with other EOs.

In general, the tested EOs were more effective against *C. jejuni* compared to the other considered microorganisms, showing inhibition haloes from 1.5 to 5-fold wider. The only exception to this observation was represented by nutmeg EO, which showed higher inhibition (comparable with the other EOs) of *E. coli* and *L. monocytogenes* but which, however, yielded the lowest effectiveness, hardly noticeable against *C. jejuni* and *S. typhimurium*.

Table 6. Inhibition zone diameters of the film disks (22 mm diameter) based chitosan-gelatin blend (CS-GL-Control) as a control and those enriched with EOs (1%, v/v).

Film sample	*C. jejuni*	*E. coli*	*L. monocytogenes*	*S. typhimurium*
CS-GL-Control	N. D.	N. D.	N. D.	N. D.
CS-GL-Cinnamon	5.3 ± 0.9^{bB}	2.7 ± 0.5^{aA}	2.0 ± 0.5^{aA}	1.0 ± 0.1^{aA}
CS-GL-Citronella	4.3 ± 1.9^{abA}	2.8 ± 0.7^{aA}	2.3 ± 0.5^{aA}	2.8 ± 0.7^{aA}
CS-GL-Pink clove	5.3 ± 0.9^{bB}	3.5 ± 0.2^{aAB}	2.4 ± 0.3^{aA}	3.0 ± 0.1^{aA}
CS-GL-Nutmeg	0.4 ± 0.1^{aA}	2.7 ± 0.3^{aC}	2.3 ± 0.5^{aBC}	1.0 ± 0.5^{aAB}
CS-GL-Thyme	11.3 ± 0.9^{cC}	5.7 ± 0.5^{bB}	3.0 ± 0.1^{aA}	6.2 ± 0.7^{bB}

Values are given as mean ± SD (n = 3). N.D means as not detected.
Different lowercase letters in the same column indicate significant differences ($p<0.05$).
Different capital letters in the same row indicate significant differences ($p<0.05$).

4. Conclusions

In this study, bio-based CS-GL blend active films enriched with cinnamon, citronella, pink clove, nutmeg and thyme EOs (1%, v/v) were developed and their physical,

optical, mechanical, water barrier and microstructural properties were evaluated for active food packaging applications. The FT-IR spectra confirmed intermolecular interactions between functional groups of the EOs with the hydroxyl and amino groups of the CS-GL film network. The results showed that the incorporation of different EOs could notably improve the UV barrier properties of CS-GL film, however, light transparency was reduced. The developed films, with special regards for those including thyme EO, possessed noticeable antimicrobial activity against common food pathogens. The moisture content and water vapor permeability of CS-GL film increased by EOs incorporation due to the microstructure change and presence of pores on the surface as confirmed by SEM. The results suggest that the CS-GL films enriched with different EOs could be used as environmentally friendly, active food packaging with antimicrobial properties and potential to extend the shelf life of food products.

Appendix A. Supplementary material

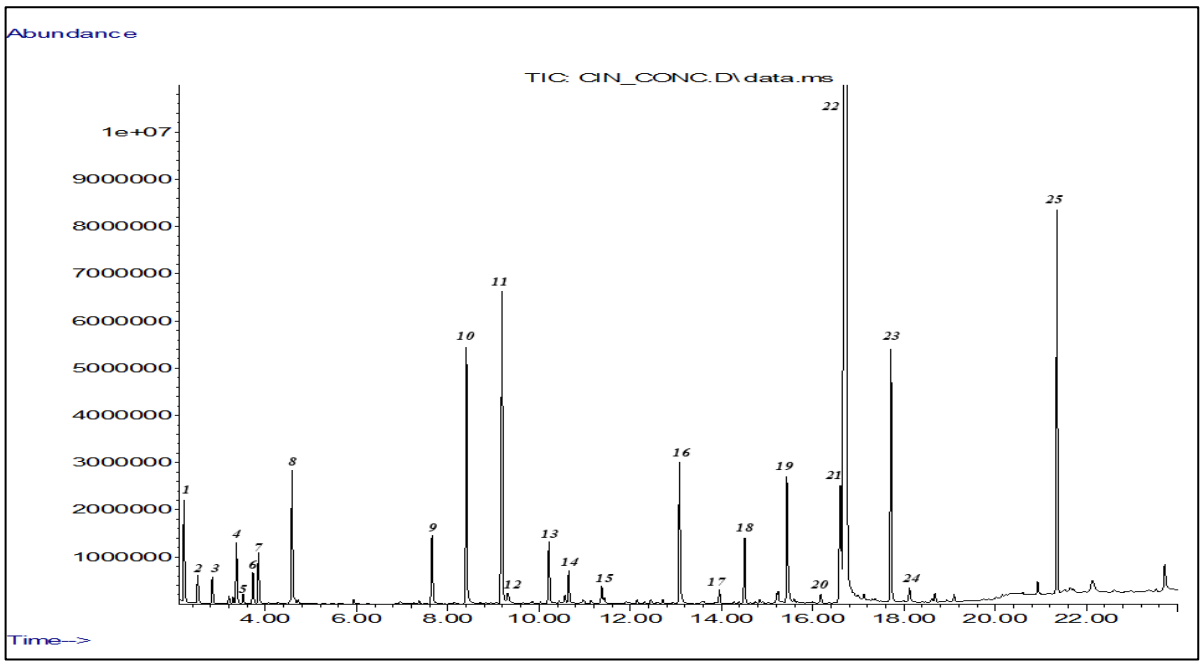

Fig. S1. Cinnamon essential oil chromatogram including: 1. α-pinene; 2. camphene; 3. β-pinene; 4. phellandrene; 5. α-terpinene; 6. limonene; 7. sabinene; 8. o-cymene; 9. α-cubebene; 10. linalool; 11. β-caryophyllene; 12. 4-terpineol; 13. α-humulene; 14. α-terpineol; 15. δ-cadinene; 16. safrole; 17. allylbenzene; 18. caryophyllene oxide; 19. cinnamaldehyde; 20. spathulenol; 21. cinnamyl acetate; 22. eugenol; 23. acethyleugenol; 24. cinnamyl alcohol; 25. benzyl benzoate

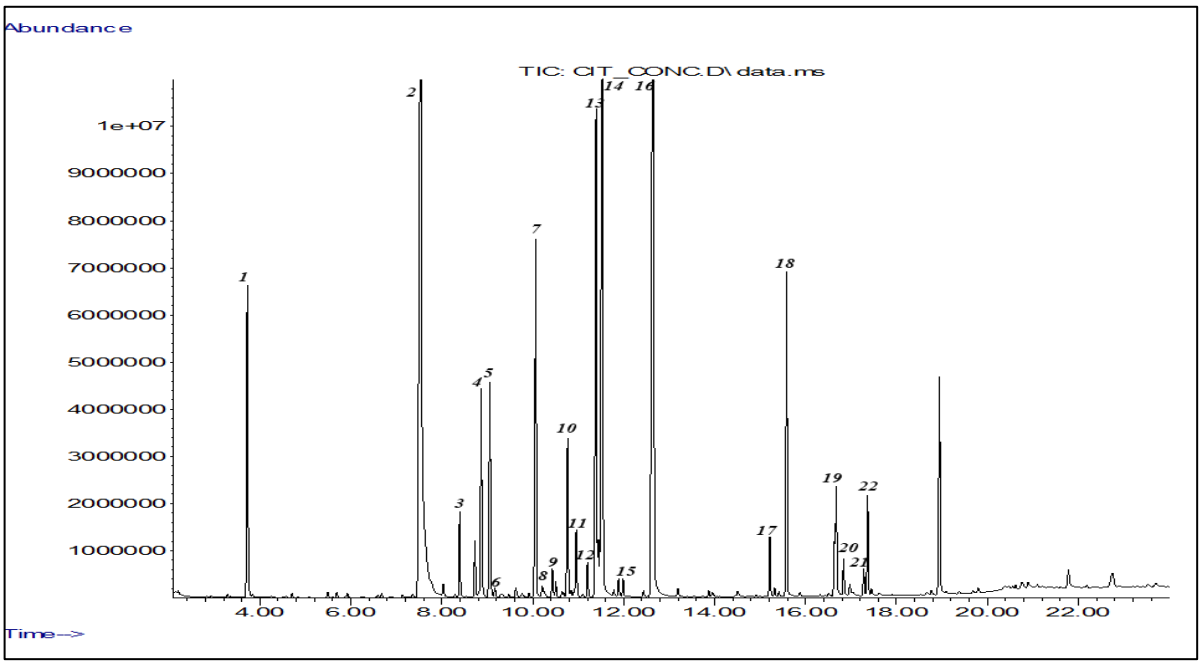

Fig. S2. Citronella essential oil chromatogram including: 1. limonene; 2. citronellal; 3. linalool; 4. isopulegol; 5. β-elemene; 6. β-caryophyllene; 7. citronellyl acetate; 8. α-humulene; 9. α-amorphene; 10. β-cubebene; 11. α-muurolene; 12. citral; 13. δ-cadinene; 14. β-citronellol; 15. nerol; 16. geraniol; 17. α amorphene; 18. elemol; 19. eugenol; 20. muurolol; 21. α-eudesmol; 22. α-cadinol

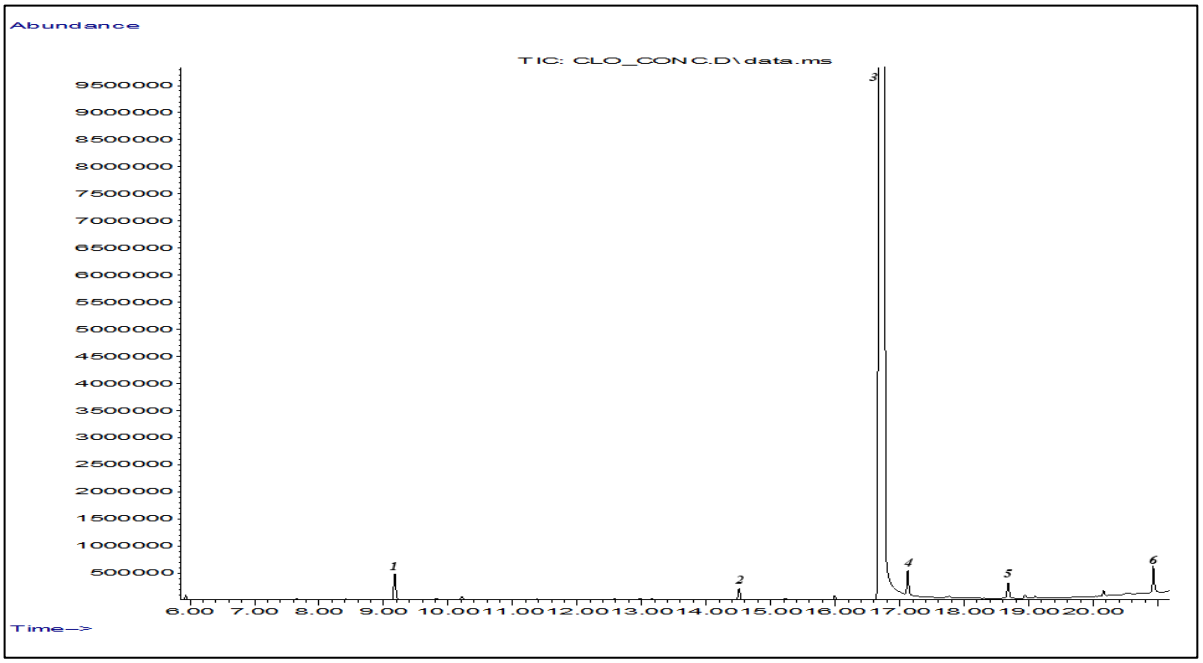

Fig. S3. Pink clove essential oil chromatogram including: 1. β-caryophyllene; 2. caryophyllene oxide; 3. eugenol; 4. carvacrol; 5. chavicol; 6. vanillin

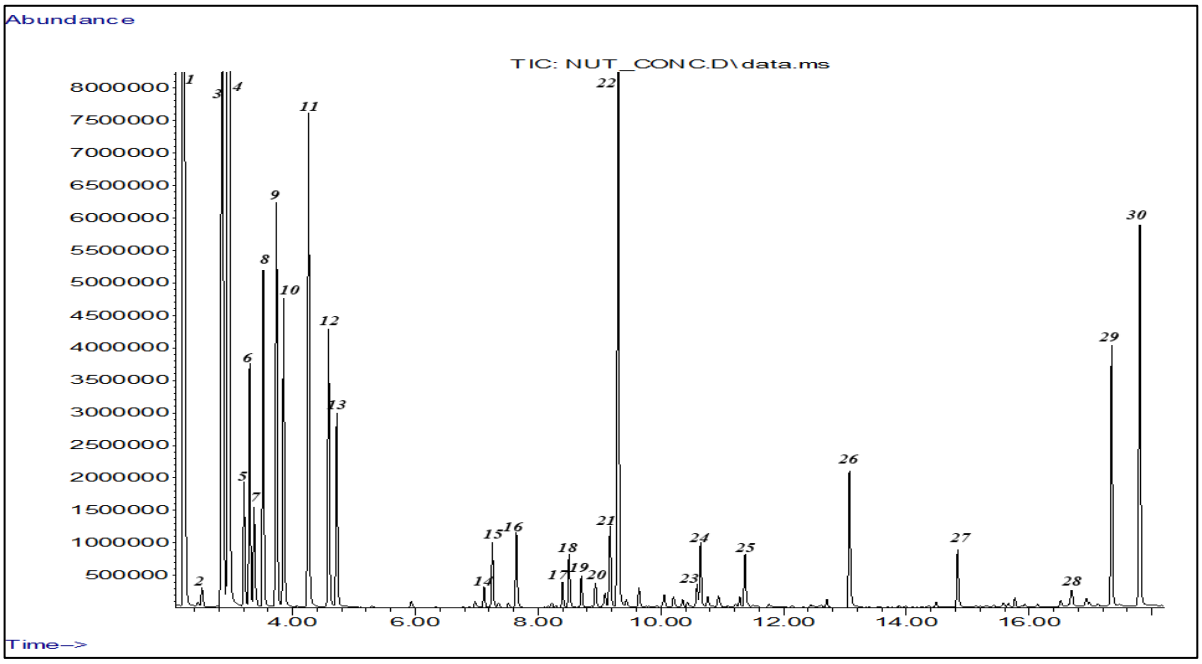

Fig. S4. Nutmeg essential oil chromatogram including:1. α-pinene; 2. camphene; 3. β-pinene; 4. sabinene; 5. δ-3-carene; 6. β-myrcene; 7. phellandrene; 8. α-terpinene; 9. limonene; 10. sabinene; 11. γ-terpinene; 12. p-cymene; 13. α-terpinolene; 14. α-cubebene; 15. trans thujan-4-ol; 16. α-copaene; 17. linalool; 18. β-terpineol; 19. 1-terpineol; 20. α-fenchyl acetate; 21. β-caryophyllene; 22. 4-terpineol; 23 camphene; 24. α-terpineol; 25. δ-cadinene; 26. safrole; 27. methyleugenol; 28. eugenol; 29. elemicin; 30. myristicin.

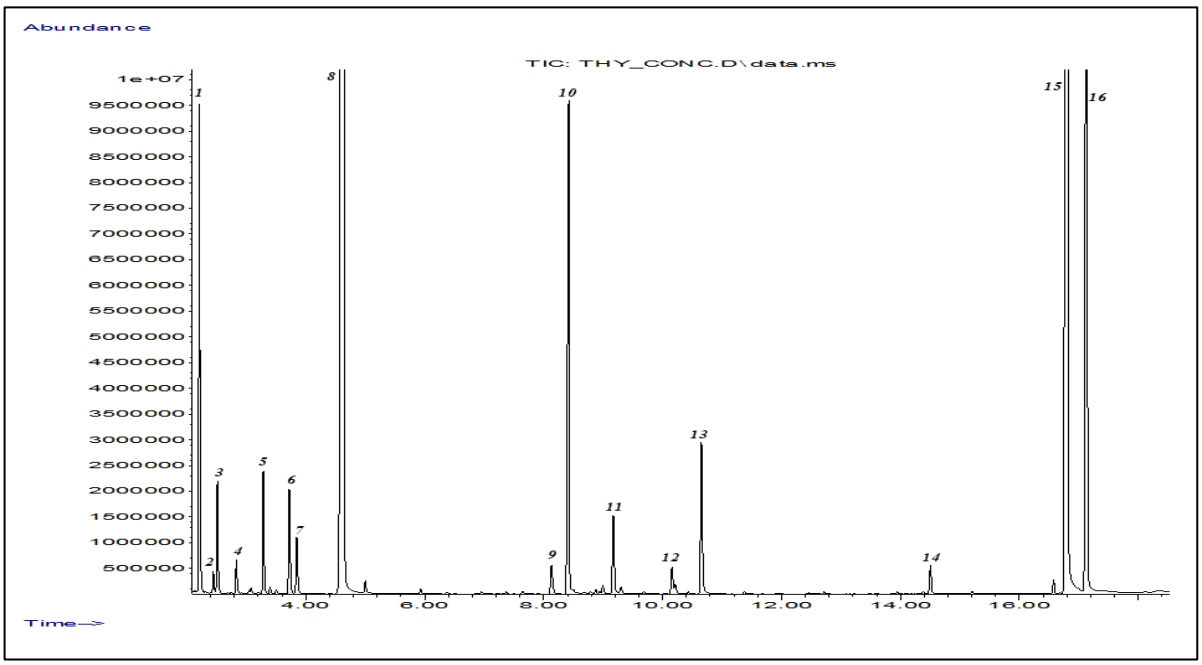

Fig. S5. Thyme essential oil chromatogram including:1. α-pinene; 2. α-fenchene; 3. camphene; 4. β-pinene; 5. β-myrcene; 6. limonene; 7. 1,8-cineole; 8. p-cymene; 9. camphor; 10. linalool; 11. β-caryophyllene; 12. isoborneol; 13. borneol; 14. caryophyllene oxide; 15. thymol; 16. carvacrol

Chapter 4

Development of antimicrobial films based on chitosan-polyvinyl alcohol blend enriched with Ethyl Lauroyl Arginate (LAE) for food packaging applications

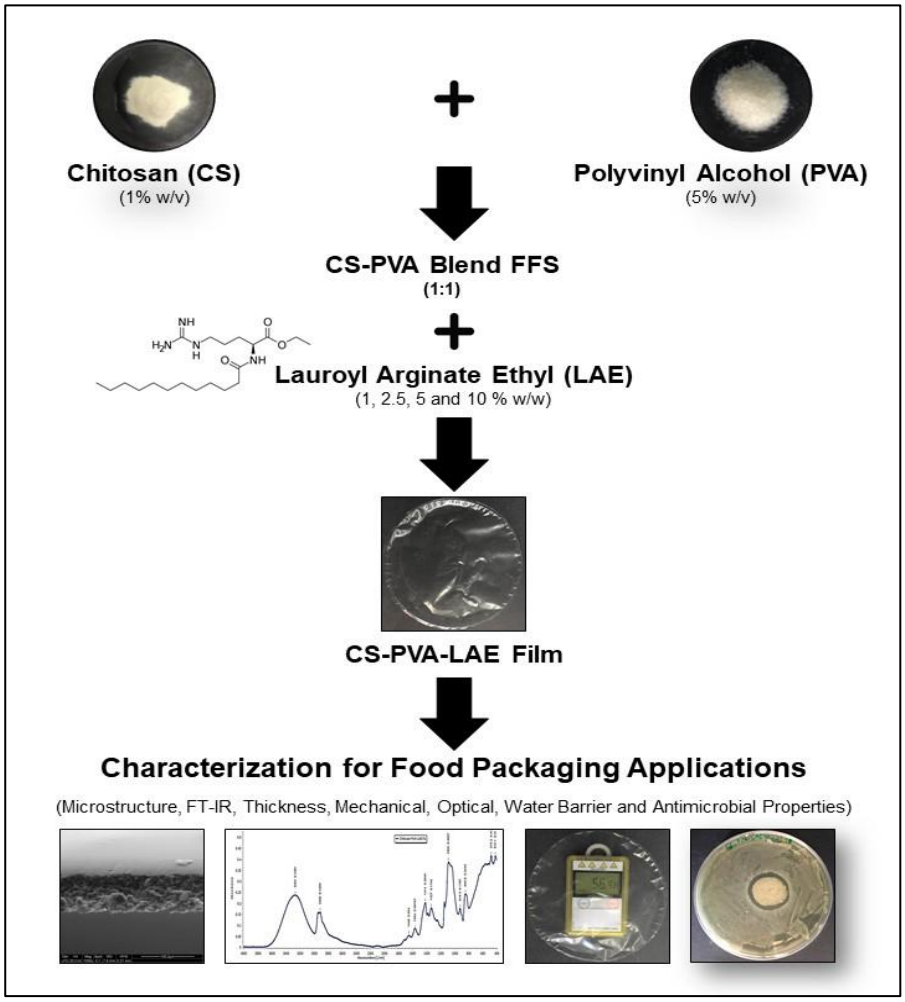

Highlights

- LAE was effectively incorporated into chitosan-polyvinyl alcohol films
- High LAE levels negatively affected mechanical and water barrier properties
- Addition of LAE improved UV barrier of chitosan-polyvinyl alcohol blend films
- The developed active films were effective against four food bacterial pathogens

Abstract

The main aim of this study was to characterize microstructural, physical, optical, mechanical, water barrier and antimicrobial properties of chitosan-polyvinyl alcohol blend films (CS-PVA) enriched with ethyl lauroyl arginate (LAE) (1-10% w/w) for food packaging applications. The film microstructure was determined by scanning electron microscopy. Active films containing 10% LAE showed cracks on the surface with irregular shape in the cross-section indicating a weaker cohesion of the CS-PVA polymer blend at high LAE concentrations. The possible interaction of CS-PVA blend film with incorporated LAE was also investigated using Fourier-transform infrared (FT-IR) spectroscopy in the attenuated total reflection (ATR) mode. ATR/FT-IR spectra showed a low molecular interaction between the CS-PVA and LAE up to 2.5% while for films containing 5 and 10% LAE such interactions between the functional groups of the CS-PVA matrix and LAE have been detected. The active films were transparent and showed barrier properties against UV and visible light. The incorporation of LAE into the CS-PVA increased the thickness, water solubility, water vapor permeability, and the b* and ΔE* values, while it decreased mechanical properties and transparency ($p<0.05$). Active films inhibited the growth of four major food bacterial pathogens including *Campylobacter jejuni*, *Escherichia coli*, *Listeria monocytogenes,* and *Salmonella typhimurium*. Particularly, films containing 5 and 10% LAE were the most effective ($p<0.05$). Overall, the characterization of functional properties revealed that CS-PVA blend film incorporated with LAE could be used as an environmentally friendly antimicrobial packaging material to extend the shelf life of food products.

1. Introduction

The current trend in food packaging is mainly oriented towards the substitution of non-biodegradable petroleum-based polymers by packaging materials that are eco-friendly and also prolong food shelf life (Kanatt, Rao, Chawla, & Sharma, 2012). In this context,

considerable research has been conducted involving the fabrication of biodegradable food packaging materials that come from renewable natural resources and agri-food industry wastes (Cazón, Vázquez, & Velazquez, 2018; Sarwar, Niazi, Jahan, Ahmad, & Hussain, 2018). Among bio-based natural polymers, chitosan (CS) has received significant attention for its potential to substitute - partially or totally - petroleum-based polymers (Leceta, Guerrero, & De La Caba, 2013). CS is a cationic linear polysaccharide consisting of poly-β-(1–4)-D-glucosamine units obtained by partial deacetylation of chitin, the major component of the insect's exoskeleton and shells of crustacean such as crab, shrimp, and crawfish. CS is the second most abundant polysaccharide after cellulose with unique biological properties such as biocompatibility, biodegradability, and non-toxicity. In addition, this amino polysaccharide has high antimicrobial activity against many pathogenic and spoilage microorganisms, including both Gram-positive and Gram-negative bacteria which makes it an excellent candidate for food packaging applications (Rubilar, Candia, Cobos, Díaz, & Pedreschi, 2016). However, there are some limitations which are associated with CS such as low mechanical strength, low thermal stability, rigid crystalline structure, and high production cost. A simple and effective alternative to overcome these drawbacks could be blending of CS with synthetic polymers. Films formed by the blending of natural and synthetic polymers represent a new class of material with modified physical and mechanical properties compared to films made of individual components. Blending CS with polyvinyl alcohol (PVA) has been intensively investigated by many researchers to gain biodegradable and antimicrobial films for food packaging applications with new and desired properties (Bonilla, Fortunati, Atarés, Chiralt, & Kenny, 2014; Kanatt et al., 2012; Liu, Wang, & Lan, 2018; Tripathi, Mehrotra, & Dutta, 2009; Parida, Nayak, Binhani, & Nayak, 2011).

PVA is a synthetic, low cost, non-toxic and water-soluble polymer commercially obtainable from hydrolysis of polyvinyl acetate with excellent film-forming properties. Despite its synthetic character, this polymer was recognized as biodegradable and it shows high tensile strength, flexibility, gas barrier properties and good resistance to acid and alkali media (Aloui et al., 2016). PVA has been evaluated for safety by the Joint FAO/WHO Expert Committee on Food Additives (JECFA) in 2003 at the 61st meeting (Bellelli, Licciardello, Pulvirenti, & Fava, 2018) and it has also been approved for use in packaging meat and poultry products by the USDA (Kanatt et al., 2012). PVA is highly miscible with other hydrophilic polymers such as CS, owing to the formation of intermolecular hydrogen bonds between hydroxyl groups of PVA and hydroxyl and amine groups of CS. Due to the high compatibility of CS and PVA, the resulting films show homogeneous structure. Moreover, blending PVA with CS is a promising strategy to reduce the production cost and improve the mechanical property and stability of CS films.

Antimicrobial packaging as a part of active packaging systems is intended to extend the shelf life of food products and assure the safety and quality of packaged foods (Tripathi, Mehrotra, & Dutta, 2008). Ethyl lauroyl arginate (LAE) is considered as an effective antimicrobial substance among novel food additives (Rubilar et al., 2016). LAE remains stable at pH 3-7 and is odorless and colorless as well (Kashiri et al., 2016). LAE is a synthetic surfactant consisting of an ethyl esterified arginine head with a lauroyl tail attached to the α-amino group that is highly active against a wide range of food pathogens and spoilage microorganisms including bacteria, yeast, and molds with a low-dose application (Becerril, Manso, Nerin, & Gómez-Lus, 2013). This cationic surfactant disrupts the cytoplasmic membrane of microorganisms and inhibits the growth of microorganisms by causing cell deformation and affecting their metabolic process negatively (Muriel-Galet, Carballo, Hernández-Muñoz, & Gavara, 2016). LAE

has been considered as GRAS (generally recognized as safe) by the U.S. Food and Drug Administration (FDA, 2005b) and has been authorized as food preservative by the European Food Safety Authority (EFSA, 2007). Incorporation of LAE as an antimicrobial compound into antimicrobial packaging to improve food safety and quality has been reported in several studies (De Leo et al., 2018; Haghighi, De Leo, et al., 2019; Higueras, López-Carballo, Hernández-Muñoz, Gavara, & Rollini, 2013; Kashiri et al., 2016; Moreno, Cárdenas, et al., 2017; Rubilar et al., 2016). However, literature concerning the effects of LAE on the functional properties of CS-PVA blend film is not available. Therefore, the objective of the present study was to develop biodegradable films based on CS-PVA blend enriched with different concentrations of LAE to evaluate microstructural, physical, optical, mechanical and water barrier properties for food packaging applications. Moreover, the antimicrobial activity of films against four common food bacterial pathogens including *Campylobacter jejuni*, *Escherichia coli*, *Listeria monocytogenes,* and *Salmonella typhimurium,* was investigated.

2. Material and methods

2.1 Materials and reagents

Chitosan (CS) with a molecular weight of 100-300 kDa was obtained from Acros Organics™ (China). Polyvinyl alcohol (PVA) with molecular weight of 27 kDa and 98% degree of hydrolysis was purchased from Fluka (Steinheim, Germany). Glycerol (≥ 99.5%) was purchased from Merck (Darmstadt, Germany). Acetic acid (≥ 99.5%) was obtained from Brenntag S.p.A (Milan, Italy). Ethyl lauroyl arginate (LAE) was kindly provided as Mirenat-D (69.3% LAE and 30.7% maltodextrin) by Vedeqsa Grupo LAMIRSA (Terrassa, Barcelona, Spain). Brain heart infusion agar (BHIA) was purchased from Biolife (Milan, Italy).

2.2. Preparation of film-forming solutions (FFSs) and films

Preparation of films was adapted from the procedures of Higueras et al., (2013) and Kanatt et al., (2012) with slight modification. In this study, four CS-PVA blend films enriched with different concentrations of LAE (1, 2.5, 5 and 10% w/w of biopolymer) were analyzed. Furthermore, a CS-PVA film-forming solution (FFS) without LAE was used to produce a control film. The CS FFS (1%, w/w) was prepared by dissolving CS in an acetic acid solution (1%, v/v) under continuous stirring at 55 °C for 60 min. The PVA FFS (5%, w/w) was prepared by dissolving PVA in distilled water at 80 °C for 60 min. Glycerol (0.5%, v/v of FFS) was then added as a plasticizer into both FFSs, followed by additional stirring for 60 min. The CS-PVA blend FFS was prepared by mixing CS and PVA FFSs at 1:1 ratio and final plasticizer content was 17 g glycerol/ 100 g dry polymer. Different amounts of LAE were added to the CS-PVA blend FFS to obtain active films with 1-10% LAE (g of LAE/100 g of dry CS-PVA blend) considering the LAE concentration (69.3%) in Mirenat-D. All FFSs were degasified with a vacuum pump (70 kPa) for 15 min to remove bubbles. Films were obtained by casting 20 mL of the FFS into Petri dishes (14.4 cm in diameter) and drying at 25 ± 2 °C in the chemical hood overnight.

2.3. Scanning electron microscopy (SEM)

The SEM images from the surface and cross-section of the films were obtained with the use of a scanning electron microscope (FEI, Quanta 200, Oregon, USA). Film samples were fixed on a stainless-steel support with a double-sided conductive adhesive. The analysis was conducted in a low vacuum (0.6 Torr) at an acceleration voltage of 20 kV.

2.4. Atomic force microscopy (AFM)

The surface morphology of the films was analyzed using an atomic force microscope (Park Scientific Instruments, South Korea). Films were fixed onto AFM specimen metal

discs using a double-sided tape and then placed to a magnetic sample holder located on the top of the scanner tube. The images were scanned in no-contact mode under ambient condition. The surface roughness (R_a) of the films was calculated on the basis of the root mean square (R_q) deviation from the average height of peaks after subtracting the background using ProScan software (version 1.51b). All samples were analyzed in triplicate.

2.5 Attenuated Total Reflection (ATR) / Fourier-Transform Infrared (FT-IR) Spectroscopy

The infrared spectra of different films were obtained using an ATR/FT-IR spectrometer (type Alpha, Bruker Optik GmbH, Ettlingen, Germany). Spectra were collected from two different locations from the top and bottom side of the same samples in the 4000 - 400 cm^{-1} wavenumber range by accumulating 64 scans with a spectral resolution of 4 cm^{-1}.

2.6. Thickness

Film thickness was measured with a digital micrometer (Model IP65, SAMA Tools, Viareggio, Italia) at five different random positions (one at the center and four at the edges). The means of these five separate measurements were recorded.

2.7. Mechanical properties

The tensile strength (TS), elongation at break (E%) and elastic modulus (EM) were determined using a dynamometer (Z1.0, Zwick/Roell, Ulm, Germany) according to ASTM standard method D882 (ASTM, 2001a). The films with known thickness were cut into rectangular strips (9.0 x 1.5 cm^2). Initial grip separation and cross-head speed were set at 70 mm and 50 mm/min, respectively. Measurements were repeated 10 times from each type of film. The software TestXpert® II (V3.31) (Zwick/Roell, Ulm, Germany) was used to record the TS curves. TS was calculated by dividing the maximum load to break the film by the cross-sectional area of the film and expressed

in MPa. The E% was calculated by dividing film elongation at rupture by the initial grip separation expressed in percentage (%). EM was calculated from the initial slope of the stress-strain curve and expressed in MPa.

2.8. UV barrier, light transmittance, and opacity value

The barrier properties of films against UV and visible light were determined at the UV (200, 280 and 350 nm) and visible (400, 500, 600, 700 and 800 nm) wavelengths. These optical characteristics were estimated with a VWR®Double Beam UV-VIS 6300PC spectrophotometer (China) using square film samples (2×2 cm^2). The opacity of the films was calculated by Eq. (1):

$$\text{Opacity value} = \frac{-\log T_{600}}{x} \quad (1)$$

where T_{600} is the fractional transmittance at 600 nm and x is the film thickness (mm). The greater opacity value represents the lower transparency of the film. For each film, four readings were taken at different positions and average values were determined.

2.9. color

The color of films was measured with a CR-400 Minolta colorimeter (Minolta Camera, Co., Ltd., Osaka, Japan) at room temperature, with D65 illuminant and 10° observer angle. The instrument was calibrated with a white standard (L* = 99.36, a* = -0.12, b* = -0.07) before measurements. Results were expressed as L* (lightness), a* (red/green) and b* (yellow/blue) parameters. The total color difference (ΔE^*) was calculated using the following Eq. (2):

$$\Delta E^* = \sqrt{[(\Delta L^*)^2 + (\Delta a^*)^2 + (\Delta b^*)^2]} \quad (2)$$

where ΔL^*, Δa^* and Δb^* are the differences between the corresponding color parameter of the samples and that of a standard white plate used as the film background. For each film, five readings were taken at different positions and the average values were determined from the top and bottom sides.

2.10. Moisture content and water solubility

Moisture content (MC) of the films (2 × 2 cm^2) was determined as the percentage of weight loss upon drying to constant weight (Md) in an oven at 105 ± 2 °C and the initial weight (Mw) according to the following Eq. (3):

$$MC\ (\%): \frac{Mw-Md}{Mw} \times 100 \quad (3)$$

The solubility of films (2 × 2 cm^2) in water was determined by drying to constant weight in an air-circulating oven at 105 ± 2 °C (Wi) and then each film was immersed in 50 mL distilled water at 25 °C following Gontard, Guilbert, & Cuq, (1992) with slight modifications. After 24 h, the film samples were dripped and dried to constant weight at 105 ± 2 °C (Wf) to determine the weight of dry matter which was not solubilized in water. The measurement of water solubility (WS) was determined according to the following Eq. (4):

$$WS\ (\%): \frac{Wi-Wf}{Wi} \times 100 \quad (4)$$

All measurements for MC and WS were made in triplicate.

2.11. Water vapor transmission rate and water vapor permeability

Water vapor transmission rate (WVTR) of the films was determined gravimetrically in triplicate according to the ASTM E96 method (ASTM, 2001b) with some modifications. Films were sealed on top of glass test cups with an internal diameter of 10 mm and a depth of 55 mm filled with 2 g anhydrous $CaCl_2$ (0% RH). The cups were placed in desiccators containing $BaCl_2$ (90% RH), which were maintained in incubators at 45 °C. WVTR was determined using the weight gain of the cups and was recorded and plotted as a function of time. Cups were weighed daily for 7 days to guarantee the steady-state permeation. The slope of the mass gain versus time was obtained by linear regression ($r^2 \geq 0.99$). WVTR (g /day m^2) and WVP (g mm/kPa day m^2) were calculated according to the following Eqs. (5) and (6):

$$WVTR = \frac{\Delta W}{\Delta t \times A} \quad (5)$$

$$WVP = \frac{WVTR \times L}{\Delta P} \quad (6)$$

where $\Delta W/\Delta t$ is the weight gain as a function of time (g/day), A is the area of the exposed film surface (m^2), L is the mean film thickness (mm) and ΔP is the difference of vapor pressure across the film (kPa).

2.12. In vitro antimicrobial activity

2.12.1. Disk diffusion assay

Antibacterial activity test on films was assessed against four typical food bacterial pathogens including *Listeria monocytogenes* (UNIMORE 19115), *Escherichia coli* (UNIMORE 40522)*, Salmonella typhimurium* (UNIMORE 14028) and *Campylobacter jejuni* (UNIMORE 33250) using the disk diffusion assay according to (Haghighi, Biard, et al., 2019). Films (sterilized with UV light) were cut into a disc shape of 22 mm diameter and placed on the surface of BHIA agar plates, which had been previously streaked with 0.1 mL of inocula containing 10^6 CFU/mL of tested bacteria. The plates were then incubated at 30 °C for 24 h (*C. jejuni* plates were incubated at 37 °C). The diameter of the inhibition zones was measured with a caliper and recorded in millimeters (mm). All tests were performed in triplicates.

2.12.2. Evaluation of antimicrobial activity in liquid medium

Antimicrobial activity of CS-PVA films enriched with LAE (1-10% w/w) evaluated against *L. monocytogenes*, *E. coli*, *S. typhimurium* and *C. jejuni* in liquid medium (Kashiri et al., 2016). A loop of each strain was transferred to 10 mL of BHIB and incubated at 30 °C (*C. jejuni* plates were incubated at 37 °C) for 24 h to obtain stationary phase (optical density of 0.9 at 600 nm). Then, cells were diluted in BHIB and incubated at 30 °C (*C. jejuni* tube was incubated at 37 °C) to obtain exponential phase (optical density of 0.2 at 600 nm). One hundred µL of microorganism in exponential phase was inoculated into tubes with 10 mL of BHIB. A 0.025 g portion of

film (1.5 x 1.5 cm^2) was added to each tube in sterile conditions. The tubes were incubated at 30 °C for 24 h. As a control, CS-PVA film without LAE was used. Depending on the turbidity of each tube, serial dilutions with NaCL were made and plated on the Petri dishes with BHIA culture medium. Colonies were counted after incubation at 30 °C for 24 h.

2.13. Statistical analysis

The statistical analysis of the data was performed through analysis of variance (ANOVA) using SPSS statistical program (SPSS 20 for Windows, SPSS INC., IBM, New York). The experiment was performed in 3 replicates and the number of repeats varied from one analysis to another and was reported in each subsection. The differences between means were evaluated by Tukey's multiple range test ($p<0.05$). The data were expressed as the mean ± SD (standard deviation).

3. Results and discussion

3.1. Scanning electron microscopy (SEM)

The surface and cross-section images of CS-PVA blend film (control) and CS-PVA film enriched with different concentrations of LAE (1-10% w/w) (active films) are presented in Fig. 1. The film microstructure greatly affects the final physical, mechanical and barrier properties. This is mainly due to the interaction between the film components and LAE. The surface of the control film was smooth and homogenous and did not show pores or cracks indicating good compatibility between CS and PVA to form a blend (Fig. 1a). This could be explained by strong molecular interaction between functional groups of chitosan and PVA. Similar results were reported by Ghaderi, Hosseini, & Gómez-Guillén (2019) and Jahan, Mathad, & Farheen (2016) who noticed that the surface of CS-PVA blend film was homogenous without pores. Addition of LAE up to 1% did not affect the surface morphology of active films (Fig. 1c) indicating LAE was evenly distributed and well dispersed in the film matrix. Small particles and

aggregations were observed at the surface of films with increasing concentration of LAE up to 10% (Fig. 1e, 1g, and 1i). A compact and continuous structure without irregularities like air bubbles and pores and any evidence of phase separation can be observed in the cross-section of the control film (Fig. 1b). The cross-section of active films containing LAE up to 2.5% showed similar results (Fig. 1d and 1f). However, active films containing 5 and10% LAE showed irregular and sponge shape structure (Fig. 1h and 1j). This effect was more obvious in CS-PVA film containing 10% LAE. This might be related to the agglomeration of LAE in the film matrix at high concentrations which resulted in disrupted structures. The interaction between the polymer chains was disturbed by interactions with functional groups of LAE, producing films with less integrity. Gaikwad, Lee, Lee, & Lee (2017) also reported that the order of low-density polyethylene (LDPE) films was interrupted by the addition of high amount of LAE powder (5 and 10%) mainly due to the inhomogeneous distribution of LAE inside the matrix and the low interfacial interaction between the LDPE and LAE powder.

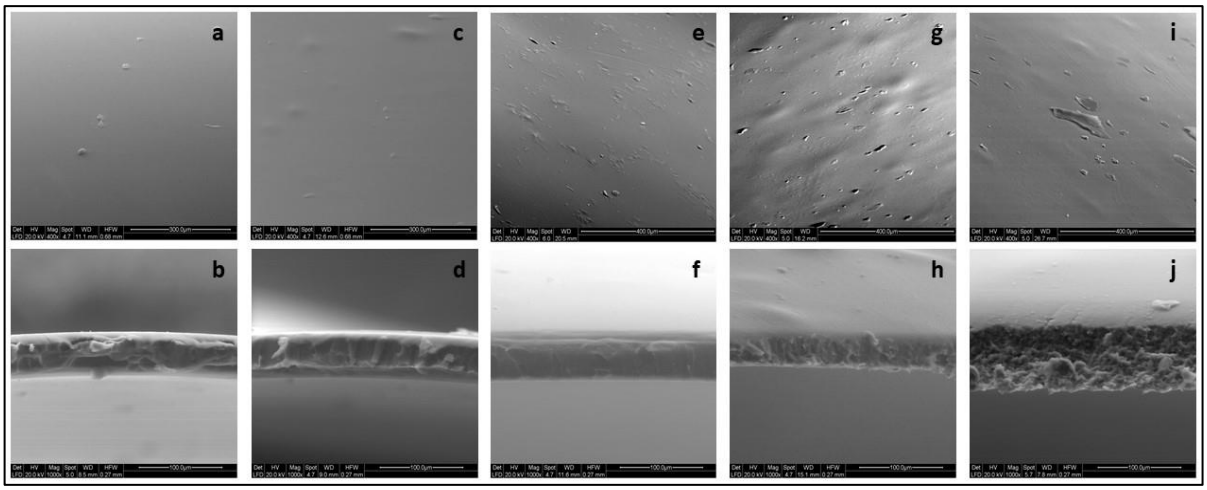

Fig. 1. Scanning electron microscopy (SEM) images of the surface and cross-section of films based on a control CS-PVA blend (CS-PVA) (a and b), CS-PVA-LAE1% (c and d), CS-PVA-LAE2.5% (e and f), CS-PVA-LAE5% (g and h) and CS-PVA-LAE10% (i and j).

3.2. Atomic force microscopy (AFM)

AFM was further performed to characterize the surface morphology of control and active films. Typical 3D surface topographic AFM images and root mean square (R_q) and roughness (R_a) values are presented in Fig. 2. The surface of control film was relatively smooth and homogenous as indicated by lower R_q and R_a values (17.1 and 12.0 nm, respectively). Increasing concentration of LAE up to 10% led to an increase in the roughness of the films, as indicated by higher R_q and R_a values. The difference in roughness value between control and active films was in accordance with the film microstructure observed by SEM analysis.

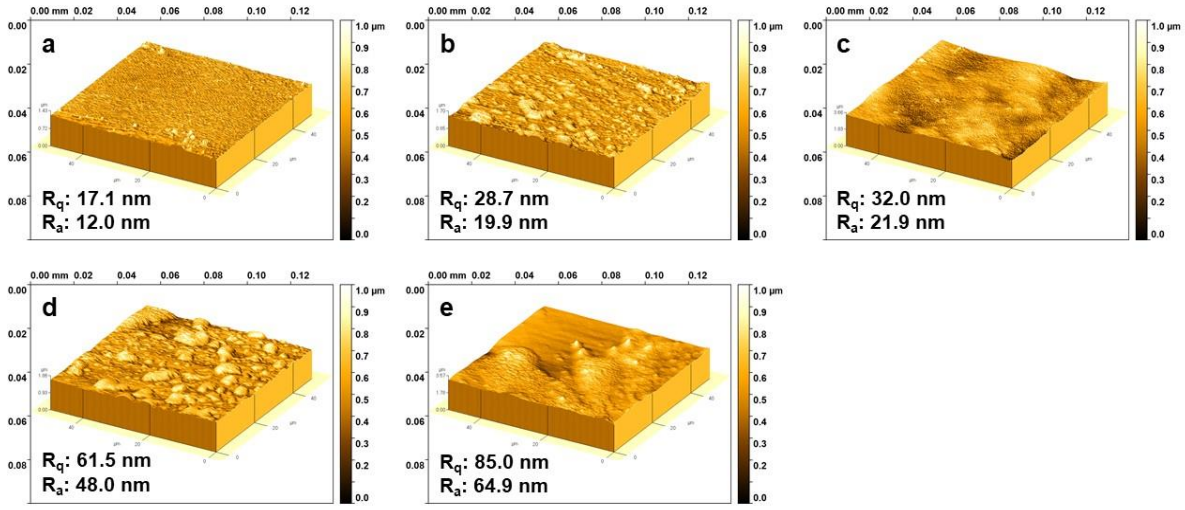

Fig. 2. 3D AFM images, root mean square (R_q) and roughness (R_a) of films based on a: control CS-PVA blend, b: CS-PVA-LAE 1%, c: CS-PVA-LAE 2.5%, d: CS-PVA-LAE 5% and e: CS-PVA-LAE 10%.

3.3. Attenuated Total Reflection (ATR) / Fourier-Transform Infrared (FT-IR) Spectroscopy

ATR/FT-IR spectroscopy was performed to characterize the structural and spectroscopic changes due to the incorporation of different amounts of LAE (1-10% w/w) into the CS-PVA film matrix by measuring the spectra in the wavenumber range of 4000 - 400 cm^{-1} at a spectral resolution of 4 cm^{-1}. The spectrum of the control CS-PVA blend (Fig. 3A, a) revealed the characteristic bands of the two polymer components (CS and PVA) with relative intensities according to the respective

composition. Under the broad and intense absorption band with the maximum at about 3270 cm^{-1}, the ν(OH), ν(NH) and $\nu_{as}(NH_2)/\nu_s(NH_2)$ absorption bands of these inter- and intramolecularly hydrogen bonded functionality of the CS and PVA blend components are superimposed (Costa-junior, Pereira, & Mansur, 2009; Santosh Kumar, Krishnakumar, Sobral, & Koh, 2019). The neighboring band doublet at about 2937/2908 cm^{-1} can be assigned to antisymmetric and symmetric $\nu_{as}(CH_2)/\nu_s(CH_2)$ and ν(CH) stretching vibrations of the corresponding polymer chain functionalities (Liu et al., 2018). Characteristic absorption bands for CS can be assigned at 1646 cm^{-1} (amide-I) due to the ν(C=O) stretching vibration, and at 1561 cm^{-1} (amide II) to a combination band of the ν(C–N) stretching and δ(N-H) bending vibrations (Costa-junior et al., 2009). Because in this study a PVA with only 98% degree of hydrolysis was used, 2% of acetate groups remained non-hydrolyzed during the manufacturing process (Koosha & Mirzadeh, 2015). Thus, the band at 1708 cm^{-1} belongs to the ν(C=O) stretching vibration of residual vinyl acetate units in the PVA backbone (Costa-junior et al., 2009). The very sharp, crystallinity-sensitive band of PVA at 1140 cm^{-1} is also observed in the CS-PVA blend (Kim, Kim, Lee, & Kim, 1992; Tripathi et al., 2009). Furthermore, absorption bands at 1413 cm^{-1} (δ(CH_2) bending vibration), between 1085 and 1045 cm^{-1} (ν(C–O) stretching vibrations), and 917 cm^{-1} (CH_2 rocking vibration) can be observed in the ATR/FT-IR spectrum of the CS-PVA blend (Pavaloiu, Stoica-Guzun, Stroescu, Jinga, & Dobre, 2014; Pereira Jr, de Arruda, & Stefani, 2015). For better visualization and understanding of the – although minor – spectral changes in the wavenumber ranges 2800 – 3000 cm^{-1} and specifically 1500 – 1800 cm^{-1} (see Fig. 3B) upon addition of LAE to the CS-PVA blends, the spectrum of pure Mirenat-D is reproduced in Fig.4. The most important absorption bands of the spectral range between 1000 and 3500 cm^{-1} can be readily assigned to the different vibrations of the chemical building blocks of this additive.

Up to 2.5% LAE content, the characteristic absorption bands in the ATR/FT-IR spectra of the CS-PVA blends (Fig. 3A, b, and c) are wavenumber invariant and do not show intensity changes, thereby suggesting low molecular interaction between the polymer and the LAE. Similar results were reported by Gaikwad, Lee, Lee, & Lee (2017); Rubilar et al. (2016) and Kashiri et al. (2016). However, CS-PVA blend films containing 5% and 10% LAE (Fig. 3A, d and e) revealed new absorption bands at 2918 cm^{-1} and 2851 cm^{-1} ($\nu_{as}(CH_2)/\nu_s(CH_2)$), 1755 cm^{-1} (ν(C=O)), 1724 cm^{-1} (ν(C=O)) and 1661/1645 cm^{-1} (ν(C=O), ν(C=N), $\delta(NH_2)$) originating from the introduction of new CH_2-segments, ester, amide, NH_2 and imine groups (Gamarra, Missagia, Urpí, Morató, & Muñoz-Guerra, 2018; Moreno, Cárdenas, et al., 2017). The evolution of the band doublet (1661/1645 cm^{-1}) from the original 1646 cm^{-1} band and the shift of the 1561 cm^{-1} band to 1557 cm^{-1} (LAE 5%) and to 1544 cm^{-1} (LAE 10%), respectively (Fig. 3B, d and e), is a clear evidence, that at elevated LAE content the C=O, NH_2 and NH functionalities of this additive contribute to competitive intermolecular interactions with the hydroxyl, amino, ether and residual acetate groups of the CS-PVA film network. Furthermore, LAE can also promote the formation of C=N groups, by reacting with both, residual acetate carbonyls of PVA and CS amino groups, as revealed by the relative intensity of the peak at 1645 cm^{-1} for LAE 10% (Fig 3B, e). Thus, the carbonyl-amino reaction to form C=N groups was enhanced by the presence of LAE (Moreno, Cárdenas, et al., 2017).

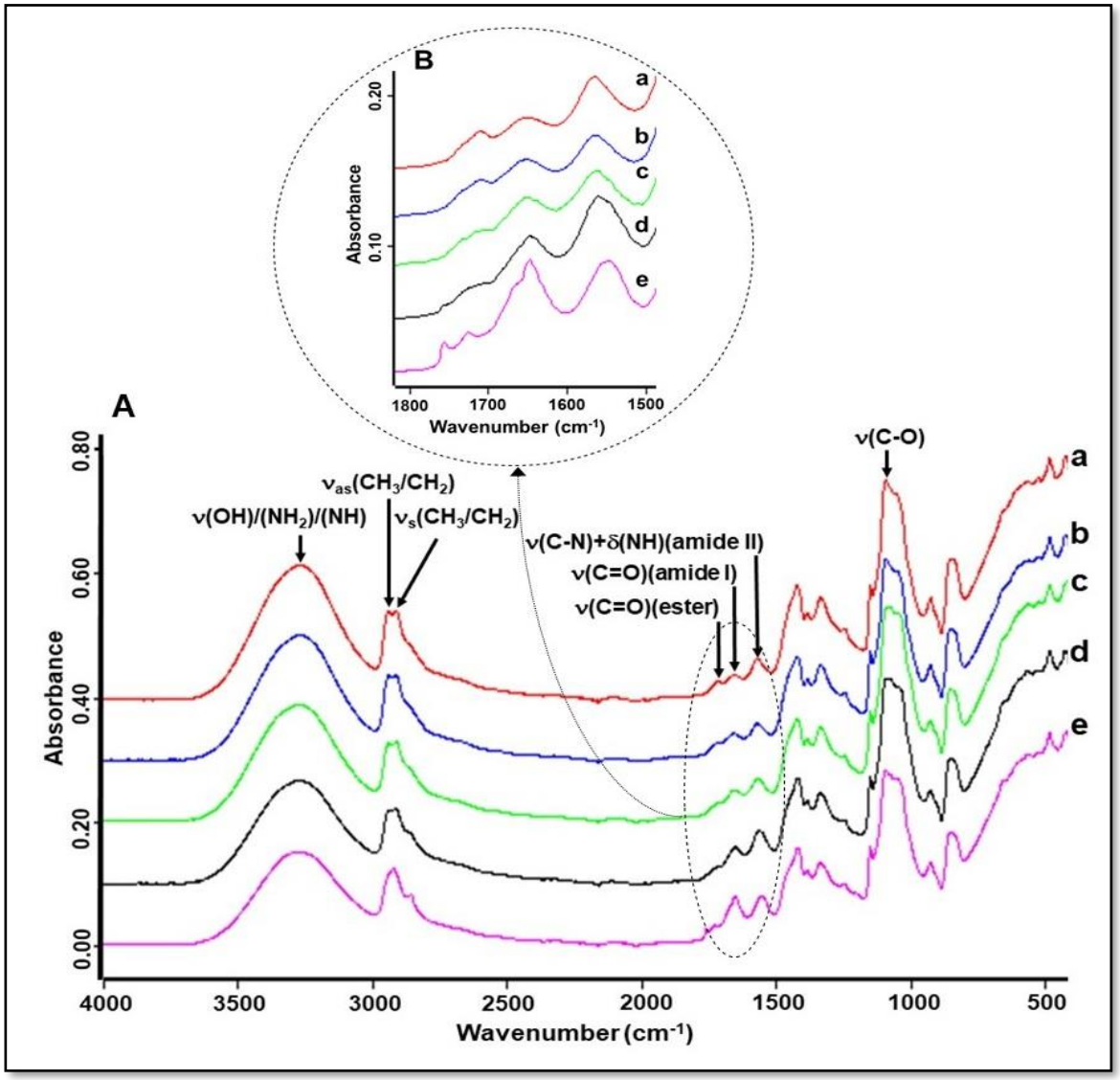

Fig. 3. ATR/FT-IR spectra (A) of films based on a: control CS-PVA blend, b: CS-PVA-LAE 1%, c: CS-PVA-LAE 2.5%, d: CS-PVA-LAE 5% films and e: CS-PVA-LAE 10%. In (B) the enlarged 1800-1500 cm^{-1} region is shown to highlight the spectral changes at elevated LAE content.

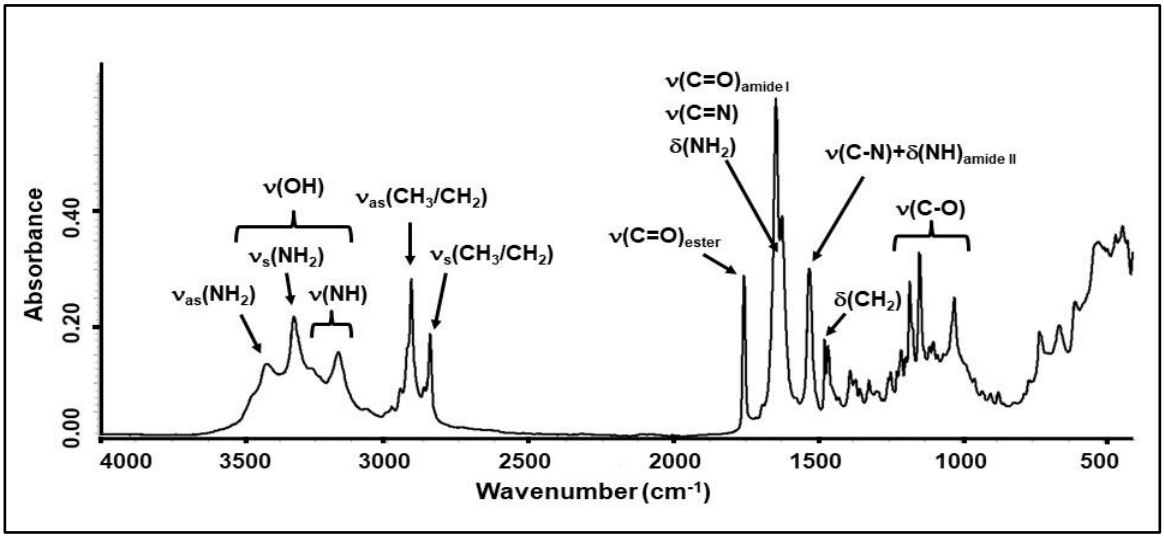

Fig. 4. ATR/FT-IR spectra of LAE formulation (Mirenat-D).

3.4. Thickness

The thickness value is a crucial parameter for determining final physical, mechanical and barrier properties of biodegradable films. The thickness values of control and active films are reported in Tab. 1. Thickness values ranged from 44.81 to 59.82 µm. The control film showed the lowest value ($p<0.05$). This is due to the well-organized and dense network structure in the CS-PVA blend film as confirmed by SEM images. The incorporation of LAE into the CS-PVA blend increased the thickness ($p<0.05$) and the CS-PVA film enriched with 10% LAE showed the highest thickness value ($p<0.05$). In this study, all films were prepared by casting a constant amount of FFS in Petri dishes with the same surface ratio, therefore differences in thickness between control and active films are due to the addition of LAE to the FFS. According to Gaikwad et al. (2017), film thickness is influenced by the solid content of the FFS. Thus, LAE might contribute to the loosen film matrix, reduce the homogeneity, and consequently increase the thickness. In contrast, Rubilar et al., (2016) reported that addition of LAE to CS films did not influence the thickness. It is noteworthy that the type of LAE applied in different studies as a powder (Mirenat-D or Mirenat-P) or dissolved in glycerol (Mirenat-G) strongly affects film thickness.

3.5. Mechanical properties

The tensile strength (TS), elongation at break (E%) and elastic modulus (EM) are three important parameters for evaluation of mechanical properties. Generally, adequate mechanical strength and extensibility are required for the development of biodegradable films for food packaging applications. The mechanical properties of control and active films are presented in Tab. 1. The control film showed the highest TS, E% and EM values. The presence of LAE greatly influenced TS and E% ($p<0.05$). Films containing LAE were less resistant and less stretchable than the control film ($p<0.05$). Incorporation of LAE up to 10% decreased the tensile strength from 42.5 to

15.7 MPa and E% from 54.2 to 14.3%. The significant deterioration of mechanical properties above 2.5% incorporation of LAE (Tab. 1) is also consistent with the ATR/FT-IR observation, that band shifts and intensity changes occur above this threshold concentration. This tendency could be explained by the fact that active films containing a high concentration of LAE are unable to form a cohesive and continuous matrix as it was confirmed by SEM analysis. This can be attributed to the competitive interaction of the functional groups of LAE and the CS-PVA blend that limit cohesion forces within the polymer in the film matrix and consequently decrease the degree of physical crosslinking by weakening the intermolecular hydrogen bonding, thereby resulting in the reduction of mechanical properties. Despite the reduction of TS after incorporation of LAE, it should be noted that the TS values for the active films containing LAE up to 2.5% were comparable with those of plastic films that are used widely in the market, such as high-density polyethylene (22-31 MPa) and polypropylene (31-38 MPa) but slightly lower than that for polystyrene (45-83 MPa) (Theinsathid, Visessanguan, Kruenate, Kingcha, & Keeratipibul, 2012). Moreno, Díaz, Atarés, & Chiralt (2016) also reported that the incorporation of LAE into starch-gelatin blend film notably reduced the stiffness and resistance to break compared to the control film. In contrast to these results, Rubilar et al. (2016) reported that the incorporation of LAE (1g/L) to CS films significantly increased TS and E% values ($p<0.05$) which might be due to the application of Mirenat-G (10% LAE, 90% glycerol) as LAE source. Hence the observed effect could be mainly due to the plasticizing effect of glycerol. Literature data regarding mechanical properties are controversial and are influenced by multiple factors such as the molecular mass of the polymer, deacetylation degree of CS, degree of hydrolysis of PVA, pH of the FFS, drying conditions and type of LAE.

Table 1. Thickness, tensile strength (TS), elongation at break (E%) and elastic modulus (EM) of the films based on control CS-PVA blend (CS-PVA) and CS-PVA enriched with LAE (1-10% w/w).

Film sample	Thickness (μm)	TS (MPa)	E (%)	EM (MPa)
CS-PVA	44.8 ± 1.0^{a}	42.5 ± 1.6^{d}	54.2 ± 2.0^{d}	1570.1 ± 139.0^{d}
CS-PVA-LAE 1%	45.1 ± 0.5^{a}	33.0 ± 2.4^{c}	38.9 ± 3.1^{c}	1153.1 ± 121.1^{bc}
CS-PVA-LAE 2.5%	49.9 ± 1.6^{b}	34.5 ± 4.2^{c}	39.0 ± 2.6^{c}	1287.3 ± 77.8^{c}
CS-PVA-LAE 5%	54.9 ± 2.7^{c}	22.2 ± 0.9^{b}	25.0 ± 2.8^{b}	1016.9 ± 90.8^{b}
CS-PVA-LAE 10%	59.6 ± 0.8^{d}	15.7 ± 1.2^{a}	14.3 ± 1.9^{a}	701.3 ± 53.8^{a}

Values are given as mean ± SD (n = 3).
Different letters in the same column indicate significant differences ($p<0.05$).

3.6. UV barrier, light transmittance and opacity value

Protecting food from the effect of UV-Vis radiation is one of the desired characteristics of packaging material due to their influence on product performance and consumer acceptance. The UV-Vis light transmittance of control and active films in the wavelength range of 200 - 800 nm is presented in Fig. 5. Control film showed a higher UV light transmittance (200 - 350 nm) compared to the active films. UV light transmittance was reduced at increasing LAE concentration and active films behaved as effective UV barriers at 200 nm since the transmittance value was below 1%. UV barrier property of films is an important parameter for food packaging applications to minimize UV-induced lipid oxidation, to preserve the organoleptic properties of the packaged food, to avoid nutrient losses, discoloration and off-flavors, thereby prolonging food shelf life (Hajji et al., 2016; Wu et al., 2017).

The transmission of visible light (400 - 800 nm) was higher than 80% for the control film. The active films containing 1 and 2.5% LAE showed similar results while active films containing 5 and 10% LAE showed lower values. Thus, once a critical LAE concentration is exceeded, aggregates are formed, that were large enough to scatter the light and thereby interfere with its transmission (Bonnaud et al., 2010). The light

barrier property is also an important factor for food preservation to avoid photo-oxidation of organic compounds and degradation of vitamins and other pigments. In addition, it provides a clear view of the food content and its condition (Figueroa-Lopez, Andrade-Mahecha, & Torres-Vargas, 2018; Yadav & Chiu, 2019).

In this study, all films can be considered as transparent due to the opacity value lower than 5 at 600 nm (Tab. 2). The higher value of this parameter represents the lower transparency of the film.

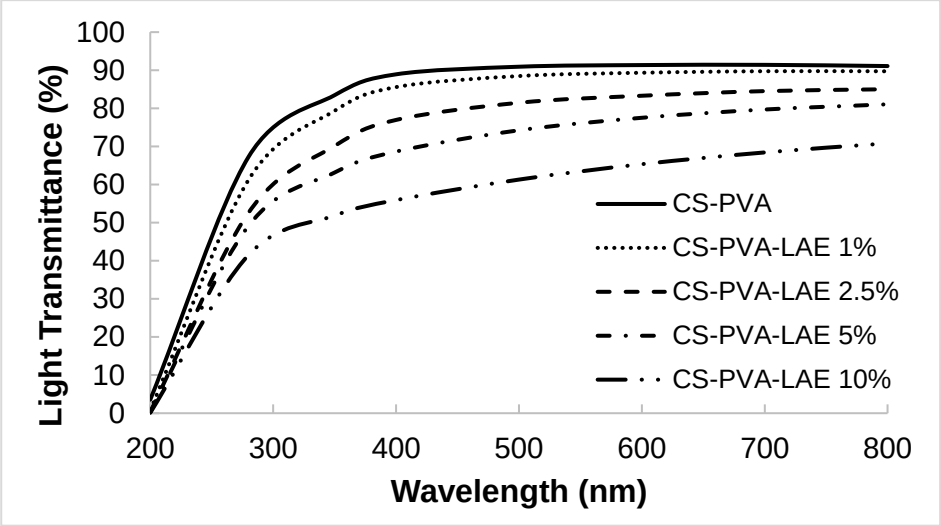

Fig. 5. UV-Vis light transmittance of the films based on a control CS-PVA blend (CS-PVA) and CS-PVA blends enriched with LAE (1-10% w/w).

3.7. Color

The color values (L*, a* and b*) and total color difference (ΔE*) of control and active films are shown in Tab. 2. The L*, a*, b* offer objective evaluation of the appearance of films while ΔE* measures the color change of treatment from a reference color. Color is an important feature of a film for food packaging applications since it evaluates the visual characteristic of the food product inside the packaging system and affects consumer purchase decisions. The L* value indicates lightness and represents the apparent proportion of incident light reflected by an object, varying between 98.2 and 99, which means that all the films were almost clear. No significant differences ($p>0.05$)

for L* between the control and active films were found. These results were in agreement with opacity values that showed all films were clear and transparent.

The a* value, expressing the green-red color component, was negative for all films, which means that films were not truly red (Muriel-Galet, López-Carballo, Hernández-Muñoz, & Gavara, 2014).

The b* value measures the blue-yellow color component. This value increased upon addition of LAE ($p<0.05$), suggesting a gain of a slight yellow color.

ΔE* was used to compare the color of active films with commercial plastic films (perceptibility threshold of ΔE* = 1). The selected value is often used as the smallest color difference that the human eye can detect (Thakhiew, Devahastin, & Soponronnarit, 2013). Control film had ΔE* value of 0.91. The ΔE* increased upon addition of LAE ($p<0.05$) and reached a value of 1.70 in the active film containing 10% LAE. This behavior might be attributed to the increase in the colorimetric coordinate b* and increase in film thickness upon addition of LAE.

In summary, the consumer might not be able to detect color difference in active films, despite the slightly higher values than the threshold. A similar result has been reported by Rubilar et al. (2016).

Table 2. Color parameters (L*, a*, and b*), total color difference (ΔE*) and opacity values of the films based on a control CS-PVA blend (CS-PVA) and CS-PVA enriched with LAE (1-10% w/w).

Film sample	Color parameters				Opacity value
	L*	a*	b*	ΔE*	(600 nm)
CS-PVA	99.0 ± 0.2^{a}	-0.3 ± 0.03^{c}	0.7 ± 0.1^{a}	0.91 ± 0.2^{a}	0.9 ± 0.01^{a}
CS-PVA-LAE 1%	98.8 ± 0.1^{a}	-0.3 ± 0.01^{c}	0.7 ± 0.1^{a}	0.99 ± 0.1^{a}	1.1 ± 0.08^{ab}
CS-PVA-LAE 2.5%	98.8 ± 0.1^{a}	-0.4 ± 0.02^{b}	1.0 ± 0.1^{b}	1.22 ± 0.1^{b}	1.6 ± 0.31^{bc}
CS-PVA-LAE 5%	98.6 ± 0.1^{a}	-0.4 ± 0.03^{a}	1.3 ± 0.2^{c}	1.63 ± 0.2^{c}	2.0 ± 0.13^{c}
CS-PVA-LAE 10%	98.7 ± 0.2^{a}	-0.5 ± 0.02^{a}	1.4 ± 0.1^{c}	1.70 ± 0.1^{c}	3.1 ± 0.27^{d}

Values are given as mean ± SD (n = 3).
Different letters in the same column indicate significant differences ($p<0.05$).

3.8. Moisture content, water solubility, water vapor transmission rate and water vapor permeability

One of the major drawbacks of biodegradable films for food packaging applications is their sensitivity to water. Due to the hydrophilic nature of CS and PVA, when these films are exposed to high relative humidity conditions, water molecules are absorbed by the polymeric chains, exerting a plasticizing effect and resulting in changes of the mechanical and barrier properties (Aguirre-Loredo, Rodríguez-Hernández, Morales-Sánchez, Gómez-Aldapa, & Velazquez, 2016). Therefore, measuring water sensitivity plays an important role in the packaging performance for the food products. The moisture content (MC), water solubility (WS), water vapor transmission rate (WVTR) and water vapor permeability (WVP) of control and active films are presented in Tab. 3. The MC value ranged from 16.4 to 17.5%. The effect of LAE incorporation on the MC was not significant ($p<0.05$). Moreno, Gil, Atarés, & Chiralt (2017) reported that the enrichment of starch-gelatin films with different LAE concentrations did not influence the MC. Solubility is defined as the content of dry matter solubilized after 24 h immersion in water. The control film showed the lowest WS value and addition of LAE increased the WS value. CS-PVA film containing 10% LAE showed the highest WS value ($p<0.05$). The higher solubility values of active films could be explained by the hydrophilic nature of CS-PVA blend film and low oil-water equilibrium partition coefficient of LAE ($K_{ow}<0.1$), which means that LAE has a high affinity to water molecules (Higueras et al., 2013; Rubilar et al., 2016).

The barrier properties of biodegradable films to water play an important role in determining the shelf life of packed foodstuffs (Del Nobile, Fava, & Piergiovanni, 2002). In this study, the WVTR was not significantly influenced by the addition of LAE, despite showing higher values in active films ($p>0.05$). However, the incorporation of LAE to CS-PVA blend film increased the WVP value. This might be due to the difference in

each film thickness considered in WVP calculation (Rubilar et al., 2016). Additionally, incorporation of LAE into the CS-PVA film network may break hydrogen bonding and disrupt the long-range ordering between CS and PVA molecules, resulting in an increase in WVP value (Ma, Zhang, & Zhong, 2016).

Table 3. Moisture content (MC), water solubility (WS), water vapor transmission rate (WVTR) and water vapor permeability (WVP) of the films based on a control CS-PVA blend (CS-PVA) and CS-PVA enriched with LAE (1-10% w/w).

Film sample	MC (%)	WS (%)	WVTR (g /day m^2)	WVP 90:0% RH (g mm/kP day m^2)
CS-PVA	16.4 ± 0.5^{a}	22.1 ± 0.4^{a}	3605.6 ± 450.8^{a}	18 ± 0.02^{a}
CS-PVA-LAE 1%	16.7 ± 0.9^{a}	23.7 ± 2.8^{ab}	3608.7 ± 362.1^{a}	19 ± 0.02^{a}
CS-PVA-LAE 2.5%	16.8 ± 0.7^{a}	25.4 ± 3.4^{ab}	3729.5 ± 369.3^{a}	21 ± 0.02^{ab}
CS-PVA-LAE 5%	17.1 ± 0.6^{a}	27.8 ± 2.1^{b}	3742.1 ± 341.5^{a}	24 ± 0.02^{b}
CS-PVA-LAE 10%	17.5 ± 0.6^{a}	33.2 ± 2.1^{c}	3808.9 ± 337.7^{a}	26 ± 0.02^{c}

Values are given as mean ± SD (n = 3).
Different letters in the same column indicate significant differences ($p<0.05$).

3.9. In vitro antimicrobial activity

3.9.1. Disk diffusion assay (DDA)

The antimicrobial activity of control and active films against common bacterial food pathogens, namely *C. jejuni*, *E. coli*, *L. monocytogenes* and *S. typhimurium*, was evaluated by the disk diffusion assay (Fig. 6) and the details are presented in Tab. 4. The control film did not show an inhibition zone against any of the tested microorganisms. The absence of inhibition zone could be explained by the limitation of CS to diffuse in agar medium (Leceta, Guerrero, Ibarburu, et al., 2013) and incapability of PVA to inhibit bacterial growth as it has been reported by other authors (Hajji et al., 2016; Tripathi et al., 2009) so that only microorganisms in direct contact with the active sites of CS in the CS-PVA film network are inhibited. Active films containing 1% LAE were only effective against *C. jejuni*. In general, LAE was more effective against *C. jejuni* compared to the other microorganisms considered, which showed inhibition

haloes ranging from 3 to 5-fold wider. No differences were observed in the inhibition zones produced by CS-PVA films incorporating 5 and 10% of LAE against all tested microorganisms. Similar results reported by Muriel-Galet, López-Carballo, Gavara, & Hernández-Muñoz (2015). Pattanayaiying, H-Kittikun, & Cutter (2015) also found that incorporation of LAE into pullulan film inhibited the growth of foodborne pathogens such as *Salmonella spp*., *L. monocytogenes* and *E. coli.* The antimicrobial activity of LAE is attributed to its action as a cationic surfactant on the cytoplasmic membranes of microorganisms, causing a disturbance in membrane potential and resulting in cell growth inhibition and loss of viability.

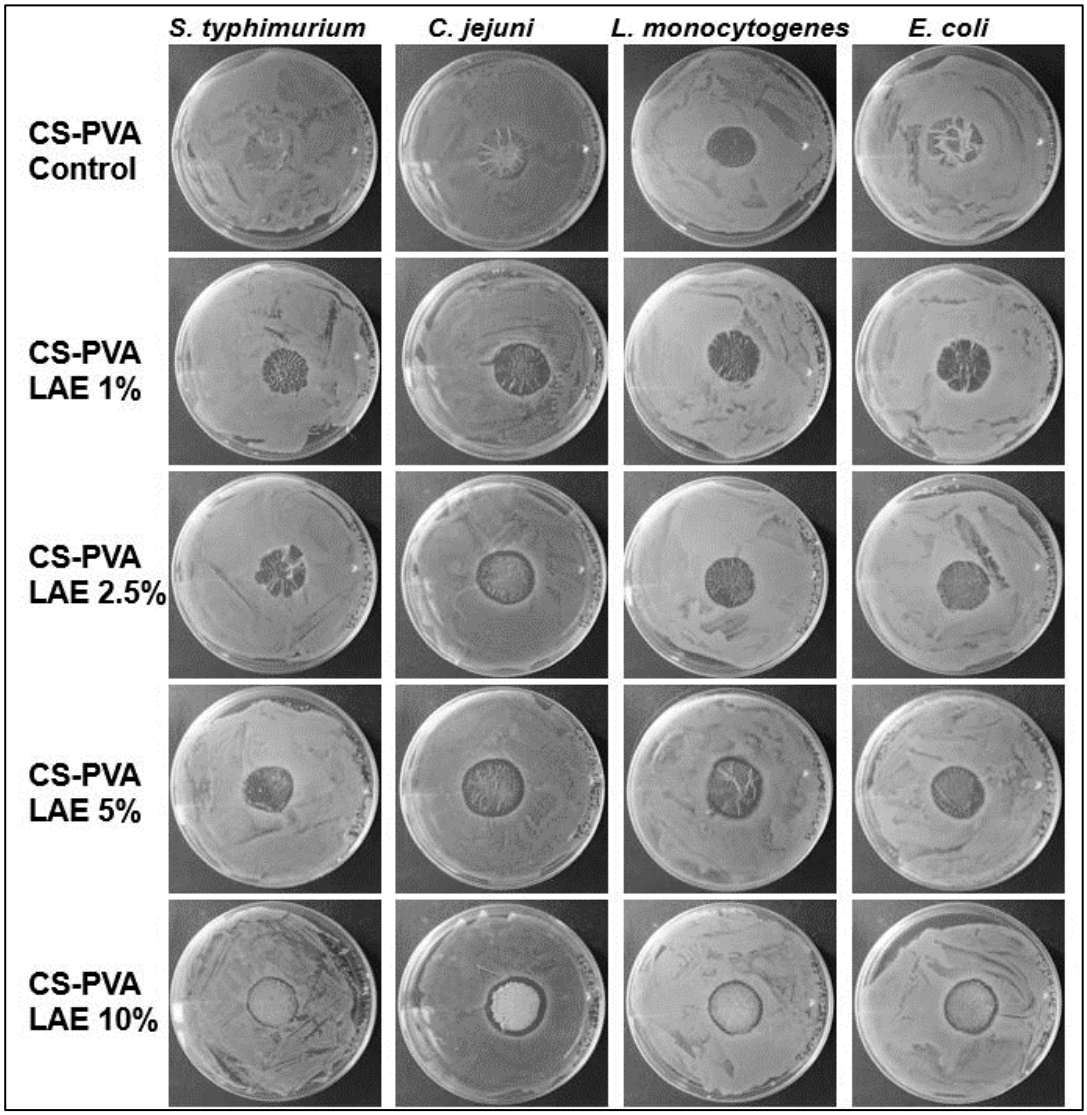

Fig. 6. Disk diffusion results of films based on a control CS-PVA blend (CS-PVA) and CS-PVA enriched with LAE (1-10% w/w).

Table 4. Inhibition zone diameters of the film disks (22 mm diameter) based on a control CS-PVA blend (CS-PVA) and CS-PVA enriched with LAE (1-10% w/w).

Film sample	*L. monocytogenes*	*E. coli*	*C. jejuni*	*S. typhimurium*
CS-PVA	N. D.	N. D.	N. D.	N. D.
CS-PVA-LAE 1%	N. D.	N. D.	1.8 ± 1.0^{aA}	N. D.
CS-PVA-LAE 2.5%	0.5 ± 0.5^{aA}	0.6 ± 0.3^{aA}	3.7 ± 1.5^{bB}	0.6 ± 0.7^{aA}
CS-PVA-LAE 5%	1.3 ± 0.7^{abA}	1.2 ± 0.9^{abA}	4.6 ± 1.8^{bB}	1.7 ± 1.1^{abA}
CS-PVA-LAE 10%	1.6 ± 0.9^{bA}	1.6 ± 1.0^{bA}	5.2 ± 1.4^{bB}	1.8 ± 1.8^{aA}

Values are given as mean ± SD (n = 3). N.D: not detected.
Different lowercase letters in the same column indicate significant differences ($p<0.05$).
Different capital letters in the same row indicate significant differences ($p<0.05$).

3.9.2. Evaluation of antimicrobial activity in liquid medium

The Antimicrobial activity of control and active films against common bacterial food pathogens including *C. jejuni*, *E. coli*, *L. monocytogenes,* and *S. typhimurium* was also evaluated in liquid medium and the details are presented in Tab. 5.

Table 5. Antimicrobial activity of films based on a control CS-PVA blend (CS-PVA) and CS-PVA enriched with LAE (1-10% w/w) expressed as logarithm of colony forming units (log CFU/ mL) and log reduction value (LRV).

Film sample	*L. monocytogenes*		*E. coli*		*C. jejuni*		*S. typhimurium*	
	log (cfu/mL)	*LRV*	*log (cfu/mL)*	*LRV*	*log (cfu/mL)*	*LRV*	*log (cfu/mL)*	*LRV*
CS-PVA	9.2 ± 0.2^{b}		9.3 ± 0.1^{c}		9.4 ± 0.1^{b}		9.5 ± 0.1^{c}	
CS-PVA-LAE1%	9.2 ± 0.2^{b}	0	9.1 ± 0.1^{bc}	0.2	9.2 ± 0.1^{b}	0.2	9.4 ± 0.1^{bc}	0.1
CS-PVA-LAE2.5%	9.0 ± 0.2^{b}	0.2	9.0 ± 0.1^{bc}	0.3	9.1 ± 0.3^{b}	0.3	9.3 ± 0.1^{bc}	0.2
CS-PVA-LAE5%	8.9 ± 0.2^{b}	0.3	8.8 ± 0.1^{b}	0.5	8.8 ± 0.1^{b}	0.6	9.2 ± 0.1^{ab}	0.3
CS-PVA-LAE10%	7.7 ± 0.8^{a}	1.5	8.3 ± 0.4^{a}	1	7.4 ± 0.1^{a}	2	9.1 ± 0.1^{a}	0.4

Values are given as mean ± SD (n = 3).
Different lowercase letters in the same column indicate significant differences ($p<0.05$).

CS-PVA film without LAE used as a control. Among tested microorganisms *C. jejuni* showed higher log reduction (2) for CS-PVA-LAE 10% films that is in agreement with

the DDA result. The incorporation of LAE (1-10% w/w) showed a log reduction against all tested microorganisms. Clearly, the higher the LAE concentration in the film, the greater the antimicrobial efficiency of the CS-PVA film. Similar results were reported by Muriel-Galet et al., (2015) and Kashiri et al., (2016).

4. Conclusions

In this study, biodegradable active films based on CS-PVA blends enriched with LAE at different concentrations (1-10%, w/w) were developed and their microstructural, physical, optical, mechanical, barrier and antimicrobial properties were evaluated for food packaging applications. The results showed that all films containing LAE were transparent. The incorporation of LAE could improve the UV and light barrier properties of CS-PVA film, which may be useful to protect food from UV degradation and photo-oxidation. The characteristic absorption bands in the ATR/FT-IR spectra of the CS-PVA blends did not show significant band shifts and intensity changes up to 2.5% LAE content, indicating low interactions between the polymer and the LAE. However, at elevated LAE content, the C=O, NH_2 and NH functionalities of this additive contribute to competitive molecular interactions with the hydroxyl, amino, ether and residual acetate groups of the CS-PVA film network. The presence of LAE greatly influenced TS and E%. Films with LAE were less resistant and less stretchable than the control film and a significant deterioration of mechanical properties occurred above 2.5% incorporation of LAE. The developed active films, especially those including 5 and 10% LAE, were effective against common bacterial food pathogens. The results suggest that the CS-PVA films enriched with different concentrations of LAE could be considered as environmentally friendly packaging material with antimicrobial properties to extend the shelf life of food products and that might be an alternative to synthetic plastics for certain applications.

Chapter 5

Concluding remarks

The recent sharp increase of sensitivity towards environmental issues and the plastic issue, in particular, has boosted interest in sustainable alternative packaging materials which would, nevertheless, offer suitable performances to the food. Applying chitosan as packaging material fulfills the environmental concerns, but carries some drawbacks in terms of thermal resistance, barrier and mechanical properties, and the cost.

Films based on chitosan-gelatin blend enriched with low concentration of LAE (0.1% v/v of FFS) were successfully developed. Blending chitosan and gelatin resulted in improvement in mechanical and water barrier properties. The chitosan-gelatin blend film was continuous, transparent and its optical properties did not present relevant changes with respect to the pure chitosan and gelatin film. The addition of LAE as an active compound even at low concentration was effective against common food bacterial pathogens.

Films based on chitosan-gelatin blend enriched with five different essential oils including cinnamon, citronella, pink clove, nutmeg, and thyme were developed. The active films showed as effective barriers against UV light. Active films inhibited the growth of four major food bacterial pathogens. Among the tested essential oils, thyme was the most effective. Overall, the characterization of functional properties revealed that chitosan-gelatin films incorporated with essential oils could be used as environmentally friendly active food packaging material with antimicrobial properties and the potential to extend the shelf-life of food products.

Active films based on chitosan-polyvinyl alcohol blend were produced and incorporating LAE (1-10% w/w of biopolymer) were developed. Increasing concentration of LAE up to 10% led to an increase in the roughness of the films. In addition, high LAE levels negatively affected mechanical and water barrier properties.

However, addition of LAE improved UV barrier of chitosan-polyvinyl alcohol blend films. In addition, the developed active films were effective against four food bacterial pathogens.

Blending chitosan with natural (gelatin) and synthetic (polyvinyl alcohol) biopolymers enriched with LAE or essential oils as active compounds could be considered as a viable strategy for the development of biodegradable packaging showing improved physical, mechanical and barrier properties with an additional bioactive function to extend the shelf life of food products.

There is huge potential for the application of biodegradable material for packaging applications. Blending chitosan with other biopolymers appears to have a very bright future for innovative active food packaging with bio-functional properties to replace (for some applications) or reduce the use of the conventional fossil-based packaging materials.

References

1. Abdelrazek, E. M., Elashmawi, I. S., & Labeeb, S. (2010). Chitosan filler effects on the experimental characterization , spectroscopic investigation and thermal studies of PVA / PVP blend films. *Physica B: Physics of Condensed Matter*, 405(8), 2021–2027. https://doi.org/10.1016/j.physb.2010.01.095

2. Abdollahi, M., Rezaei, M., & Farzi, G. (2012). Improvement of active chitosan film properties with rosemary essential oil for food packaging. *International Journal of Food Science and Technology*, 47(4), 847–853. https://doi.org/10.1111/j.1365-2621.2011.02917.x

3. Acevedo-Fani, A., Salvia-Trujillo, L., Rojas-Graü, M. A., & Martín-Belloso, O. (2015). Edible films from essential-oil-loaded nanoemulsions: Physicochemical characterization and antimicrobial properties. *Food Hydrocolloids*, 47, 168–177. https://doi.org/10.1016/j.foodhyd.2015.01.032

4. Acosta, S., Jiménez, A., Cháfer, M., González-Martínez, C., & Chiralt, A. (2015). Physical properties and stability of starch-gelatin based films as affected by the addition of esters of fatty acids. *Food Hydrocolloids*, 49, 135–143. https://doi.org/10.1016/j.foodhyd.2015.03.015

5. Águila-Almanza, E., Salgado-Delgado, R., Vargas-Galarza, Z., García-Hernández, E., & Hernández-Cocoletzi, H. (2019). Enzymatic depolymerization of chitosan for the preparation of functional membranes. *Journal of Chemistry*, *2019*, 1–8. https://doi.org/10.1155/2019/5416297

6. Aguirre-Loredo, R. Y., Rodríguez-Hernández, A. I., Morales-Sánchez, E., Gómez-Aldapa, C. A., & Velazquez, G. (2016). Effect of equilibrium moisture content on barrier, mechanical and thermal properties of chitosan films. *Food Chemistry*, 196, 560–566. https://doi.org/10.1016/j.foodchem.2015.09.065

7. Ahmed, J., Mulla, M., Arfat, Y. A., & Thai T, A. L. (2017). Mechanical, thermal, structural and barrier properties of crab shell chitosan/graphene oxide composite films. *Food Hydrocolloids*, 71, 141–148. https://doi.org/10.1016/j.foodhyd.2017.05.013

8. Ahmed, S., & Ikram, S. (2016). Chitosan and gelatin based biodegradable packaging films with UV-light protection. *Journal of Photochemistry and Photobiology B: Biology*, 163, 115–124. https://doi.org/10.1016/j.jphotobiol.2016.08.023

9. Ahmed, S., & Ikram, S. (2017). Chitin and chitosan: history, composition and properties. In S. Ahmed & S. Ikram (Eds.), *Chitosan: Derivatives, Composites and Applications* (pp. 1–24). Scrivener Publishing LLC.

10. Aloui, H., Khwaldia, K., Hamdi, M., Fortunati, E., Kenny, J. M., Buonocore, G. G., & Lavorgna, M. (2016). Synergistic effect of halloysite and cellulose nanocrystals on the functional properties of PVA based nanocomposites. A*CS Sustainable Chemistry and Engineering*, 4(3), 794–800. https://doi.org/10.1021/acssuschemeng.5b00806

11. Arfat, Y. A., Ahmed, J., Hiremath, N., Auras, R., & Joseph, A. (2017). Thermo-mechanical, rheological, structural and antimicrobial properties of bionanocomposite films based on fish skin gelatin and silver-copper nanoparticles. *Food Hydrocolloids*, 62, 191–202. https://doi.org/10.1016/j.foodhyd.2016.08.009

12. Argüelles-Monal, W. M., Lizardi-Mendoza, J., Fernández-Quiroz, D., Recillas-Mota, M. T., & Montiel-Herrera, M. (2018). Chitosan derivatives: introducing new

functionalities with a controlled molecular architecture for innovative materials. *Polymers*, 10(3), 342. https://doi.org/10.3390/polym10030342

13. Arikan, E. B., & Ozsoy, H. D. (2015). A review: investigation of bioplastics. *Journal of Civil Engineering and Architecture*, *9*(2), 188–192. https://doi.org/10.17265/1934-7359/2015.02.007

14. Asker, D., Weiss, J., & McClements, D. J. (2009). Analysis of the interactions of a cationic surfactant (Lauric arginate) with an anionic biopolymer (Pectin): Isothermal titration calorimetry, light scattering and microelectrophoresis. *Langmuir*, 25(1), 116–122. https://doi.org/10.1021/la803038w

15. ASTM. (2001a). Standard test method for tensile properties of thin plastic sheeting. Annual books of ASTM Standards. Designation D882-01, Philadelphia: ASTM, American Society for Testing Materials.

16. ASTM. (2001b). Standard test method for water vapor transmission of materials. Annual books of ASTM Standards. Designation E 96-01, Philadelphia: ASTM, American Society for Testing Materials.

17. Atarés, L., Bonilla, J., & Chiralt, A. (2010). Characterization of SPI-based edible films incorporated with cinnamon or ginger essential oils. *Journal of Food Engineering*, 99, 384–391. https://doi.org/10.1016/j.jfoodeng.2010.03.004

18. Badawy, M. E. I., Rabea, E. I., & El-Nouby, M. A. M. (2016). Preparation, physicochemical characterizations, and the antioxidant activity of the biopolymer films based on modified chitosan with starch, gelatin, and plasticizers. *Journal of Polymer Materials*, 33(1), 17–32. https://doi.org/10.1007/s10924-013-0621-z

19. Baron, R. D., Pérez, L. L., Salcedo, J. M., Córdoba, L. P., & Sobral, P. J. do A. (2017). Production and characterization of films based on blends of chitosan from blue crab (Callinectes sapidus) waste and pectin from Orange (Citrus sinensis Osbeck) peel. *International Journal of Biological Macromolecules*, 98, 676–683. https://doi.org/10.1016/j.ijbiomac.2017.02.004

20. Basta, A. H., Khwaldia, K., Aloui, H., & El-Saied, H. (2015). Enhancing the performance of carboxymethyl cellulose by chitosan in producing barrier coated paper sheets. *Nordic Pulp and Paper Research Journal*, 30(4), 617–625. https://doi.org/10.3183/npprj-2015-30-04-p617-625

21. Becerril, R., Manso, S., Nerin, C., & Gomez-Lus, R. (2013). Antimicrobial activity of Lauroyl Arginate Ethyl (LAE), against selected food-borne bacteria. *Food Control*, 32(2), 404–408. https://doi.org/10.1016/j.foodcont.2013.01.003

22. Bellelli, M., Licciardello, F., Pulvirenti, A., & Fava, P. (2018). Properties of poly(vinyl alcohol) films as determined by thermal curing and addition of polyfunctional organic acids. *Food Packaging and Shelf Life*, 18, 95–100. https://doi.org/10.1016/j.fpsl.2018.10.004

23. Bellich, B., D'Agostino, I., Semeraro, S., Gamini, A., & Cesàro, A. (2016). "The good, the bad and the ugly" of chitosans. *Marine Drugs*. 14(5), 99. https://doi.org/10.3390/md14050099

24. Benbettaïeb, N., Kurek, M., Bornaz, S., & Debeaufort, F. (2014). Barrier, structural and mechanical properties of bovine gelatin-chitosan blend films related to biopolymer interactions. *Journal of the Science of Food and Agriculture*, 94(12), 2409–2419. https://doi.org/10.1002/jsfa.6570

25. Bhuimbar, M. V., Bhagwat, P. K., & Dandge, P. B. (2019). Extraction and characterization of acid soluble collagen from fish waste: Development of collagen-chitosan blend as food packaging film. *Journal of Environmental Chemical Engineering*, 7(2), 102983. https://doi.org/10.1016/j.jece.2019.102983

26. Bonilla, J., Fortunati, E., Atarés, L., Chiralt, A., & Kenny, J. M. (2014). Physical, structural and antimicrobial properties of poly vinyl alcohol- chitosan biodegradable films. *Food Hydrocolloids*, 35, 463–470. https://doi.org/10.1016/j.foodhyd.2013.07.002

27. Bonilla, J., Poloni, T., Lourenço, R. V., & Sobral, P. J. A. (2018). Antioxidant potential of eugenol and ginger essential oils with gelatin/chitosan films. *Food Bioscience*, 23, 107–114. https://doi.org/10.1016/j.fbio.2018.03.007

28. Bonilla, J., & Sobral, P. J. A. (2016). Investigation of the physicochemical, antimicrobial and antioxidant properties of gelatin-chitosan edible film mixed with plant ethanolic extracts. *Food Bioscience*, 16, 17–25. https://doi.org/10.1016/j.fbio.2016.07.003

29. Bonnaud, M., Weiss, J., & McClements, D. J. (2010). Interaction of a food-grade cationic surfactant (Lauric Arginate) with food-grade biopolymers (pectin, carrageenan, xanthan, alginate, dextran and chitosan). *Journal of Agricultural and Food Chemistry*, 58(17), 9770–9777. https://doi.org/10.1021/jf101309h

30. Bourakadi, K. El, Merghoub, N., Fardioui, M., Mekhzoum, M. E. M., Kadmiri, I. M., Essassi, E. M., Qaiss, A. E. K., Bouhfid, R. (2019). Chitosan/polyvinyl alcohol/thiabendazoluim-montmorillonite bio-nanocomposite films: Mechanical, morphological and antimicrobial properties. *Composites Part B: Engineering*, 172, 103–110. https://doi.org/10.1016/j.compositesb.2019.05.042

31. Burt, S. (2004). Essential oils: their antibacterial properties and potential applications in foods—a review. *International Journal of Food Microbiology*, 94 (3), 223–253. https://doi.org/10.1016/j.ijfoodmicro.2004.03.022

32. Cao, N., Yang, X., & Fu, Y. (2009). Effects of various plasticizers on mechanical and water vapor barrier properties of gelatin films. *Food Hydrocolloids*, 23 (3), 729-735. https://doi.org/10.1016/j.foodhyd.2008.07.017

33. Cao, T. L., Yang, S. Y., & Song, K. Bin. (2018). Development of burdock root inulin/chitosan blend films containing oregano and thyme essential oils. International *Journal of Molecular Sciences*, 19(1), 131. https://doi.org/10.3390/ijms19010131

34. Campos, C. A., Gerschenson, L. N., & Flores, S. K. (2011). Development of edible films and coatings with antimicrobial activity. *Food and Bioprocess Technology*, 4(6), 849–875. https://doi.org/10.1007/s11947-010-0434-1

35. Cárdenas, G., Díaz, J., Meléndrez, M. F., & Cruzat, C. (2008). Physicochemical properties of edible films from chitosan composites obtained by microwave heating. *Polymer Bulletin*, 61(6), 737–748. https://doi.org/10.1007/s00289-008-0994-7

36. Cardoso, G. P., Dutra, M. P., Fontes, P. R., Ramos, A. de L. S., Gomide, L. A. de M., & Ramos, E. M. (2016). Selection of a chitosan gelatin-based edible coating for color preservation of beef in retail display. *Meat Science*, 114, 85–94. https://doi.org/10.1016/j.meatsci.2015.12.012

37. Caro, N., Medina, E., Díaz-Dosque, M., López, L., Abugoch, L., & Tapia, C. (2016). Novel active packaging based on films of chitosan and chitosan/quinoa protein printed with chitosan-tripolyphosphate-thymol nanoparticles via thermal ink-jet printing.

Food Hydrocolloids, 52, 520–532. https://doi.org/10.1016/j.foodhyd.2015.07.028

38. Cazón, P., Vázquez, M., & Velazquez, G. (2018). Composite films of regenerate cellulose with chitosan and polyvinyl alcohol: Evaluation of water adsorption, mechanical and optical properties. *International Journal of Biological Macromolecules*, 117, 235–246. https://doi.org/10.1016/j.ijbiomac.2018.05.148

39. Cazón, P., & Vázquez, M. (2019). Mechanical and barrier properties of chitosan combined with other components as food packaging film. *Environmental Chemistry Letters*, in press. https://doi.org/10.1007/s10311-019-00936-3

40. Chen, Q., Xu, S., Wu, T., Guo, J., S, S., Zheng, X., & Yu, T. (2014). Effect of citronella essential oil on the inhibition of postharvest Alternaria alternata in cherry tomato. *Journal of the Science of Food and Agriculture*, 94(12), 2441-2447. https://doi.org/10.1002/jsfa.6576

41. Costa-junior, E. D. S., Pereira, M. M., & Mansur, H. S. (2009). Properties and biocompatibility of chitosan films modified by blending with PVA and chemically crosslinked. *Journal of Materials Science: Materials in Medicine*, 20(2), 553–561. https://doi.org/10.1007/s10856-008-3627-7

42. Dangaran, K., Tomasula, P. M., & Qi, P. (2009). Structure and function of protein-based edible films and coatings. In K. Huber & M. Embuscado (Eds.) Edible films and coatings for food applications (pp. 25-56). Springer: New York, NY, USA. https://doi.org/10.1007/978-0-387-92824-1_2

43. Darmon, S. E., & Rudall, K. M. (1950). Infra-red and X-ray studies on chitin. *Discussion Faraday Soc.*, *9*, 251.

44. De Leo, R., Quartieri, A., Haghighi, H., Gigliano, S., Bedin, E., & Pulvirenti, A. (2018). Application of pectin-alginate and pectin-alginate-lauroyl arginate ethyl coatings to eliminate Salmonella enteritidis cross contamination in egg shells. *Journal of Food Safety*, 1–9. https://doi.org/10.1111/jfs.12567

45. De Moraes Crizel, T., de Oliveira Rios, A., D. Alves, V., Bandarra, N., Moldão-Martins, M., & Hickmann Flôres, S. (2018). Active food packaging prepared with chitosan and olive pomace. *Food Hydrocolloids*, 74, 139–150. https://doi.org/10.1016/j.foodhyd.2017.08.007

46. Del Nobile, M.A., Di Benedetto, N., Suriano, N., Conte, A., Corbo, M.R., & Sinigaglia, M. (2009). Combined effects of chitosan and MAP to improve the microbial quality of amaranth homemade fresh pasta. *Food Microbiology*, 26 (6), 587-591. https://doi.org/10.1016/j.fm.2009.03.012

47. Del Nobile, M. A., Fava, P., & Piergiovanni, L. (2002). Water transport properties of cellophane flexible films intended for food packaging applications. *Journal of Food Engineering*, 53(4), 295–300. https://doi.org/10.1016/S0260-8774(01)00168-6

48. EFSA. (2007). Opinion of the scientific panel on food additives, flavourings , processing aids and materials in contact with food on a request from the commission related to an application on the use of ethyl lauroyl arginate as a food additive. *The EFSA Journal*, 511, 1–27. https://doi.org/10.2903/j.efsa.2007.511

49. Elsabee, M. Z., & Abdou, E. S. (2013). Chitosan based edible films and coatings: A review. *Materials Science and Engineering C*, 33(4), 1819–1841. https://doi.org/10.1016/j.msec.2013.01.010

50. FDA (2005a). US Food and Drugs Administration. Center for Food Safety and Applied Nutrition, U.S. Agency Response Letter GRAS Notice No. GRN 170. https://www.accessdata.fda.gov/scripts/fdcc/?set=GRASNotices&id=170&sort=FDA_s_Letter&order=ASC&startrow=1&type=basic&search=443

51. FDA (2005b). US Food and Drugs Administration. Center for Food Safety and Applied Nutrition, U.S. Agency Response Letter GRAS Notice No. GRN 000164. https://www.accessdata.fda.gov/scripts/fdcc/index.cfm?set=GRASNotices&id=164&sort=GRN_No&order=DESC&startrow=1&type=advanced&search=%C2%A4%C2%A4%C2%A4

52. FDA (2013). US Food and Drug Administration, Department of Health And Human Services. Code of Federal Regulations part 182: Substances Generally Recognized as Safe sec. 182.20 Essential oils, oleoresins (solvent-free), and natural extractives (including distillates). CFR-Code of Federal Regulations Title 21, volume 3. https://www.accessdata.fda.gov/scripts/cdrh/cfdocs/cfcfr/cfrsearch.cfm?fr=182.20

53. Figueroa-Lopez, K. J., Andrade-Mahecha, M. M., & Torres-Vargas, O. L. (2018). Development of antimicrobial biocomposite films to preserve the quality of bread. *Molecules*, 23(1), 212. https://doi.org/10.3390/molecules23010212

54. Gaikwad, K. K., Lee, S. M., Lee, J. S., & Lee, Y. S. (2017). Development of antimicrobial polyolefin films containing lauroyl arginate and their use in the packaging of strawberries. *Journal of Food Measurement and Characterization*, 11(4), 1706–1716. https://doi.org/10.1007/s11694-017-9551-0

55. Galus, S., & Kadzińska, J. (2015). Food applications of emulsion-based edible films and coatings. T*rends in Food Science & Technology*, 45(2), 273–283. https://doi.org/10.1016/j.tifs.2015.07.011

56. Gamarra, A., Missagia, B., Urpí, L., Morató, J., & Muñoz-guerra, S. (2018). Ionic coupling of hyaluronic acid with ethyl *N*-lauroyl L-arginate (LAE): Structure, properties and biocide activity of complexes. *Carbohydrate Polymers*, 197, 109–116. https://doi.org/10.1016/j.carbpol.2018.05.057

57. Gartner, H., Li, Y., & Almenar, E. (2015). Improved wettability and adhesion of polylactic acid/chitosan coating for bio-based multilayer film development. *Applied Surface Science*, 332, 488–493. https://doi.org/10.1016/j.apsusc.2015.01.157

58. Ghaderi, J., Hosseini, S. F., Keyvani, N., & Gómez-Guillén, M. C. (2019). Polymer blending effects on the physicochemical and structural features of the chitosan/poly(vinyl alcohol)/fish gelatin ternary biodegradable films. *Food Hydrocolloids*, 95, 122–132. https://doi.org/10.1016/j.foodhyd.2019.04.021

59. Giannakas, A., Vlacha, M., Salmas, C., Leontiou, A., Katapodis, P., Stamatis, H., Barkoula, N-M., Ladavos, A. (2016). Preparation, characterization, mechanical, barrier and antimicrobial properties of chitosan/PVOH/clay nanocomposites. *Carbohydrate Polymers*, 140, 408–415. https://doi.org/10.1016/j.carbpol.2015.12.072

60. Gómez-Estaca, J., López de Lacey, A., López-Caballero, M. E., Gómez-Guillén, M. C., & Montero, P. (2010). Biodegradable gelatin-chitosan films incorporated with essential oils as antimicrobial agents for fish preservation. *Food Microbiology*, 27(7), 889–896. https://doi.org/10.1016/j.fm.2010.05.012

61. Gómez-Guillén, M. C., Giménez, B., López-Caballero, M. E., & Montero, M. P. (2011). Functional and bioactive properties of collagen and gelatin from alternative

source: A review. *Food Chemistry*, 25(8), 1813–1827. https://doi.org/10.1016/j.foodhyd.2011.02.007

62. Gontard, N., Guilbert, S., & Cuq, J. (1992). Edible wheat gluten films: Influence of the main process variables on film properties using response surface methodology. *Journal of Food Science*, 57(1), 190–195. https://doi.org/10.1111/j.1365-2621.1992.tb05453.x.

63. Guo, Y., Chen, X., Yang, F., Wang, T., Ni, M., Chen, Y., Yang, F., Huang, D., Fu, C., Wang, S. (2019). Preparation and characterization of chitosan-based ternary blend edible films with efficient antimicrobial activities for food packaging applications. *Journal of Food Science*, 84(6), 1411–1419. https://doi.org/10.1111/1750-3841.14650

64. Gutiérrez, T. J. (2017). Chitosan applications for the food industry. In S. Ahmed & I. Saiqa (Eds.), *Chitosan: Derivatives, Composites and Applications* (pp. 183–232). https://doi.org/10.1002/9781119364849.ch8

65. Haghighi, H., Biard, S., Bigi, F., Leo, R. De, Bedin, E., Pfeifer, F. Siesler, H. W., Licciardello, F., & Pulvirenti, A. (2019). Comprehensive characterization of active chitosan-gelatin blend films enriched with different essential oils. *Food Hydrocolloids*, 95, 33–42. https://doi.org/10.1016/j.foodhyd.2019.04.019

66. Haghighi, H., De Leo, R., Bedin, E., Pfeifer, F., Siesler, H. W., & Pulvirenti, A. (2019). Comparative analysis of blend and bilayer films based on chitosan and gelatin enriched with LAE (lauroyl arginate ethyl) with antimicrobial activity for food packaging applications. *Food Packaging and Shelf Life*, 19, 31–39. https://doi.org/10.1016/j.fpsl.2018.11.015

67. Haghighi, H., Leugoue, S. K., Pfeifer, F., Siesler, H. W., Licciardello, F., Fava, P., & Pulvirenti, A. (2020). Development of antimicrobial films based on chitosan-polyvinyl alcohol blend enriched with ethyl lauroyl arginate (LAE) for food packaging applications. *Food Hydrocolloids*, 100, 105419. https://doi.org/10.1016/j.foodhyd.2019.105419

68. Hajji, S., Chaker, A., Jridi, M., Maalej, H., Jellouli, K., Boufi, S., & Nasri, M. (2016). Structural analysis , and antioxidant and antibacterial properties of chitosan-poly (vinyl alcohol) biodegradable films. *Environmental Science and Pollution Research*, 23(15), 15310–15320. https://doi.org/10.1007/s11356-016-6699-9

69. Hasanpour Ardekani-Zadeh, A., & Hosseini, S. F. (2019). Electrospun essential oil-doped chitosan/poly(ε-caprolactone) hybrid nanofibrous mats for antimicrobial food biopackaging exploits. *Carbohydrate Polymers*, 223, 115108. https://doi.org/10.1016/j.carbpol.2019.115108

70. Higueras, L., López-Carballo, G., Hernández-Muñoz, P., Gavara, R., & Rollini, M. (2013). Development of a novel antimicrobial film based on chitosan with LAE (ethyl-Nα-dodecanoyl-L-arginate) and its application to fresh chicken. International *Journal of Food Microbiology*, 165(3), 339–345. https://doi.org/10.1016/j.ijfoodmicro.2013.06.003

71. Hosseini, S. F., Rezaei, M., Zandi, M., & Ghavi, F. F. (2013). Preparation and functional properties of fish gelatin-chitosan blend edible films. *Food Chemistry*, 136(3–4), 1490–1495. https://doi.org/10.1016/j.foodchem.2012.09.081

72. Hosseini, S. F., Rezaei, M., Zandi, M., & Ghavi, F.F. (2015). Fabrication of bio-nanocomposite films based on fish gelatin reinforced with chitosan nanoparticles. *Food*

Hydrocolloids, 44, 172–182. https://doi.org/10.1016/j.foodhyd.2014.09.004

73. Hou, C., Gao, L., Wang, Z., Rao, W., Du, M., & Zhang, D. (2019). Mechanical properties, thermal stability, and solubility of sheep bone collagen–chitosan films. *Journal of Food Process Engineering*, e13086. https://doi.org/10.1111/jfpe.13086

74. Hu, D., Wang, H., & Wang, L. (2016). Physical properties and antibacterial activity of quaternized chitosan/carboxymethyl cellulose blend films. *LWT - Food Science and Technology*. https://doi.org/10.1016/j.lwt.2015.08.033

75. Huang, L. H., & Zhang, Y. H. (2015). Effects of chitosan and microfluidization pretreatment on physicochemical and mechanical properties of vicilin-rich protein isolate (Phaseolus aureus) films. *Digest Journal of Nanomaterials and Biostructures*, 10(2), 513–519.

76. Jackson, M., & Mantsch, H. H. (1995). The use and misuse of FTIR spectroscopy in the determination of protein structure. *Critical Reviews in Biochemistry and Molecular Biology*, 30(2), 95-120. https://doi.org/10.3109/10409239509085140

77. Jahan, F., Mathad, R. D., & Farheen, S. (2016). Effect of mechanical strength on chitosan-PVA blend through ionic crosslinking for food packaging application. *Materials Today: Proceedings*, 3(10), 3689–3696. https://doi.org/10.1016/j.matpr.2016.11.014

78. Jamróz, E., Juszczak, L., & Kucharek, M. (2018). Investigation of the physical properties, antioxidant and antimicrobial activity of ternary potato starch-furcellaran-gelatin films incorporated with lavender essential oil. *International Journal of Biological Macromolecules*, 114, 1094–1101. https://doi.org/10.1016/j.ijbiomac.2018.04.014

79. Jantrawut, P., Chaiwarit, T., Jantanasakulwong, K., Brachais, C., & Chambin, O. (2017). Effect of plasticizer type on tensile property and In Vitro indomethacin release of thin films based on low-methoxyl pectin. *Polymers*, 9(7), 289. https://doi.org/10.3390/polym9070289

80. Jouki, M., Yazdia, F. T., Mortazavi, S. A., Koocheki, A., & Khazaei, N. (2014). Effect of quince seed mucilage edible films incorporated with oregano or thyme essential oil on shelf life extension of refrigerated rainbow trout fillets. I*nternational Journal of Food Microbiology*, 174, 88-97. https://doi.org/10.1016/j.ijfoodmicro.2014.01.001

81. Jridi, M., Hajji, S., Ben Ayed, H., Lassoued, I., Mbarek, A., Kammoun, M., Souissi, N., Nasri, M. (2014). Physical, structural, antioxidant and antimicrobial properties of gelatin-chitosan composite edible films. *International Journal of Biological Macromolecules*, 67, 373–379. https://doi.org/10.1016/j.ijbiomac.2014.03.054

82. Jridi, M., Souissi, N., Mbarek, A., Chadeyron, G., Kammoun, M., & Nasri, M. (2013). Comparative study of physico-mechanical and antioxidant properties of edible gelatin films from the skin of cuttlefish. *International Journal of Biological Macromolecules*, 61, 17–25. https://doi.org/10.1016/j.ijbiomac.2013.06.040

83. Kakaei, S., & Shahbazi, Y. (2016). Effect of chitosan-gelatin film incorporated with ethanolic red grape seed extract and Ziziphora clinopodioides essential oil on survival of Listeria monocytogenes and chemical, microbial and sensory properties of minced trout fillet. *LWT - Food Science and Technology*, 72, 432–438. https://doi.org/10.1016/j.lwt.2016.05.021

84. Kan, J., Liu, J., Yong, H., Liu, Y., Qin, Y., & Liu, J. (2019). Development of active

packaging based on chitosan-gelatin blend films functionalized with Chinese hawthorn (Crataegus pinnatifida) fruit extract. *International Journal of Biological Macromolecules*, 140, 384–392. https://doi.org/10.1016/j.ijbiomac.2019.08.155

85. Kanatt, S. R., Rao, M. S., Chawla, S. P., & Sharma, A. (2012). Active chitosan-polyvinyl alcohol films with natural extracts. *Food Hydrocolloids*, 29(2), 290–297. https://doi.org/10.1016/j.foodhyd.2012.03.005

86. Kashiri, M., Cerisuelo, J. P., Domínguez, I., López-Carballo, G., Hernández-Muñoz, P., & Gavara, R. (2016). Novel antimicrobial zein film for controlled release of lauroyl arginate (LAE). *Food Hydrocolloids*, 61, 547–554. https://doi.org/10.1016/j.foodhyd.2016.06.012

87. Khan, I., Mansha, M., & Mazumder, M. A. J. (2018). Polymer blends. In M. J. Mazumder, H. Sheardown, & A. Al-Ahmed (Eds.), *Functional Polymers* (pp. 1–38). https://doi.org/10.3139/9781569905586.007

88. Khezrian, A., & Shahbazi, Y. (2018). Application of nanocompostie chitosan and carboxymethyl cellulose films containing natural preservative compounds in minced camel's meat. *International Journal of Biological Macromolecules*, 106, 1146–1158. https://doi.org/10.1016/j.ijbiomac.2017.08.117

89. Khwaldia, K., Basta, A. H., Aloui, H., & El-Saied, H. (2014). Chitosan-caseinate bilayer coatings for paper packaging materials. *Carbohydrate Polymers*, 99(2014), 508–516. https://doi.org/10.1016/j.carbpol.2013.08.086

90. Kim, H., Beak, S. E., & Song, K. B. (2018). Development of a hagfish skin gelatin film containing cinnamon bark essential oil. *Lwt/Food Science and Technology*, 96, 583–588. https://doi.org/10.1016/j.lwt.2018.06.016

91. Kim, J. H., Kim, J. Y., Lee, Y. M., & Kim, K. Y. (1992). Properties and swelling characteristics of cross-linked poly (vinyl alcohol)/ chitosan blend membrane. J*ournal of Applied Polymer Science*, 45(10), 1711–1717. https://doi.org/10.1002/app.1992.070451004

92. Koosha, M., & Mirzadeh, H. (2015). Electrospinning, mechanical properties, and cell behavior study of chitosan/PVA nanofibers. *Journal of Biomedical Materials Research - Part A*, 103(9), 3081–3093. https://doi.org/10.1002/jbm.a.35443

93. Kumar, S., Krishnakumar, B., Sobral, A. J. F. N., & Koh, J. (2019). Bio-based (chitosan/PVA/ ZnO) nanocomposites film : Thermally stable and photoluminescence material for removal of organic dye. *Carbohydrate Polymers*, 205, 559–564. https://doi.org/10.1016/j.carbpol.2018.10.108

94. Leceta, I., Guerrero, P., & De La Caba, K. (2013). Functional properties of chitosan-based films. *Carbohydrate Polymers*, 93(1), 339–346. https://doi.org/10.1016/j.carbpol.2012.04.031

95. Leceta, I., Guerrero, P., Ibarburu, I., Dueñas, M. T., & De La Caba, K. (2013). Characterization and antimicrobial analysis of chitosan-based films. *Journal of Food Engineering*, 116(4), 889–899. https://doi.org/10.1016/j.jfoodeng.2013.01.022

96. Lee, J.-H., Lee, J.-H., Yang, H.-J., & Song, K. bin. (2015). Preparation and characterization of brewer's spent grain protein-chitosan composite films. *Journal of Food Science and Technology*, 52(11), 7549–7555. https://doi.org/10.1007/s13197-015-1941-x

97. Li, J. (2008). Characterization and Performance Improvement of Chitosan Films As Affected by Preparation Method, Synthetic Polymers , and Blend Ratios (University of Tennessee, Knoxville). Retrieved from http://trace.tennessee.edu/utk_graddiss/464

98. Li, K., Jin, S., Liu, X., Chen, H., He, J., & Li, J. (2017). Preparation and characterization of chitosan/soy protein isolate nanocomposite film reinforced by Cu nanoclusters. *Polymers*, 9(7): 247. https://doi.org/10.3390/polym9070247

99. Li, W., Zheng, K., Chen, H., Feng, S., Wang, W., & Qin, C. (2019). Influence of Nano Titanium Dioxide and Clove Oil on Chitosan–Starch Film Characteristics. *Polymers*, 11(9), 1418. https://doi.org/10.3390/polym11091418

100. Liu, F., Antoniou, J., Li, Y., Yi, J., Yokoyama, W., Ma, J., & Zhong, F. (2015). Preparation of gelatin films incorporated with tea polyphenol nanoparticles for enhancing controlled-release antioxidant properties. *Journal of Agricultural and Food Chemistry*, 63(15), 3987–3995. https://doi.org/10.1021/acs.jafc.5b00003

101. Liu, Y., Wang, S., & Lan, W. (2018). Fabrication of antibacterial chitosan-PVA blended film using electrospray technique for food packaging applications. *International Journal of Biological Macromolecules*, 107(PartA), 848–854. https://doi.org/10.1016/j.ijbiomac.2017.09.044

102. Liu, Y., Wang, S., Zhang, R., Lan, W., & Qin, W. (2017). Development of poly(lactic acid)/chitosan fibers loaded with essential oil for antimicrobial applications. *Nanomaterials*, 7(7),194. https://doi.org/10.3390/nano7070194

103. Lozano-Navarro, J. I., Díaz-Zavala, N. P., Velasco-Santos, C., Martínez-Hernández, A. L., Tijerina-Ramos, B. I., García-Hernández, M., … Reyes-de la Torre, A. I. (2017). Antimicrobial, optical and mechanical properties of Chitosan–Starch films with natural extracts. *International Journal of Molecular Sciences*, 18(5), 1–18. https://doi.org/10.3390/ijms18050997

104. Luchese, C. L., Pavoni, J. M. F., dos Santos, N. Z., Quines, L. K., Pollo, L. D., Spada, J. C., & Tessaro, I. C. (2018). Effect of chitosan addition on the properties of films prepared with corn and cassava starches. *Journal of Food Science and Technology*, 55(8), 2963–2973. https://doi.org/10.1007/s13197-018-3214-y

105. Luzi, F., Fortunati, E., Giovanale, G., Mazzaglia, A., Torre, L., & Balestra, G. M. (2017). Cellulose nanocrystals from Actinidia deliciosa pruning residues combined with carvacrol in PVA_CH films with antioxidant/antimicrobial properties for packaging applications. *International Journal of Biological Macromolecules*, 104, 43–55. https://doi.org/10.1016/j.ijbiomac.2017.05.176

106. Ma, Q., Davidson, P. M., Critzer, F., & Zhong, Q. (2016). Antimicrobial activities of lauric arginate and cinnamon oil combination against foodborne pathogens: Improvement by ethylenediaminetetraacetate and possible mechanisms. *LWT - Food Science and Technology*, 72, 9–18. https://doi.org/10.1016/j.lwt.2016.04.021

107. Ma, Q., Zhang, Y., & Zhong, Q. (2016). Physical and antimicrobial properties of chitosan films incorporated with lauric arginate, cinnamon oil, and ethylenediaminetetraacetate. *LWT - Food Science and Technology*, 65, 173–179. https://doi.org/10.1016/j.lwt.2015.08.012

108. Ma, W., Tang, C. H., Yin, S. W., Yang, X. Q., Wang, Q., Liu, F., & Wei, Z. H. (2012). Characterization of gelatin-based edible films incorporated with olive oil. *Food Research International*, 49(1), 572–579. https://doi.org/10.1016/j.foodres.2012.07.037

109. McHugh, T. H., Avena–Bustillos, R.J., Krochta, J. M. (1993). Hydrophilic edible films: modified procedure for water vapor permeability and explanation of related thickness effects. J*ournal of Food Science*, 58, 899–903. https://doi.org/10.1111/j.1365-2621.1993.tb09387.x

110. Mohammadi, R., Mohammadifar, M. A., Rouhi, M., Kariminejad, M., Mortazavian, A. M., Sadeghi, E., & Hasanvand, S. (2018). Physico-mechanical and structural properties of eggshell membrane gelatin- chitosan blend edible films. *International Journal of Biological Macromolecules*, 107, 406–412. https://doi.org/10.1016/j.ijbiomac.2017.09.003

111. Moreno, O., Cárdenas, J., Atarés, L., & Chiralt, A. (2017). Influence of starch oxidation on the functionality of starch-gelatin based active films. *Carbohydrate Polymers*, 178, 147–158. https://doi.org/10.1016/j.carbpol.2017.08.128

112. Moreno, O., Díaz, R., Atarés, L., & Chiralt, A. (2016). Influence of the processing method and antimicrobial agents on properties of starch-gelatin biodegradable films. *Polymer International*, 65(8), 905–914. https://doi.org/10.1002/pi.5115

113. Moreno, O., Gil, À., Atarés, L., & Chiralt, A. (2017). Active starch-gelatin films for shelf-life extension of marinated salmon. *LWT - Food Science and Technology*, 84, 189–195. https://doi.org/10.1016/j.lwt.2017.05.005

114. Morsy, N. F. S. (2016). A comprtive study of nutmeg (Myristica fragrans Houtt.) oleoresins obtained by conventionl and green extraction techniques. *Journal of Foos Science and Technology* 53(10), 3770-3777. https://doi.org/10.1007/s13197-016-2363-0

115. Muriel-Galet, V., Carballo, G. L., Hernández-Muñoz, P., & Gavara, R. (2016). Ethyl Lauroyl Arginate (LAE): usage and potential in antimicrobial packaging. In J. Barros-Velázquez (Ed.) *Antimicrobial Food Packaging* (pp. 313–318), Elsevier Science. London. https://doi.org/10.1016/B978-0-12-800723-5.00024-3

116. Muriel-Galet, López-Carballo, G., Gavara, R., & Hernández-Muñoz, P. (2015). Antimicrobial effectiveness of lauroyl arginate incorporated into ethylene vinyl alcohol copolymers to extend the shelf-life of chicken stock and surimi sticks. *Food and Bioprocess Technology*, 8(1), 208–217. https://doi.org/10.1007/s11947-014-1391-x

117. Muriel-Galet, V., López-Carballo, G., Hernández-Muñoz, P., & Gavara, R. (2014). Characterization of ethylene-vinyl alcohol copolymer containing lauril arginate (LAE) as material for active antimicrobial food packaging. *Food Packaging and Shelf Life*, 1(1), 10–18. https://doi.org/10.1016/j.fpsl.2013.09.002

118. Muriel-Galet, V., López-Carballo, G., Gavara, R., & Hernández-Muñoz, P. (2012). Antimicrobial food packaging film based on the release of LAE from EVOH. *International Journal of Food Microbiology*, 157(2), 239–244. https://doi.org/10.1016/j.ijfoodmicro.2012.05.009

119. Musso, Y. S., Salgado, P. R., & Mauri, A. N. (2017). Smart edible films based on gelatin and curcumin. *Food Hydrocolloids*, 66, 8–15. https://doi.org/10.1016/j.foodhyd.2016.11.007

120. Nisar, T., Wang, Z. C., Yang, X., Tian, Y., Iqbal, M., & Guo, Y. (2018). Characterization of citrus pectin films integrated with clove bud essential oil: Physical, thermal, barrier, antioxidant and antibacterial properties. *International Journal of Biological Macromolecules*, 106, 670–680.

https://doi.org/10.1016/j.ijbiomac.2017.08.068

121. No, H. K., Meyers, S. P., Prinyawiwatkul, W., & Xu, Z. (2007). Applications of chitosan for improvement of quality and shelf life of foods: A review. *Journal of Food Science*, 72(5), 87–100. https://doi.org/10.1111/j.1750-3841.2007.00383.x

122. Ojagh, S. M., Rezaei, M., Razavi, S. H., & Hosseini, S. M. H. (2010). Development and evaluation of a novel biodegradable film made from chitosan and cinnamon essential oil with low affinity toward water. *Food Chemistry*, 122(1), 161–166. https://doi.org/10.1016/j.foodchem.2010.02.033

123. Parida, U. K., Nayak, A. K., Binhani, B. K., & Nayak, P. L. (2011). Synthesis and characterization of chitosan-polyvinyl alcohol blended with cloisite 30B for controlled release of the anticancer drug curcumin. *Journal of Biomaterials and Nanobiotechnology*, 2, 414–425. https://doi.org/10.4236/jbnb.2011.24051

124. Pattanayaiying, R., H-Kittikun, A., & Cutter, C. N. (2015). Incorporation of nisin Z and lauric arginate into pullulan films to inhibit foodborne pathogens associated with fresh and ready-to-eat muscle foods. *International Journal of Food Microbiology*, 207, 77–82. https://doi.org/10.1016/j.ijfoodmicro.2015.04.045

125. Pavaloiu, R. D., Stoica-Guzun, A., Stroescu, M., Jinga, S. I., & Dobre, T. (2014). Composite films of poly(vinyl alcohol)-chitosan-bacterial cellulose for drug controlled release. *International Journal of Biological Macromolecules*, 68, 117–124. https://doi.org/10.1016/j.ijbiomac.2014.04.040

126. Peelman, N., Ragaert, P., De Meulenaer, B., Adons, D., Peeters, R., Cardon, L., Van Impe, F., & Devlieghere, F. (2013). Application of bioplastics for food packaging. *Trends in Food Science and Technology*, 32(2), 128–141. https://doi.org/10.1016/j.tifs.2013.06.003

127. Peng, Y., & Li, Y. (2014). Combined effects of two kinds of essential oils on physical, mechanical and structural properties of chitosan films. *Food Hydrocolloids*, 36, 287–293. https://doi.org/10.1016/j.foodhyd.2013.10.013

128. Pereda, M., Ponce, A. G., Marcovich, N. E., Ruseckaite, R. A., & Martucci, J. F. (2011). Chitosan-gelatin composites and bi-layer films with potential antimicrobial activity. *Food Hydrocolloids*, 25(5), 1372–1381. https://doi.org/10.1016/j.foodhyd.2011.01.001

129. Pereira Jr, V. A., de Arruda, I. N. Q., & Stefani, R. (2015). Active chitosan/PVA films with anthocyanins from Brassica oleraceae (Red Cabbage) as Time-Temperature Indicators for application in intelligent food packaging. *Food Hydrocolloids*, 43, 180–188. https://doi.org/10.1016/j.foodhyd.2014.05.014

130. Perumal, A. B., Sellamuthu, P. S., Nambiar, R. B., & Sadiku, E. R. (2018). Development of polyvinyl alcohol/chitosan bio-nanocomposite films reinforced with cellulose nanocrystals isolated from rice straw. *Applied Surface Science*, 449, 591–602. https://doi.org/10.1016/j.apsusc.2018.01.022

131. Pezo, D., Navascués, B., Salafranca, J., & Nerín, C. (2012). Analytical procedure for the determination of Ethyl Lauroyl Arginate (LAE) to assess the kinetics and specific migration from a new antimicrobial active food packaging. *Analytica Chimica Acta*, 745, 92–98. https://doi.org/10.1016/j.aca.2012.07.038

132. Qu, L., Chen, G., Dong, S., Huo, Y., Yin, Z., Li, S., & Chen, Y. (2019). Improved mechanical and antimicrobial properties of zein/chitosan films by adding highly

dispersed nano-TiO_2. *Industrial Crops and Products*, 130, 450–458. https://doi.org/10.1016/j.indcrop.2018.12.093

133. Peng, Y., & Li, Y. (2014). Combined effects of two kinds of essential oils on physical, mechanical and structural properties of chitosan films. *Food Hydrocolloids*, 36, 287–293. https://doi.org/10.1016/j.foodhyd.2013.10.013

134. Ponce, A. G., Roura, S. I., del Valle, C. E., & Moreira, M. R. (2008). Antimicrobial and antioxidant activities of edible coatings enriched with natural plant extracts: In vitro and in vivo studies. *Postharvest Biology and Technology*, 49(2), 294–300. https://doi.org/10.1016/j.postharvbio.2008.02.013

135. Poverenov, E., Rutenberg, R., Danino, S., Horev, B., & Rodov, V. (2014). Gelatin-Chitosan composite films and edible coatings to enhance the quality of food products: Layer-by-Layer vs. Blended formulations. *Food and Bioprocess Technology*, 7(11), 3319–3327. https://doi.org/10.1007/s11947-014-1333-7

136. Pranoto, Y., Rakshit, S. K., & Salokhe, V. M. (2005). Enhancing antimicrobial activity of chitosan films by incorporating garlic oil, potassium sorbate and nisin. *LWT - Food Science and Technology*, 38(8), 859–865. https://doi.org/10.1016/j.lwt.2004.09.014

137. Qiao, C., Ma, X., Zhang, J., & Yao, J. (2017). Molecular interactions in gelatin/chitosan composite films. *Food Chemistry*, 235, 45–50. https://doi.org/10.1016/j.foodchem.2017.05.045

138. Raafat, D., & Sahl, H. G. (2009). Chitosan and its antimicrobial potential - A critical literature survey. *Microbial Biotechnology*, 2(2), 186–201. https://doi.org/10.1111/j.1751-7915.2008.00080.x

139. Ramos, M., Valdés, A., Beltrán, A., & Garrigós, M. (2016). Gelatin-based films and coatings for food packaging applications. *Coatings*, 6(4), 41. https://doi.org/10.3390/coatings6040041

140. Ramziia, S., Ma, H., Yao, Y., Wei, K., & Huang, Y. (2018). Enhanced antioxidant activity of fish gelatin–chitosan edible films incorporated with procyanidin. *Journal of Applied Polymer Science*, 135(10), 1–10. https://doi.org/10.1002/app.45781

141. Ren, L., Yan, X., Zhou, J., Tong, J., & Su, X. (2017). Influence of chitosan concentration on mechanical and barrier properties of corn starch/chitosan films. *International Journal of Biological Macromolecules*, *105*, 1636–1643. https://doi.org/10.1016/j.ijbiomac.2017.02.008

142. Rezaee, M., Askari, G., EmamDjomeh, Z., & Salami, M. (2018). Effect of organic additives on physiochemical properties and anti-oxidant release from chitosan-gelatin composite films to fatty food simulant. *International Journal of Biological Macromolecules*, 114, 844–850. https://doi.org/10.1016/j.ijbiomac.2018.03.122

143. Richards, A. G. (1951). The integument of arthropods: the chemical components and their properties, the anatomy and development, and the permeability. University of Minnesota Press, Minneapolis.

144. Ritchie, H., & Roser, M. (2018). Plastic pollution. *Our World In Data*. Retrieved from https://ourworldindata.org/plastic-pollution

145. Rivero, S., García, M. A., & Pinotti, A. (2009). Composite and bi-layer films based on gelatin and chitosan. *Journal of Food Engineering*, 90(4), 531–539.

https://doi.org/10.1016/j.jfoodeng.2008.07.021

146. Rouget, C. (1859). Des substances amylacees dans Ie tissue des animaux, specialement les Atricules (Chitine). *Comp. Rend*, 48, 792–795

147. Rubilar, J. F., Candia, D., Cobos, A., Díaz, O., & Pedreschi, F. (2016). Effect of nanoclay and ethyl-Nα-dodecanoyl-L-arginate hydrochloride (LAE) on physico-mechanical properties of chitosan films. *LWT - Food Science and Technology*, 72(2016), 206–214. https://doi.org/10.1016/j.lwt.2016.04.057

148. Rujnić-Sokele, M., & Pilipović, A. (2017). Challenges and opportunities of biodegradable plastics: A mini review. *Waste Management and Research*, 35(2), 132–140. https://doi.org/10.1177/0734242X16683272

149. Sadeghi, K., & Shahedi, M. (2016). Physical, mechanical, and antimicrobial properties of ethylene vinyl alcohol copolymer/chitosan/nano-ZnO (ECNZn) nanocomposite films incorporating glycerol plasticizer. *Journal of Food Measurement and Characterization*, *10*(1), 137–147. https://doi.org/10.1007/s11694-015-9287-7

150. Salgado, P. R., López-Caballero, M. E., Gómez-Guillén, M. C., Mauri, A. N., & Montero, M. P. (2013). Sunflower protein films incorporated with clove essential oil have potential application for the preservation of fish patties. *Food Hydrocolloids*, 33(1), 74–84. https://doi.org/10.1016/j.foodhyd.2013.02.008

151. Salvia-Trujillo, L., Rojas-Graü, A., Soliva-Fortuny, R., & Martín-Belloso, O. (2015). Physicochemical characterization and antimicrobial activity of food-grade emulsions and nanoemulsions incorporating essential oils. *Food Hydrocolloids*, 43, 547–556. https://doi.org/10.1016/j.foodhyd.2014.07.012

152. Sarwar, M. S., Niazi, M. B. K., Jahan, Z., Ahmad, T., & Hussain, A. (2018). Preparation and characterization of PVA/nanocellulose/Ag nanocomposite films for antimicrobial food packaging. *Carbohydrate Polymers*, 184, 453–464. https://doi.org/10.1016/j.carbpol.2017.12.068

153. Shahbazi, M., Rajabzadeh, G., & Ahmadi, S. J. (2017). Characterization of nanocomposite film based on chitosan intercalated in clay platelets by electron beam irradiation. *Carbohydrate Polymers*, 157, 226–235. https://doi.org/10.1016/j.carbpol.2016.09.018

154. Shapi'i, R. A., & Othman, S. H. (2016). Effect of concentration of chitosan on the mechanical, morphological and optical properties of tapioca starch film. *International Food Research Journal*, 23, S187–S193. http://www.ifrj.upm.edu.my/23%20(06)%202016%20supplementary/(27)%20IFRJ-16271%20Othman.pdf

155. Shen, Z., & Kamdem, D. P. (2015). Development and characterization of biodegradable chitosan films containing two essential oils. *International Journal of Biological Macromolecules*, 74, 289–296. https://doi.org/10.1016/j.ijbiomac.2014.11.046

156. Shin, J., & Selke, S. E. M. (2014). Food Packaging. In S. SteClark, S. Lamsal, & J. Buddhi (Eds.), *Food processing: principles and applications*. https://doi.org/10.1002/9781118846315.ch11

157. Siracusa, V., Rocculi, P., Romani, S., & Rosa, M. D. (2008). Biodegradable polymers for food packaging: a review. *Trends in Food Science and Technology*, 19(12), 634–643. https://doi.org/10.1016/j.tifs.2008.07.003

158. Siracusa, V., Romani, S., Gigli, M., Mannozzi, C., Cecchini, J., Tylewicz, U., & Lotti, N. (2018). Characterization of active edible films based on citral essential oil, alginate and pectin. *Materials*, 11(10), 1980. https://doi.org/10.3390/ma11101980

159. Souza, V. G. L., Fernando, A. L., Pires, J. R. A., Rodrigues, P. F., Lopes, A. A. S., & Fernandes, F. M. B. (2017). Physical properties of chitosan films incorporated with natural antioxidants. *Industrial Crops and Products*, 107, 565–572. https://doi.org/10.1016/j.indcrop.2017.04.056

160. Staroszczyk, H., Sztuka, K., Wolska, J., Wojtasz-Pająk, A., & Kołodziejska, I. (2014). Interactions of fish gelatin and chitosan in uncrosslinked and crosslinked with EDC films: FT-IR study. *Spectrochimica Acta - Part A: Molecular and Biomolecular Spectroscopy*, 117, 707–712. https://doi.org/10.1016/j.saa.2013.09.044

161. Thakhiew, W., Devahastin, S., & Soponronnarit, S. (2013). Physical and mechanical properties of chitosan films as affected by drying methods and addition of antimicrobial agent. *Journal of Food Engineering*, 119(1), 140–149. https://doi.org/10.1016/j.jfoodeng.2013.05.020

162. Theinsathid, P., Visessanguan, W., Kruenate, J., Kingcha, Y., & Keeratipibul, S. (2012). Antimicrobial activity of lauric arginate-coated polylactic acid films against Listeria monocytogenes and Salmonella Typhimurium on cooked sliced ham. *Journal of Food Science*, 77(2), 142–149. https://doi.org/10.1111/j.1750-3841.2011.02526.x

163. Tripathi, S., Mehrotra, G. K., & Dutta, P. K. (2009). Physicochemical and bioactivity of cross-linked chitosan–PVA film for food packaging applications. International J*ournal of Biological Macromolecules*, 45(4), 372–376. https://doi.org/10.1016/j.ijbiomac.2009.07.006

164. Tripathi, S., Mehrotra, G. K., & Dutta, P. K. (2008). Chitosan based antimicrobial films for food packaging applications. *e-Polymers*, 8(1), 093. https://doi.org/10.1515/epoly.2008.8.1.1082

165. Unger, M., Sedlmair, J., Siesler, H. W., & Hirschmugl, C. (2014). 3D FT-IR imaging spectroscopy of phase-separation in a poly(3-hydroxybutyrate)/poly(L-lactic acid) blend. *Vibrational Spectroscopy*, 75, 169–172. https://doi.org/10.1016/j.vibspec.2014.07.007

166. Uranga, J., Puertas, A. I., Etxabide, A., Dueñas, M. T., Guerrero, P., & De La Caba, K. (2019). Citric acid-incorporated fish gelatin/chitosan composite films. *Food Hydrocolloids*, 86, 95–103. https://doi.org/10.1016/j.foodhyd.2018.02.018

167. Valizadeh, S., Naseri, M., Babaei, S., Hosseini, S. M. H., & Imani, A. (2019). Development of bioactive composite films from chitosan and carboxymethyl cellulose using glutaraldehyde, cinnamon essential oil and oleic acid. *International Journal of Biological Macromolecules*, 134, 604–612. https://doi.org/10.1016/j.ijbiomac.2019.05.071

168. Van den Broek, L. A. M., Knoop, R. J. I., Kappen, F. H. J., & Boeriu, C. G. (2015). Chitosan films and blends for packaging material. *Carbohydrate Polymers*, 116, 237–242. https://doi.org/10.1016/j.carbpol.2014.07.039

169. Van den Oever, M., Molenveld, K., van der Zee, M., & Bos, H. (2017). Bio-based and biodegradable plastics - facts and figures. https://doi.org/10.18174/408350

170. Vodnar, D. C., Pop, O. L., Dulf, F. V., & Socaciu, C. (2015). Antimicrobial efficiency of edible films in food industry. *Notulae Botanicae Horti Agrobotanici Cluj-*

Napoca, 43(2), 302–312. https://doi.org/10.15835/nbha43210048

171. Wang, H., Qian, J., & Ding, F. (2018). Emerging Chitosan-Based Films for Food Packaging Applications. *Journal of Agricultural and Food Chemistry*, 66, 395–413. https://doi.org/10.1021/acs.jafc.7b04528

172. Wang, X. Y., Wang, C. S., & Heuzey, M. C. (2016). Complexation of chitosan and gelatin: From soluble complexes to colloidal gel. *International Journal of Polymeric Materials and Polymeric Biomaterials*, 65(2), 96–104. https://doi.org/10.1080/00914037.2015.1074908

173. Wang, Y., Zhang, Y., Shi, Y., Pan, X., Lu, Y., & Cao, P. (2018). Antibacterial effects of cinnamon (Cinnamomum zeylanicum) bark essential oil on Porphyromonas gingivalis. *Microbial Pathogenesis*, 116, 26–32. https://doi.org/10.1016/j.micpath.2018.01.009

174. Wu, H., Lei, Y., Lu, J., Zhu, R., Xiao, D., Jiao, C., Xia, R., Zhang, Z., Shen, G., Liu, Y., Li, S., Li, M. (2019). Effect of citric acid induced crosslinking on the structure and properties of potato starch/chitosan composite films. *Food Hydrocolloids*, 97, 105208. https://doi.org/10.1016/j.foodhyd.2019.105208

175. Wu, J., Sun, X., Guo, X., Ge, S., & Zhang, Q. (2017). Physicochemical properties, antimicrobial activity and oil release of fish gelatin films incorporated with cinnamon essential oil. Aquaculture and Fisheries, 2(4), 185–192. https://doi.org/10.1016/j.aaf.2017.06.004

176. Wu, Y., Ying, Y., Liu, Y., Zhang, H., & Huang, J. (2018). Preparation of chitosan/poly vinyl alcohol films and their inhibition of biofilm formation against Pseudomonas aeruginosa PAO1. *International Journal of Biological Macromolecules*, 118, 2131–2137. https://doi.org/10.1016/j.ijbiomac.2018.07.061

177. Xing, F., Zhang, S., Li, J., Li, L., & Shi, J. (2018). Crosslinked chitosan-based biocomposite films modified with soy protein isolate. *Polymer Composites*, 39(3), 942–949. https://doi.org/10.1002/pc.24024

178. Xu, J., Xia, R., Zheng, L., Yuan, T., & Sun, R. (2019). Plasticized hemicelluloses/chitosan-based edible films reinforced by cellulose nanofiber with enhanced mechanical properties. *Carbohydrate Polymers*, 224, 115164. https://doi.org/10.1016/j.carbpol.2019.115164

179. Xu, T., Gao, C. C., Feng, X., Yang, Y., Shen, X., & Tang, X. (2019). Structure, physical and antioxidant properties of chitosan-gum arabic edible films incorporated with cinnamon essential oil. *International Journal of Biological Macromolecules*, 134, 230–236. https://doi.org/10.1016/j.ijbiomac.2019.04.189

180. Yadav, M., & Chiu, F. C. (2019). Cellulose nanocrystals reinforced κ-carrageenan based UV resistant transparent bionanocomposite films for sustainable packaging applications. *Carbohydrate Polymers*, 211, 181–194. https://doi.org/10.1016/j.carbpol.2019.01.114

181. Yang, W., Owczarek, J. S., Fortunati, E., Kozanecki, M., Mazzaglia, A., Balestra, G. M., Kenny, J. M., Torre, L., Puglia, D. (2016). Antioxidant and antibacterial lignin nanoparticles in polyvinyl alcohol/chitosan films for active packaging. *Industrial Crops and Products*, 94, 800–811. https://doi.org/10.1016/j.indcrop.2016.09.061

182. Yao, Y., Ding, D., Shao, H., Peng, Q., & Huang, Y. (2017). Antibacterial activity and physical properties of fish gelatin-chitosan edible films supplemented with D-

Limonene. *International Journal of Polymer Science*, (2017), 1-9. https://doi.org/10.1155/2017/1837171

183. Yoon, S. Do, Kim, Y. M., Kim, B. Il, & Je, J. Y. (2017). Preparation and antibacterial activities of chitosan-gallic acid/polyvinyl alcohol blend film by LED-UV irradiation. *Journal of Photochemistry and Photobiology B: Biology*, 176, 145–149. https://doi.org/10.1016/j.jphotobiol.2017.09.024

184. Youssef, A. M., El-Sayed, S. M., El-Sayed, H. S., Salama, H. H., & Dufresne, A. (2016). Enhancement of Egyptian soft white cheese shelf life using a novel chitosan/carboxymethyl cellulose/zinc oxide bionanocomposite film. *Carbohydrate Polymers*, 151, 9–19. https://doi.org/10.1016/j.carbpol.2016.05.023

185. Yu, Z., Li, B., Chu, J., & Zhang, P. (2018). Silica in situ enhanced PVA/chitosan biodegradable films for food packages. *Carbohydrate Polymers*, 184, 214–220. https://doi.org/10.1016/j.carbpol.2017.12.043

186. Yuan, G., Chen, X., & Li, D. (2016). Chitosan films and coatings containing essential oils: The antioxidant and antimicrobial activity, and application in food systems. *Food Research International*, 89, 117–128. https://doi.org/10.1016/j.foodres.2016.10.004

187. Yun, Y. H., Lee, C. M., Kim, Y. S., & Yoon, S. Do. (2017). Preparation of chitosan/polyvinyl alcohol blended films containing sulfosuccinic acid as the crosslinking agent using UV curing process. *Food Research International*, 100(part 1), 377–386. https://doi.org/10.1016/j.foodres.2017.07.030

188. Zargar, V., Asghari, M., & Dashti, A. (2015). A Review on chitin and chitosan polymers: structure, chemistry, solubility, derivatives, and applications. *ChemBioEng Reviews*, 2(3), 204–226. https://doi.org/10.1002/cben.201400025

189. Zhang, L., Wang, H., Jin, C., Zhang, R., Li, L., Li, X., & Jiang, S. (2017). Sodium lactate loaded chitosan-polyvinyl alcohol/montmorillonite composite film towards active food packaging. *Innovative Food Science and Emerging Technologies*, 42, 101–108. https://doi.org/10.1016/j.ifset.2017.06.007

190. Zhang, Y., Ma, Q., Critzer, F., Davidson, P. M., & Zhong, Q. (2015). Physical and antibacterial properties of alginate films containing cinnamon bark oil and soybean oil. *LWT - Food Science and Technology*, 64(1), 423–430. https://doi.org/10.1016/j.lwt.2015.05.008

191. Zhao, Y., Teixeira, J. S., Gänzle, M. M., & Saldaña, M. D. A. (2018). Development of antimicrobial films based on cassava starch, chitosan and gallic acid using subcritical water technology. *Journal of Supercritical Fluids*, 137, 101–110. https://doi.org/10.1016/j.supflu.2018.03.010

192. Zheng, K., Li, W., Fu, B., Fu, M., Ren, Q., Yang, F., & Qin, C. (2018). Physical, antibacterial and antioxidant properties of chitosan films containing hardleaf oatchestnut starch and Litsea cubeba oil. *International Journal of Biological Macromolecules*, 118, 707–715. https://doi.org/10.1016/j.ijbiomac.2018.06.126

193. Zimet, P., Mombrú, Á., Mombrú, D., Castro, A., Villanueva, J., Pardo, H., & Rufo, C. (2019). Physico-chemical and antilisterial properties of nisin-incorporated chitosan/carboxymethyl chitosan films. *Carbohydrate Polymers*, 219, 334–343. https://doi.org/10.1016/j.carbpol.2019.05.013

Acknowledgment

Three years of Ph.D. life passed quickly. I could never have made such an achievement without the people who were beside me. I would like to express my deepest gratitude to my supervisor Prof. Dr. Andrea Pulvirenti for his invaluable enthusiasm, guidance, encouragement, and advice during the entire study. I am grateful to him for having believed in my research capabilities and providing me with the utmost independence at work. All my respects are due to this wonderful person. I would also like to express my sincere thanks to my co-supervisor Prof. Dr. Fabio Licciardello for sharing his knowledge in this field and for his suggestions and advice for performing experiments and revising articles. I am thankful to Prof. Dr. Heinz Wilhelm Siesler, our collaborator from University of Duisburg-Essen, Germany, who warmly accepted me during research visit period at his lab and for his great suggestions to improve this work.

Most importantly, I would like to thank my wife, my parents and my sister for their encouragement and support throughout all my choices in life.

I also want to give my deep appreciation to both referees for spending their valuable time reading my thesis.

Many thanks to Prof. Dr. Alessandro Ulrici, Prof. Dr. Luisa Volpelli, and Prof. Dr. Patrizia Fava for all their important contributions during my studies. I would like to acknowledge Dr. Massimo Tonelli for his constant help to carry out SEM analysis.

I would also like to thank Luca and Alexandra; you made my studying life great. I enjoyed every day, during lunch break, after-work parties, and the time we hung out together.

All the friends and colleagues at Kennedy lab, they make the end of the day more enjoyable especially thanks to Ricky, Francesco, Elisa, Andrea, Anna, Corina, Serena, Salvo, Estefania, Federica, Marco, Veronica, Silvia, Massimo, Sai, Luciana, Maria, Paola, Stefano, Alessandro, and all the others.
Thank you all!

List of Publications

1. **Haghighi H**, Kameni Leuguue S, Pfeifer F, Siesler HW, Licciardello F, Fava P, Pulvirenti A (2020) Development of antimicrobial films based on chitosan-polyvinyl alcohol blend enriched with ethyl lauroyl arginate (LAE) for food packaging applications. *Food Hydrocolloids.* 100:105419*.* https://doi.org/10.1016/j.foodhyd.2019.105419

2. **Haghighi H,** Biard S, Bigi F, De Leo R, Bedin E, Pfeifer F, Siesler HW, Licciardello F, Pulvirenti A (2019) Comprehensive characterization of active chitosan-gelatin blend films enriched with different essential oils. *Food Hydrocolloids.* 95: 33-42. https://doi.org/10.1016/j.foodhyd.2019.04.019

3. **Haghighi H,** Del Leo R, Bedin E, Pfeifer F, Siesler HW, Pulvirenti A (2019) Comparative analysis of blend and bilayer films based on chitosan and gelatin enriched with LAE (Lauroyl Arginate Ethyl) with antimicrobial activity for food packaging applications. *Food Packaging and Shelf Life*.19: 31-39. https://doi.org/10.1016/j.fpsl.2018.11.015

4. **Haghighi H,** Licciardello F, Fava P, Siesler HW, Pulvirenti A. Recent advances of chitosan-based films for sustainable food packaging applications. Proposal of submission to *Trends in Food Science and Technology.*

Congress contributions

1. **Haghighi H**, La China S, Gullo M, Pulvirenti A (2019) Preparation and characterization of active chitosan/bacterial cellulose nano-whisker composite film enriched with lauroyl arginate ethyl for food packaging applications. *5th International Conference on Microbial Diversity*. 25-27 Sep. 2019. Catania, Italy **(Best Poster Award)**

2. **Haghighi H,** Siesler HW, Licciardello F, Pulvirenti A (2019) Features of chitosan-gelatin films loaded with plant extracts. Proceedings of the 9th Shelf Life International Meeting (SLIM 2019). *Italian Journal of Food Science*, 31(5), 128-133.

3. **Haghighi H**, Siesler HW, Licciardello F, Pulvirenti A (2019) Characterization of active chitosan-gelatin blend films enriched with different essential oils for food packaging applications. *SLIM 2019-9° Shelf Life International Meeting*. 17-20 Jun. 2019. Naples, Italy **(Oral presentation)**

4. **Haghighi H**, De Leo R, Bedin E, Siesler HW, Pulvirenti A (2019) Development of active composite films based on chitosan and gelatin enriched with lauroyl arginate ethyl for food packaging applications. *SLIM 2019-9° Shelf Life International Meeting*. 17-20 Jun. 2019. Naples, Italy **(Poster)**

5. **Haghighi H,** Pulvirenti A (2017) Effect of drying conditions and plasticizer type on the development and characterization of bioactive edible films based on natural fibers. *XXII Workshop on the developments in the Italian PhD research on food science, technology, and biotechnology*. 20-22 Sep. 2017. Bolzano, Italy **(Poster)**